Biomedicine & Pharmacotherapy 186 (2025) 117995

Contents lists available at ScienceDirect

Biomedicine & Pharmacotherapy

journal homepage: www.elsevier.com/locate/biopha

Discovery of new dual butyrylcholinesterase (BuChE) inhibitors and 5-HT$_7$ receptor antagonists as compounds used to treat Alzheimer's disease symptoms

Damian Kułaga [a,*], Anna K. Drabczyk [a], Przemysław Zaręba [a], Jolanta Jaśkowska [a], Grzegorz Satała [b], Paula Zaręba [c], Anna Więckowska [c], Modesto de Candia [d], Rosa Purgatorio [d], Anna Boguszewska-Czubara [e], Sylwia Sudoł-Tałaj [f], Gniewomir Latacz [f], Damian Plażuk [g]

[a] Cracow University of Technology, Faculty of Chemical Engineering and Technology, 24 Warszawska Street, Cracow 31-155, Poland
[b] Maj Institute of Pharmacology, Polish Academy of Sciences Department of Medicinal Chemistry, 12 Smętna Street, Cracow 31-343, Poland
[c] Jagiellonian University Medical College, Department of Physicochemical Drug Analysis, Faculty of Pharmacy, 9 Medyczna Street, Cracow 30-688, Poland
[d] University of Bari "Aldo Moro", Department of Pharmacy-Pharmaceutical Sciences, 4 E. Orabona Street, Bari I-70125, Italy
[e] Medical University of Lublin, Department of Medical Chemistry, 4a Chodźki Street, Lublin 20-093, Poland
[f] Jagiellonian University Medical College, Department of Technology and Biotechnology of Drugs, Faculty of Pharmacy, 9 Medyczna Street, Kraków 30-688, Poland
[g] Laboratory of Molecular Spectroscopy, Department of Organic Chemistry, Faculty of Chemistry, University of Lodz, 12 Tamka Street, Łódz 91-403, Poland

ARTICLE INFO

Keywords:
5-HT$_7$ receptor antagonists
Butyrylcholinesterase inhibitors
Alzheimer's disease
Cognitive enhancement therapies
Dual-target strategy
Triazines

ABSTRACT

Alzheimer's disease is a neurodegenerative condition with no effective cure, and current therapies, like donepezil, only alleviate symptoms. Research has explored cholinesterase inhibitors and strategies targeting tau protein, often combining inhibitors with 5-HT receptor antagonists, particularly 5-HT$_6$. However, dual-action BuChE inhibitors and 5-HT$_7$ antagonists have not been studied until now. This study evaluated such compounds in an animal model, focusing on two candidates: compound **18** (BuChE IC$_{50}$ = 4.75 μM; 5-HT$_7$ K_i = 7 nM) and compound **50** (BuChE IC$_{50}$ = 2.53 μM; 5-HT$_7$ K_i = 1 nM). Compound **50** showed robust cognitive improvements, enhancing memory consolidation and acquisition, particularly in reversing scopolamine-induced deficits. In contrast, compound **18** exhibited limited or dose-dependent efficacy, potentially limiting its applicability. These findings highlight the strong potential of compound **50** for cognitive enhancement therapies and suggest it warrants further investigation.

1. Introduction

Alzheimer's Disease (AD) is an age-relative neurodegenerative, untreatable illness in which dementia is the main symptom. The other symptoms may include deterioration in cognition, behavioral function and memory [1]. According to recent statistics, over 6.9 million American people suffer from AD at the age of 65. It is estimated that in 2060 that number may increase up to 13.8 million [2]. Considering its incurability, many research groups have proposed potential treatment paths. Post-mortem analysis of AD brains revealed accumulation of amyloid β protein plaques or tau protein neurofibrillary tangles which may be responsible for neurodegeneration in AD [3]. This hypothesis is increasingly being questioned due to the failure of compounds designed as Aβ inhibitors or anti-tau agents to demonstrate effectiveness in clinical trials [4,5]. The recent research suggested that neurotransmitter system (including cholinergic and serotonin) may have influence on AD treatment [6]. The recent research suggests that affecting the cholinergic and/or serotonergic system may play a significant role in treating memory impairments associated with Alzheimer's disease.

Acetylcholine (AC) is a neurotransmitter present in cholinergic neurons located mostly in the brain. The highest density of this system is located in the medial habenula, spinal cord or basal forebrain. The cholinergic system plays a role in learning processes, modulation of acquisition, consolidation or in memory processes [7]. Reduced cholinergic neurotransmission function contributes to the pathophysiology of learning and memory impairments seen in adult-onset dementia disorders, including AD [8]. In the brain acetylcholine is decomposed to choline via enzymes: acetylcholinesterase (AChE) and

* Corresponding author.
E-mail address: damian.kulaga@pk.edu.pl (D. Kułaga).

https://doi.org/10.1016/j.biopha.2025.117995
Received 13 February 2025; Received in revised form 11 March 2025; Accepted 13 March 2025
Available online 18 March 2025

butyrylcholinesterase (BuChE). Inhibition of these enzymes is a treatment strategy which prevents AC decomposition, increasing neurotransmitter levels in the cholinergic system. It has been proved that in AD patient brains, AChE levels are higher than those of BuChE. On the other hand, during AD progression the activity of AChE decreases in the temporal lobe and hippocampus while that of BuChE increases [9]. Researchers initially focused more on the identification of compounds being AChE inhibitors but further studies disclosed the therapeutic significance of both AChE and BuChE [10]. Donepezil (Aricept), rivastigmine (Exelon), and galantamine (Razadyne) are three drugs commonly used for the symptomatic treatment of Alzheimer's disease (Fig. 1). However, some meta-analyses have shown that these drugs provide modest overall benefits in stabilizing or slowing the decline in cognition, function, behavior, and the clinical global change [11].

Serotonin (5-hydroxytryptamine, 5-HT) is another type of neurotransmitter and neuromodulator located in serotoninergic neurons [12]. In addition to performing basic functions such as controlling body temperature, circadian rhythms, and mood, serotonin significantly influences brain neuroplasticity and the formation of new neural connections, which consequently affects the regulation of memory and learning abilities [13]. It was proved that SSRIs (selective serotonin reuptake inhibitors) reduce the production of toxic amyloid and amyloid plaques by increasing serotonin levels in the serotonin cleft. The 5-HT_6 receptor (5-HT_6R) belongs to the GPCR superfamily of drug targets and activates adenylate cyclase upon stimulation. The latest findings suggest that it is involved in learning and memory processes [14,15]. SB-258585, SB-399885 (Fig. 1) being 5-HT_6 receptor antagonists were able to inhibit the formation of Aβ aggregates and tau protein due to CDK5 kinase activation [13,16]. In addition, they protected neurons against Aβ neurotoxicity, oxidative stress, neuroinflammation or apoptosis. Therefore, the 5-HT_6 receptor may serve as a useful target in AD; however, the known limitations [17] may reduce the chances of developing 5-HT_6 antagonists as effective treatments for AD. The 5-HT_7 receptor (5-HT_7R, similarly to 5-HT_6R) is a G-protein coupled receptor which activates adenylate cyclase upon stimulation. It plays important functions in circadian rhythms, thermoregulation, mood regulation, learning and memory or pain modulation [16]. The latest findings show that the 5-HT_7 receptor takes part in neuronal morphology processes including growth, branching and formation of dendritic spines. These properties of 5-HT_7R suggest that it may be involved in memory formation [18,19]. For instance, selective 5-HT_7 receptor antagonist SB-269970 (Fig. 1) shows significant procognitive effects in mice, while vortioxetine and lurasidone (also 5-HT_7 receptor antagonists) have been approved as procognitive antidepressant and antipsychotic drugs, respectively. Until recently, the 5-HT_7 receptor was mainly considered a target for addressing behavioral and cognitive impairments caused by neurodegeneration in AD [20–22]. However, recent studies suggest that 5-HT_7 receptors may also play a role in controlling the formation of β-amyloid plaques and tau protein aggregates [66].

From the pharmacological point of view, multitarget approach, by incorporating in the same molecule the pharmacophore features able to address simultaneously more than one target involved in disease onset and progression, seems to be more effective than single action in the case of potential anti-AD treatment [23,24]. Many strategies have been developed to treat AD (Fig. 1), such as AChE/miRNA [23], GSK-3β/ROCK-1 [25], 5-HT_6/AChE, 5-HT_6/BuChE [26], 5-HT_6/5-HT_{2A} [27], BuChE/Aβ-inhibitors [28]. Based on the evidence that targeting the 5-HT_7 receptor and the cholinergic system can improve memory and cognitive functions in induced Alzheimer's disease (AD), we decided to obtain dual 5-HT_7/BuChE ligands to validate our hypothesis for the first time. To the best of our knowledge, such strategy has never been tested before.

1,3,5-triazines are a very useful core in medicinal chemistry which can be easily modified. Compounds being 1,3,5-triazine derivatives exhibit various potential bioactivities including anticancer [65] and antimalarial [65], acting as 5-HT_6R [27], 5-HT_7R [29] or 5-HT_{2A}R [27] ligands. They also have neuroprotective properties as well as AChE and/or BuChE activity or anti-Aβ aggregation activity [15,26,30]. In recent years, we developed a series of 1,3,5-triazines being selective 5-HT_7 receptor antagonists that could be used to treat CNS (central nervous system) disorders [31,32]. In our studies, we performed an SAR study and identified the key structural fragments for achieving high 5-HT_7R affinity. In 2017, Tiwari and Hoda described very potent AChE/BuChE inhibitors with potential anti-Aβ aggregation being 1,3,5-triazine derivatives [33]. This library of compounds was an inspiration and starting point to designing dual 5HT_7/BuChE agents. First of all, during the whole design process we tried to maximally optimize 5-HT_7R binding. The first set of compounds was similar to those reported by

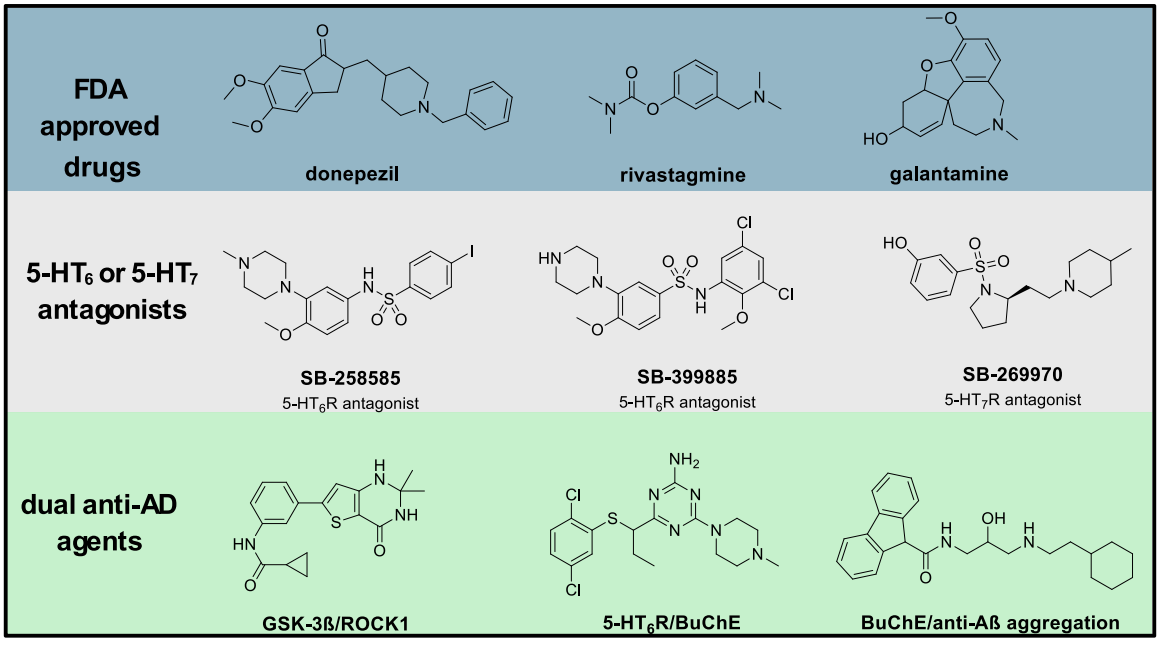

Fig. 1. Examples of compounds used in the treatment of AD (donepezil, rivastigmine, and galantamine) and compounds in the preclinical research phase (5-HT_6 or 5-HT_7 antagonists and dual anti-AD agents).

Tiwari and Hoda with cholinergic activity (Fig. 2). At this stage we decided to substitute the chlorine atom with an NH_2 group because of the potential formation of a hydrogen bond with the E7.34 amino acid in the 5-HT_7 receptor [34]. The triazolopyrimidine motif was substituted on the methyl (**1**), unsubstituted aromatic ring (**2**), with a benzyl substituent (**3**). The choice of these substituents was guided by the evaluation of the influence of: a simple methyl group, an aromatic system and a benzyl substituent allowing for the rotation of the aromatic group relative to piperazine on the affinity for the 5-HT_7 receptor. On the other hand substituting methyl by phenyl and benzyl fragments is expected to significative changing in physicochemical properties (log P, pKa) that can affect binding interactions with investigated targets.

In the next stage (set II), the aniline group was exchanged to a tryptamine moiety because of the proved activity toward 5-HT_7R [31]. Herein, our goal was to determine whether the rigidity of piperazine compared to piperidine, along with the presence of a methylene spacer, influences receptor binding. Unsatisfactory results prompted us to revisit the previously synthetized hybrid compounds containing the tryptaminotriazine core functionalized with ethyl chain arylpiperazine (Fig. 2) [31]. In set III, various arylpiperazines were tested in terms of 5-HT_7 binding. Leopoldo M. et al [35]. reported that substituted 2-biphenyl-piperazines (especially *para*-substituted) exhibited high selectivity and affinity toward the 5-HT_7 receptor with the antagonistic mode. Instead of directly attaching 2-biphenyl-piperazines to the triazine core, we chose to incorporate an ethyl linker for spacing (the direct attachment of arylpiperazine to the triazine core causes a loss of 5-HT_7R binding [31]). Since the 5-HT_7 and 5-HT_{1A} receptors share similar binding pockets and surrounding amino acid residues, we also assessed the affinity of active compounds from this set for the 5-HT_{1A} receptor as a potential off-target interaction. According our previous research [31], compounds that did not contain a long-chain arylpiperazine moiety maximally minimized the risk of affinity for serotonin receptors other than 5-HT_7, as well as the dopamine D_2 receptor. Within a new series of compounds (Fig. 3), exploration of the phenylethylamine (derivatives of compound **24** [31]) motif is justified due to the preliminary data suggesting its potential as a highly potent scaffold for affinity toward the 5-HT_7 receptor [29,31]. In set IV various phenethylamine as well as heterocyclic derivatives were tested. Another unexplored region in this set of compounds is the amine position (set V). We have established that halogens are not tolerated because of lost interaction with E7.34 and introduction of various amines (aromatic, cyclic and acyclic) was planned. Furthermore, we decided to examine the influence of other electron-donating groups (EDG) on 5-HT_7R affinity. In recent years, numerous data have shown that the incorporation of deuterium instead of the proton in the molecule may be beneficial in terms of PK improvement or toxicity reduction. For example in deutenzalutamide the introduction of a -CD_3 group achieved PK improvement and reduced the formation of metabolites associated with side effects [36]. In the current work, we tested this approach and replaced the -NH_2 group of compound **24** with an -ND_2 group to asses any binding changes as well as changes in metabolic stability. We also introduced the final structural modification (set VI) by reducing the nitrogen atom in the triazine ring, leading to the formation of pyrimidine derivatives (Fig. 3).

From each set, representative compounds with high affinity to 5-HT_7R ($K_i < 100$ nM) were chosen for AChE and BuChE screening as well as intrinsic function assessment. Subsequently, a comprehensive SAR study was performed, followed by molecular modeling analysis. Finaly the ADME-T screening panel was performed using *in vitro* conditions as well as *in vivo* on *Danio rerio*. Procognitive and memory improvement was evaluated using a mouse *in vivo* model in locomotor activity and passive avoidance tests.

2. Material and methods

2.1. Chemistry

All commercially available reagents: amines, arylpiperazines, catalysts, TLC plates, and silica gel were purchased from Chemat. Solvents used for purification were purchased from Krakchemia. Solvents for LC-MS were purchased from Thermo Scientific. ^{1}H NMR and ^{13}C NMR spectra were recorded using Bruker 400 MHz systems with TMS as an internal standard. Melting points were determined with the Böetius apparatus. Analytical thin-layer chromatography (TLC) was performed using 0.2 mm silica gel precoated aluminum sheets (60 F254, Merck) and UV light at 254 nm was used for visualization. **LC-MS chromatography, method A:** HPLC-MS analyses were performed on a Shimadzu Nexera XR system equipped with PDA (SPD-M40) and LCMS-

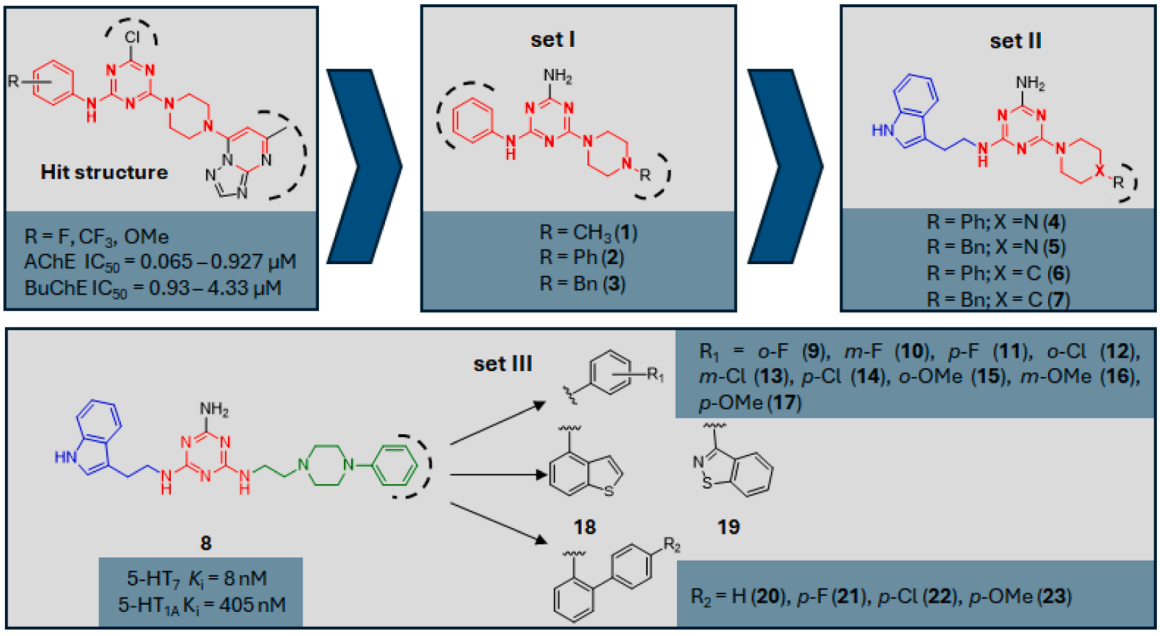

Fig. 2. Design novel 5-HT_7R ligands (set I – III) using known AChE/BuChE inhibitors. The aryl ring of parent compound **8** [31] in set III was replaced by various substituted phenyls and fused heterocycles. The dashed line indicates the structure modifications.

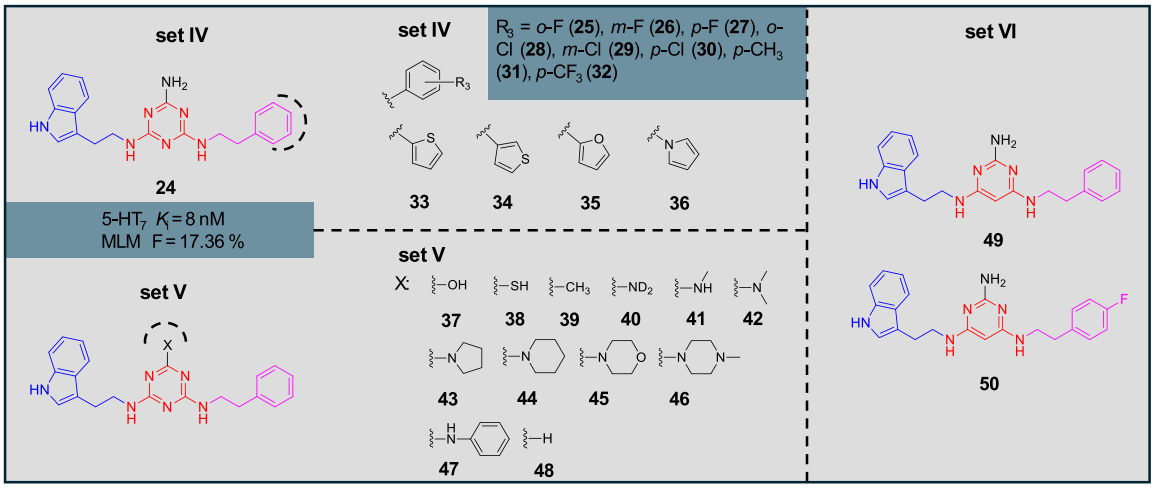

Fig. 3. Design novel 5-HT$_7$ receptor antagonists (sets IV - VI). In set IV and set V, the aryl ring of parent compound **24** was replaced by various substituted phenyls/heterocycles and various X substituents respectively. MLM – mouse liver microsomes. F – % remaining compound after 2 h of incubation with MLM. The dashed line indicates the structure modifications.

2020 detectors. Analyses were performed on a Phenomenex XB-C18 1.7 μm (50 ×2.1 mm) column (method 1 A) with a gradient of solvents as the mobile phase: Solvent A (0.01 % HCOOH in water) and B (0.01 % HCOOH in methanol); t = 0 min, 10 % of B, t = 4 min, 90 % of B, t = 6 min, 90 % of B, t = 6.1 min 10 % of B, stop time 11 min or a Phenomenex C18 1.7 μm (50 ×2.1 mm) column (method 2 A) with a gradient of solvents as the mobile phase: Solvent A (0.01 % HCOOH in water) and Solvent B (0.01 % HCOOH in MeOH): t = 0 min 5 % of B, t = 3 min 90 % of B, t = 4 min 90 % of B, t = 4.5 min 5 % of B stop time 7 min; flow rate 0.4 mL min^{-1}; UV–VIS detection was performed in a range of 240–700 nm, MS data were collected in the ESI + mode in an *m/z* range of 100–800 with a scan speed of 15000 u/s and an event time of 0.1 s. **LC-MS chromatography, method B:** UPLC-MS/MS system: Waters Acquity Premier (Waters Corporation, Milford, MA, USA) coupled to a Waters Xevo TQ-S Cronos mass spectrometer (electrospray ionization mode: ESI). Chromatographic separations were carried out using an Acquity UPLC BEH (bridged ethylene hybrid) C18 column; 2.1 × 100 mm, and 1.7 μm particle size, equipped with an Acquity UPLC BEH C18 VanGuard pre-column; 2.1 × 5 mm, and 1.7 μm particle size. The column was maintained at 40°C and eluted under gradient conditions using 95–0 % of eluent A over 10 min, subsequently 100 % of eluent B over 3 min, at a flow rate of 0.3 mL min^{-1}. Eluent A: water/formic acid (0.1 %, v/v); eluent B: acetonitrile/formic acid (0.1 %, v/v). Chromatograms were recorded using a Waters eλ PDA detector. Spectra were analyzed in the 200–700 nm range with 1.2 nm resolution and a sampling rate of 20 points/s. MS detection settings of the Waters Xevo TQ-S Cronos mass spectrometer were as follows: source temperature 150°C, desolvation temperature 350°C, desolvation gas flow rate 600 L h^{-1}, cone gas flow 100 L h^{-1}, capillary potential 3.00 kV, cone potential 30 V. Nitrogen was used as both nebulizing and drying gas. The data were obtained in a scan mode ranging from 50 to 1000 *m/z* in 0.5 s time intervals. Data acquisition software was MassLynx V 4.2 (Waters). The synthesis of final compounds was performed on a CEM Discover™ Focused Microwave System at 50 W power for all microwave-assisted reactions to obtain final compounds.

2.2. General procedure for the synthesis of final compounds 1–36

Intermediates **51** or **55** (1.5 mmol), amines **52–57**, **89–103**, **114–125** (3.75 mmol), potassium carbonate (4.5 mmol) and TBAB (0.15 mmol) were ground in a mortar and transferred to a sealed tube. For solid amines, all reagents were ground together. For liquid amines, the solid reagents were ground first, transferred to a sealed tube, and then an appropriate amount of liquid amine was added to the mixture. Subsequently, 5 wt% DMF was added. The mixture was reacted in a microwave reactor at 50 W for 2.5 minutes. Reaction progress was monitored via TLC (chloroform: MeOH 90:10 v/v). The mixture was cooled down and extracted with chloroform (3 ×20 mL). Organic layers were combined, dried over $MgSO_4$ and concentrated. The crude product was purified *via* column chromatography with elution using chloroform 100 % then chloroform: MeOH 97:3 v/v, then chloroform: MeOH 95:5 v/v, then chloroform: MeOH 93:7 v/v, then chloroform: MeOH 90:10 v/v. The colorless oil was then dissolved in acetone and pH was adjusted to 2–3 with 4 M HCl in 1,4-dioxane. The precipitating white solid was additionally crushed by the addition of cold diethyl ether. The white powder was filtered and rinsed with cold diethyl ether and then dried to yield title compounds.

Intermediates **51** and **55** were obtained according the previously published paper [37].

6-(4-methylpiperazin-1-yl)-N^2-phenyl-1,3,5-triazine-2,4-diamine hydrochloride (1)

White solid, yield 72 %, mp: 176–180 °C, ^{1}H NMR (600 MHz, DMSO) δ 11.71 (s, 1H), 10.39 (s, 1H), 7.90 (s, 2H), 7.61 (dd, *J* = 8.5, 0.9 Hz, 2H), 7.40–7.33 (m, 2H), 7.13 (t, *J* = 7.4 Hz, 1H), 4.61 (s, 2H), 3.6–3.45 (m, 4H), 3.09 (s, 2H), 2.76 (s, 3H); ^{13}C NMR (151 MHz, DMSO) δ 161.69, 160.12, 158.41, 138.07, 129.25, 124.51, 121.87, 52.00, 42.51, 41.01; UHPLC-MS analysis: t = 2.09 min (100 % purity, method B), calc. for base $C_{14}H_{19}N_7$ *m/z* = 285.35, found *m/z* = 286.23 $[M+H]^+$

N^2-phenyl-6-(4-phenylpiperazin-1-yl)-1,3,5-triazine-2,4-diamine hydrochloride (2)

Creamy solid, yield 68 %, mp: 165–168 °C; ^{1}H NMR (600 MHz, DMSO) δ 10.75 (s, 1H), 8.30 (s, 2H), 7.61 (d, *J* = 7.8 Hz, 2H), 7.39 (t, *J* = 7.9 Hz, 2H), 7.32 (t, *J* = 7.9 Hz, 2H), 7.23–7.15 (m, 3H), 6.98 (t, *J* = 7.2 Hz, 1H), 4.05 (s, 4H), 3.41–3.36 (m, 4H); ^{13}C NMR (151 MHz, DMSO) δ 157.86, 149.15, 137.53, 129.69, 129.49, 129.32, 125.07, 122.24, 122.13, 117.60, 116.71, 49.55, 43.73; UHPLC-MS analysis: t = 5.87 min (98.6 % purity, method B), calc. for base $C_{19}H_{21}N_7$ *m/z* = 347.42, found *m/z* = 348.31 $[M+H]^+$

6-(4-benzylpiperazin-1-yl)-N^2-phenyl-1,3,5-triazine-2,4-diamine hydrochloride (3)

Beige solid, yield 81 %, mp: 188–189 °C;^{1}H NMR (600 MHz, DMSO) δ 12.06 (s, 1H), 10.80 (s, 1H), 8.26 (s, 2H), 7.67 (dd, *J* = 6.0, 2.9 Hz, 2H), 7.59 (d, *J* = 7.9 Hz, 2H), 7.49–7.43 (m, 3H), 7.37 (t, *J* = 7.8 Hz, 2H), 7.14 (t, *J* = 7.3 Hz, 1H), 4.62 (s, 2H), 4.33 (s, 2H), 3.62 (s, 2H), 3.41

(s, 2H), 3.11 (s, 2H); ^{13}C NMR (151 MHz, DMSO) δ 161.42, 157.83, 137.55, 131.98, 129.98, 129.85, 129.41, 129.26, 124.83, 121.85, 59.11, 50.12, 40.90, 40.50, 40.38, 40.24, 40.10, 39.96, 39.82, 39.68, 39.55; UHPLC-MS analysis: t = 3.61 min (97.2 % purity, method B), calc. for base $C_{20}H_{23}N_7$ *m/z* = 361,44, found *m/z* = 362.26 $[M+H]^+$

N^2-(2-(1H-indol-3-yl)ethyl)-6-(4-benzylpiperazin-1-yl)-1,3,5-triazine-2,4-diamine hydrochloride (5)

White solid, yield 78 %, mp: 195–199 °C; ^{1}H NMR (600 MHz, MeOD) δ 7.63 (dd, *J* = 6.4, 2.8 Hz, 2H), 7.57–7.51 (m, 4H), 7.36 (d, *J* = 8.1 Hz, 1H), 7.11 (s, 1H), 7.08 (t, *J* = 7.5 Hz, 1H), 7.00 (t, *J* = 7.4 Hz, 1H), 4.38 (s, 2H), 3.76 (t, *J* = 6.4 Hz, 2H), 3.622—3.09 (m, 8H), 3.05 (t, *J* = 6.6 Hz, 2H); ^{13}C NMR (151 MHz, MeOD) δ 162.28, 156.81, 155.31, 136.82, 131.20, 130.02, 129.03, 128.50, 127.35, 122.68, 121.08, 118.31, 117.73, 111.28, 111.11, 60.15, 50.65, 41.22, 40.11, 24.81; UHPLC-MS analysis: t = 7.39 min (100 % purity, method A), calc. for base $C_{24}H_{28}N_8$ *m/z* = 428.53, found *m/z* = 362.26 $[M+H]^+$

N^2-(2-(1H-indol-3-yl)ethyl)-6-(4-phenylpiperidin-1-yl)-1,3,5-triazine-2,4-diamine hydrochloride (6)

White solid, yield 53 %, mp: 143–146 °C; ^{1}H NMR (400 MHz, MeOD) δ 7.57 (d, *J* = 7.8 Hz, 1H), 7.35 (d, *J* = 8.1 Hz, 1H), 7.33–7.27 (m, 2H), 7.26–7.17 (m, 3H), 7.12–7.06 (m, 1H), 6.99 (d, *J* = 7.2 Hz, 2H), 3.75 (brs, 2H), 3.08 (t, *J* = 6.9 Hz, 2H), 2.99 (brs, 2H), 2.84 (t, *J* = 12.1 Hz, 2H), 2.81 (t, *J*=11.2, 1H), 1.89 (d, *J* = 12.3 Hz, 2H), 1.62 (brs, 2H); ^{13}C NMR (101 MHz, MeOD) δ 156.40, 145.22, 136.82, 128.38, 128.16, 127.31, 126.61, 126.40, 126.07, 122.41, 121.03, 118.28, 117.66, 111.26, 110.99, 44.37, 42.32, 41.22, 32.92, 24.71. UHPLC-MS analysis: t = 11.53 min (96.6 % purity, method A), calc. for base $C_{24}H_{27}N_7$ *m/z* = 413.52, found *m/z* = 414.6 $[M+H]^+$

N^2-(2-(1H-indol-3-yl)ethyl)-6-(4-benzylpiperidin-1-yl)-1,3,5-triazine-2,4-diamine hydrochloride (7)

Beige solid, yield 59 %, mp: 124–129 °C; ^{1}H NMR (400 MHz, MeOD) δ 7.55 (d, *J* = 7.6 Hz, 1H), 7.35 (d, *J* = 8.0 Hz, 1H), 7.29 (t, *J* = 7.0 Hz, 2H), 7.19 (t, *J* = 8.3 Hz, 3H), 7.09–6.99 (m, 3H), 4.70 (brs, 2H), 3.70 (brs, 2H), 3.06 (t, *J* = 6.4 Hz, 2H), 2.84 (brs, 2H), 2.56 (d, *J* = 6.8 Hz, 2H), 1.85 (brs, 1H), 1.69 (d, *J* = 11.4 Hz, 2H), 1.13 (d, *J* = 10.6 Hz, 2H); ^{13}C NMR (101 MHz, MeOD) δ 161.18, 156.33, 139.92, 136.81, 128.84, 128.77, 127.90, 127.30, 125.66, 122.38, 121.01, 118.27, 117.65, 111.23, 110.99, 44.01, 42.29, 41.21, 37.84, 31.59, 24.68, 19.51, 12.51; UHPLC-MS analysis: t = 3.69 min (97.0 % purity, method A), calc. for base $C_{25}H_{29}N_7$ *m/z* = 427.54, found *m/z* = 428.7 $[M+H]^+$

N^2-(2-(1H-indol-3-yl)ethyl)-N^4-(2-(4-(2-fluorophenyl)piperazin-1-yl) ethyl)-1,3,5-triazine-2,4,6-triamine hydrochloride (8)

white solid, yield 64 %, mp: 163–166 °C; ^{1}H NMR (600 MHz, MeOD) δ 7.59 (dd, *J* = 14.6, 7.7 Hz, 1H), 7.36 (t, *J* = 7.3 Hz, 1H), 7.16–6.99 (m, 7H), 3.88 (brs, 2H), 3.81 (t, *J* = 6.9 Hz, 1H), 3.75 (t, *J* = 6.0 Hz, 1H), 3.66 (t, *J* = 6.0 Hz, 1H), 3.55 (brs, 2H), 3.46 (brs, 1H), 3.41–3.14 (m, 6H), 3.09 (brs, 2H); ^{13}C NMR (151 MHz, MeOD) δ 156.54, 156.27, 154.91, 138.04, 136.77, 127.28, 124.58, 123.88, 122.45, 121.05, 119.48, 118.37, 117.82, 115.90, 115.77, 111.43, 110.96, 52.45, 52.14, 41.38, 34.91, 24.86, 24.49; UHPLC-MS analysis: t = 11.95 min (97.1 % purity, method A), calc. for base $C_{25}H_{30}FN_9$ *m/z* = 475.56, found *m/z* = 476.6 $[M+H]^+$

N^2-(2-(1H-indol-3-yl)ethyl)-N^4-(2-(4-(3-fluorophenyl)piperazin-1-yl) ethyl)-1,3,5-triazine-2,4,6-triamine hydrochloride (9)

beige solid, yield 51 %, mp: 170–173 °C; ^{1}H NMR (600 MHz, MeOD) δ 7.60 (dd, *J* = 23.6, 7.8 Hz, 1H), 7.37 (t, *J* = 6.8 Hz, 1H), 7.30–7.23 (m, 1H), 7.17–7.09 (m, 2H), 7.08–7.01 (m, 1H), 6.80 (dd, *J* = 29.4, 9.4 Hz, 1H), 6.66 (dt, *J* = 16.4, 7.4 Hz, 2H), 3.87 (brs, *J* = 23.6, 16.5 Hz, 3H), 3.82 (t, *J* = 6.5 Hz, 1H), 3.74 (t, *J* = 7.1 Hz, 1H), 3.69–3.61 (m, 2H), 3.56 (d, *J* = 7.8 Hz, 1H), 3.46 (s, *J* = 5.0 Hz, 1H), 3.31–3.18 (m, 3H), 3.14–3.04 (m, 4H); ^{13}C NMR (151 MHz, MeOD) δ 164.61, 163.00, 156.28, 151.22, 136.78, 130.29, 127.29, 122.42, 121.23, 118.38, 117.80, 111.70, 110.96, 106.87, 103.02, 54.96, 51.94, 45.59, 41.31, 34.87, 24.87; UHPLC-MS analysis: t = 3.65 min (95.0 % purity, method B), calc. for base $C_{25}H_{30}FN_9$ *m/z* = 475.56, found *m/z* = 476.5 $[M+H]^+$

N^2-(2-(1H-indol-3-yl)ethyl)-N^4-(2-(4-(4-fluorophenyl)piperazin-1-yl) ethyl)-1,3,5-triazine-2,4,6-triamine hydrochloride (10)

white solid, yield 89 %, mp: 180–183 °C; ^{1}H NMR (600 MHz, MeOD) δ 7.60 (dd, *J* = 20.5, 7.8 Hz, 1H), 7.37 (d, *J* = 7.9 Hz, 1H), 7.16 (d, *J* = 11.1 Hz, 1H), 7.13–7.09 (m, 1H), 7.08–6.99 (m, 4H), 6.90 (dd, *J* = 8.8, 4.4 Hz, 1H), 3.87 (brs, 2H), 3.81 (t, *J* = 7.1 Hz, 1H), 3.74 (t, *J* = 7.1 Hz, 2H), 3.69–3.66 (m, 1H), 3.56 (brs, 1H), 3.45 (brs, 2H), 3.28 (t, *J* = 6.2 Hz, 2H), 3.18 (brs, 1H), 3.08 (dd, *J* = 14.0, 7.0 Hz, 4H); ^{13}C NMR (151 MHz, MeOD) δ 158.87, 157.28, 156.28, 146.28, 136.79, 127.31, 122.42, 121.23, 121.07, 118.72, 118.40, 117.83, 115.37, 111.48, 110.99, 52.23, 51.92, 47.01, 41.32, 34.91, 24.88; UHPLC-MS analysis: t = 4.85 min (100 % purity, method A), calc. for base $C_{25}H_{30}FN_9$ *m/z* = 475.56, found *m/z* = 476.24 $[M+H]^+$

N^2-(2-(1H-indol-3-yl)ethyl)-N^4-(2-(4-(2-chlorophenyl)piperazin-1-yl) ethyl)-1,3,5-triazine-2,4,6-triamine hydrochloride (11)

white solid, yield 76 %, mp: 163–165 °C; ^{1}H NMR (600 MHz, MeOD) δ 7.62–7.56 (m, 1H), 7.43 (brs, 1H), 7.38–7.29 (m, 2H), 7.22–7.01 (m, 5H), 3.89 (brs, 2H), 3.83–3.79 (m, 1H), 3.75 (brs, 1H), 3.68 (s, 1H), 3.61–3.46 (m, 4H), 3.42–3.34 (m, 2H), 3.26–3.18 (m, 2H), 3.17–3.06 (m, 3H); ^{13}C NMR (151 MHz, MeOD) δ 156.78, 147.29, 136.83, 130.35, 128.62, 127.82, 127.27, 124.99, 122.44, 121.17, 121.04, 120.70, 118.36, 117.81, 117.72, 110.93, 52.70, 52.38, 41.40, 41.19, 34.81, 24.44; UHPLC-MS analysis: t = 4.77 min (96 % purity, method B), calc. for base $C_{25}H_{30}ClN_9$ *m/z* = 492.02, found *m/z* = 492.27 $[M]^+$

N^2-(2-(1H-indol-3-yl)ethyl)-N^4-(2-(4-(3-chlorophenyl)piperazin-1-yl) ethyl)-1,3,5-triazine-2,4,6-triamine hydrochloride (12)

white solid, yield 45 %, mp: 172–174 °C; ^{1}H NMR (600 MHz, MeOD) δ 7.60 (dd, *J* = 25.5, 7.8 Hz, 1H), 7.39–7.31 (m, 1H), 7.25 (dt, *J* = 12.8, 8.1 Hz, 1H), 7.18–7.10 (m, 2H), 7.09–7.01 (m, 2H), 6.94 (dd, *J* = 21.4, 9.5 Hz, 2H), 3.87 (d, *J* = 4.7 Hz, 2H), 3.83 (t, *J* = 7.0 Hz, 1H), 3.75 (brs, 1H), 3.67 (t, *J* = 6.3 Hz, 1H), 3.64–3.54 (m, 2H), 3.47 (brs, *J* = 3.8 Hz, 1H), 3.33–3.18 (m, 4H), 3.12–3.06 (m, 4H); ^{13}C NMR (151 MHz, MeOD) δ 150.73, 136.80, 134.79, 130.19, 127.29, 122.38, 121.24, 121.06, 120.43, 118.52, 118.36, 117.78, 116.19, 114.54, 111.22, 110.95, 51.66, 45.84, 45.64, 41.31, 34.85, 24.86; UHPLC-MS analysis: t = 3.88 min (96.6 % purity, method A), calc. for base $C_{25}H_{30}ClN_9$ *m/z* = 492.02, found *m/z* = 492.5 $[M]^+$

N^2-(2-(1H-indol-3-yl)ethyl)-N^4-(2-(4-(4-chlorophenyl)piperazin-1-yl) ethyl)-1,3,5-triazine-2,4,6-triamine hydrochloride (13)

white solid, yield 57 %, mp: 160–163 °C; ^{1}H NMR (600 MHz, MeOD) δ 7.60 (dd, *J* = 22.5, 7.8 Hz, 1H), 7.36 (dd, *J* = 14.4, 9.1 Hz, 1H), 7.29–7.23 (m, 2H), 7.18–7.09 (m, 2H), 7.06–6.98 (m, 2H), 6.86 (d, *J* = 8.8 Hz, 1H), 3.87 (brs, 2H), 3.82 (t, *J*=7.0, 2H), 3.74 (t, *J* = 7.1 Hz, 1H), 3.69–3.67 (m, 1H), 3.57 (brs, 1H), 3.46 (brs, 2H), 3.32–3.27 (m, 2H), 3.20 (brs, 1H), 3.08 (dd, *J* = 13.8, 6.8 Hz, 4H); ^{13}C NMR (151 MHz, MeOD) δ 161.21, 158.47, 156.27, 148.14, 136.79, 128.80, 127.31, 125.86, 122.40, 121.24, 121.06, 118.38, 117.95, 111.48, 110.98, 52.03, 51.71, 46.03, 41.31, 34.89, 24.88; UHPLC-MS analysis: t = 3.86 min (96.3 % purity, method A), calc. for base $C_{25}H_{30}ClN_9$ *m/z* = 492.02, found *m/z* = 492.5 $[M]^+$

N^2-(2-(1H-indol-3-yl)ethyl)-N^4-(2-(4-(2-methoxyphenyl)piperazin-1-yl) ethyl)-1,3,5-triazine-2,4,6-triamine hydrochloride (14)

beige solid, yield 50 %, mp: 173–176 °C; ^{1}H NMR (600 MHz, MeOD)

δ 7.59 (dd, $J = 13.1$, 7.6 Hz, 1H), 7.35 (d, $J = 7.5$ Hz, 1H), 7.17–6.92 (m, 7H), 3.92–3.78 (m, 7H), 3.75 (brs, 1H), 3.67 (t, $J = 6.1$ Hz, 1H), 3.63–3.56 (m, 1H), 3.55 (t, $J = 6.0$ Hz, 1H), 3.48–3.42 (m, 2H), 3.38 (dd, $J = 6.3$, 3.3 Hz, 1H), 3.32 (t, $J = 6.1$ Hz, 1H), 3.24 (dd, $J = 15.8$, 10.3 Hz, 2H), 3.09 (t, $J = 5.9$ Hz, 2H); ^{13}C NMR (151 MHz, MeOD) δ 171.04, 152.51, 138.46, 136.78, 130.70, 127.60, 127.29, 124.54, 122.47, 121.05, 120.91, 118.94, 118.74, 117.77, 111.75, 110.96, 54.78, 52.47, 43.37, 41.41, 34.83, 24.94, 23.52; UHPLC-MS analysis: t = 4.49 min (96 % purity, method B), calc. for base $C_{26}H_{33}N_9O$ $m/z = 487.60$, found $m/z = 488$ $[M+H]^+$

N^2-(2-(1H-indol-3-yl)ethyl)-N^4-(2-(4-(3-methoxyphenyl)piperazin-1-yl) ethyl)-1,3,5-triazine-2,4,6-triamine hydrochloride (15)

white solid, yield 64 %, mp: 160–166 °C; ^{1}H NMR (400 MHz, MeOD) δ 7.59 (dd, $J = 14.3$, 7.8 Hz, 1H), 7.37 (d, $J = 7.9$ Hz, 1H), 7.23–7.02 (m, 4H), 6.65–6.48 (m, 3H), 3.94–3.80 (m, 4H), 3.78 (s, 3H), 3.74 (t, $J = 7.0$ Hz, 1H), 3.68–3.50 (m, 3H), 3.45 (brs, 1H), 3.31–2.87 (m, 7H); ^{13}C NMR (101 MHz, MeOD) δ 160.82, 156.25, 150.75, 136.76, 129.73, 127.27, 122.42, 121.20, 121.04, 118.50, 117.77, 111.42, 111.19, 110.95, 109.05, 106.11, 103.05, 54.32, 52.07, 51.76, 46.43, 41.33, 34.87, 24.87; UHPLC-MS analysis: t = 3.70 min (100 % purity, method A), calc. for base $C_{26}H_{33}N_9O$ $m/z = 487.60$, found $m/z = 488.7$ $[M+H]^+$

N^2-(2-(1H-indol-3-yl)ethyl)-N^4-(2-(4-(4-methoxyphenyl)piperazin-1-yl) ethyl)-1,3,5-triazine-2,4,6-triamine hydrochloride (16)

white solid, yield 78 %, mp: 97–100 °C; ^{1}H NMR (600 MHz, MeOD) δ 7.60 (dd, $J = 19.3$, 7.6 Hz, 1H), 7.37 (d, $J = 8.0$ Hz, 1H), 7.17–7.04 (m, 4H), 6.97–6.88 (m, 3H), 3.88 (brs, 2H), 3.84–3.80 (m, 1H), 3.77 (s, 3H), 3.75 (t, $J = 6.3$ Hz, 1H), 3.67 (t, $J = 6.0$ Hz, 1H), 3.58 (brs, 1H), 3.46 (brs, 2H), 3.36–3.22 (m, 6H), 3.12–3.07 (m, 2H); ^{13}C NMR (151 MHz, MeOD) δ 156.27, 155.92, 142.51, 136.79, 127.29, 122.42, 121.20, 121.04, 119.60, 119.33, 119.13, 118.50, 118.36, 117.79, 114.40, 111.45, 110.96, 54.63, 52.04, 43.17, 41.35, 34.93, 24.87, 23.42; UHPLC-MS analysis: t = 3.70 min (100 % purity, method A), calc. for base $C_{26}H_{33}N_9O$ $m/z = 487.60$, found $m/z = 488.4$ $[M+H]^+$

N^2-(2-(1H-indol-3-yl)ethyl)-N^4-(2-(4-(benzo[b]thiophen-4-yl)piperazin-1-yl)ethyl)-1,3,5-triazine-2,4,6-triamine hydrochloride (17)

white solid, yield 61 %, mp: 179–182 °C; ^{1}H NMR (600 MHz, MeOD) δ 7.65 (d, $J = 8.0$ Hz, 1H), 7.59 (dd, $J = 9.6$, 5.8 Hz, 2H), 7.49 (t, $J = 9.2$ Hz, 1H), 7.41–7.28 (m, 2H), 7.13–6.97 (m, 3H), 3.90 (brs, 2H), 3.81 (t, $J = 6.9$ Hz, 1H), 3.76–3.69 (m, 2H), 3.62 (d, $J = 11.5$ Hz, 2H), 3.50 (brs, 2H), 3.44 (d, $J = 12.7$ Hz, 1H), 3.39–3.27 (m, 4H), 3.19 (t, $J = 11.8$ Hz, 1H), 3.09 (brs, 2H); ^{13}C NMR (151 MHz, MeOD) δ 156.29, 146.27, 146.13, 141.41, 136.78, 134.06, 127.29, 125.77, 124.66, 122.46, 121.18, 120.98, 118.48, 117.99, 117.83, 112.50, 111.43, 111.16, 110.95, 52.77, 52.47, 48.66, 41.43, 34.99, 24.87; UHPLC-MS analysis: t = 3.94 min (96.4 % purity, method A), calc. for base $C_{27}H_{31}N_9S$ $m/z = 513.66$, found $m/z = 514.6$ $[M+H]^+$

N^2-(2-(1H-indol-3-yl)ethyl)-N^4-(2-(4-(benzo[d]isothiazol-3-yl)piperazin-1-yl)ethyl)-1,3,5-triazine-2,4,6-triamine hydrochloride (18)

white solid, yield 69 %, mp: 176–179 °C; ^{1}H NMR (600 MHz, MeOD) δ 8.05 (dd, $J = 18.6$, 7.4 Hz, 1H), 7.95 (d, $J = 8.1$ Hz, 2H), 7.58 (dd, $J = 13.2$, 6.2 Hz, 2H), 7.50–7.45 (m, 1H), 7.37–7.29 (m, 1H), 7.09–7.01 (m, 2H), 4.19 (brs, 1H), 4.01 (brs, 1H), 3.89 (brs, 3H), 3.80 (t, $J = 6.9$ Hz, 1H), 3.76 (s, 1H), 3.68 (t, $J = 6.0$ Hz, 1H), 3.63–3.43 (m, 6H), 3.08 (t, $J = 7.0$ Hz, 2H); ^{13}C NMR (151 MHz, MeOD) δ 162.10, 161.97, 156.31, 152.86, 136.76, 127.96, 127.28, 127.18, 124.40, 123.42, 122.46, 121.15, 120.41, 118.45, 117.82, 111.41, 111.14, 110.97, 51.85, 46.61, 41.37, 34.89, 24.88, 24.49; UHPLC-MS analysis: t = 3.89 min (99.3 % purity, method A), calc. for base $C_{26}H_{30}N_{10}S$ $m/z = 514.65$, found $m/z = 515.7$ $[M+1]^+$

N^2-(2-(1H-indol-3-yl)ethyl)-N^4-(2-(4-([1,1'-biphenyl]-2-yl)piperazin-1-yl) ethyl)-1,3,5-triazine-2,4,6-triamine hydrochloride (19)

white solid, yield 34 % mp: 173–178 °C; ^{1}H NMR (600 MHz, MeOD) δ 7.61 (d, $J = 6.7$ Hz, 1H), 7.55 (t, $J = 7.8$ Hz, 2H), 7.44 (dt, $J = 15.4$, 7.4 Hz, 2H), 7.37–7.30 (m, 3H), 7.26 (s, $J = 8.2$ Hz, 1H), 7.20–6.99 (m, 5H), 3.79 (s, 1H), 3.77–3.71 (m, 2H), 3.64 (d, $J = 5.9$ Hz, 1H), 3.57 (t, $J = 6.1$ Hz, 1H), 3.38 (brs, 2H), 3.28–3.18 (m, 2H), 3.10–2.80 (m, 7H); ^{13}C NMR (151 MHz, MeOD) δ 156.25, 147.99, 147.85, 140.50, 136.78, 135.43, 131.20, 128.52, 128.26, 127.26, 126.85, 123.88, 122.46, 121.16, 121.04, 118.35, 117.80, 117.67, 111.35, 111.13, 110.95, 52.46, 52.18, 41.34, 41.20, 34.83, 24.85; UHPLC-MS analysis: t = 4.19 min (94.9 % purity, method A), calc. for base $C_{31}H_{35}N_9$ $m/z = 533.67$, found $m/z = 534.7$ $[M+1]^+$

N^2-(2-(1H-indol-3-yl)ethyl)-N^4-(2-(4-(4'-fluoro-[1,1'-biphenyl]-2-yl) piperazin-1-yl)ethyl)-1,3,5-triazine-2,4,6-triamine hydrochloride (20)

white solid, yield 21 %, mp: 168–172 °C; ^{1}H NMR (600 MHz, MeOD) δ 7.63 (d, $J = 5.2$ Hz, 1H), 7.59–7.52 (m, 2H), 7.34 (dd, $J = 14.4$, 7.1 Hz, 2H), 7.26 (dd, $J = 13.3$, 7.3 Hz, 1H), 7.22–6.99 (m, 7H), 3.79 (d, $J = 16.2$ Hz, 1H), 3.77–3.70 (m, 2H), 3.67–3.54 (m, 2H), 3.39 (s, 1H), 3.24–2.84 (m, 10H); ^{13}C NMR (151 MHz, MeOD) δ 162.88, 161.26, 156.26, 148.05, 136.76, 134.47, 131.07, 130.43, 128.47, 127.26, 124.04, 122.45, 121.16, 121.05, 118.56, 118.42, 117.81, 117.69, 115.09, 111.35, 110.95, 52.43, 41.33, 41.18, 34.83, 24.83, 24.47; UHPLC-MS analysis: t = 4.32 min (99 % purity, method A), calc. for base $C_{31}H_{34}FN_9$ $m/z = 551.66$, found $m/z = 552.7$ $[M+1]^+$

N^2-(2-(1H-indol-3-yl)ethyl)-N^4-(2-(4-(4'-chloro-[1,1'-biphenyl]-2-yl) piperazin-1-yl)ethyl)-1,3,5-triazine-2,4,6-triamine hydrochloride (21)

white solid, yield 15 %, mp: 184–187 °C; ^{1}H NMR (600 MHz, MeOD) δ 7.62 (d, $J = 7.4$ Hz, 1H), 7.54 (dd, $J = 19.0$, 7.9 Hz, 2H), 7.44 (dd, $J = 31.4$, 7.3 Hz, 2H), 7.34 (dd, $J = 20.3$, 8.0 Hz, 2H), 7.25 (dd, $J = 14.1$, 7.3 Hz, 1H), 7.21–6.98 (m, 5H), 3.80 (s, 1H), 3.77–3.64 (m, 3H), 3.59 (t, $J = 6.0$ Hz, 1H), 3.40 (s, 1H), 3.25–2.83 (m, 10H); ^{13}C NMR (151 MHz, MeOD) δ 156.24, 154.81, 148.04, 139.03, 136.74, 134.16, 132.73, 131.07, 130.17, 128.71, 128.44, 127.26, 124.10, 122.46, 121.05, 118.63, 118.44, 117.71, 111.36, 111.14, 110.96, 52.39, 52.11, 41.33, 41.19, 34.83, 24.86; UHPLC-MS analysis: t = 4.71 min (99 % purity, method A), calc. for base $C_{31}H_{34}ClN_9$ $m/z = 568.11$, found $m/z = 568.6$ $[M]^+$

N^2-(2-(1H-indol-3-yl)ethyl)-N^4-(2-(4-(4'-methoxy-[1,1'-biphenyl]-2-yl) piperazin-1-yl)ethyl)-1,3,5-triazine-2,4,6-triamine hydrochloride (22)

white solid, yield 24 %, mp: 170–174 °C; ^{1}H NMR (600 MHz, MeOD) δ 7.55 (d, $J = 7.8$ Hz, 2H), 7.48 (d, $J = 8.5$ Hz, 1H), 7.37–7.27 (m, 2H), 7.22 (d, $J = 7.8$ Hz, 1H), 7.16–6.96 (m, 7H), 3.81 (dd, $J = 18.1$, 7.0 Hz, 4H), 3.73 (dt, $J = 13.6$, 6.7 Hz, 2H), 3.64 (brs, 1H), 3.57 (t, $J = 6.2$ Hz, 1H), 3.39 (brs, 2H), 3.28–3.18 (m, 2H), 3.12–2.84 (m, 7H); ^{13}C NMR (151 MHz, MeOD) δ 158.98, 156.23, 147.98, 136.76, 135.01, 132.61, 131.06, 129.60, 127.86, 127.26, 123.82, 122.49, 121.17, 121.05, 118.44, 118.20, 117.71, 113.70, 111.37, 111.15, 110.97, 54.36, 52.49, 52.22, 41.32, 41.19, 34.83, 24.85; UHPLC-MS analysis: t = 4.20 min (97 % purity, method A), calc. for base $C_{32}H_{37}N_9O$ $m/z = 563.70$, found $m/z = 564.7$ $[M+1]^+$

N^2-(2-(1H-indol-3-yl)ethyl)-N^4-(2-fluorophenethyl)-1,3,5-triazine-2,4,6-triamine hydrochloride (23)

white solid, yield 88 %, mp: 185–189 °C; ^{1}H NMR (600 MHz, MeOD) δ 7.55 (d, $J = 7.9$ Hz, 1H), 7.35 (t, $J = 7.5$ Hz, 1H), 7.31–7.16 (m, 2H), 7.13–6.90 (m, 5H), 3.73 (t, $J = 7.1$ Hz, 1H), 3.70 (t, $J = 6.5$ Hz, 1H), 3.63 (t, $J = 6.9$ Hz, 1H), 3.55 (t, $J = 7.2$ Hz, 1H), 3.05 (t, $J = 7.0$ Hz, 2H), 2.95 (t, $J = 6.3$ Hz, 1H), 2.90 (t, $J = 7.1$ Hz, 1H); ^{13}C NMR (151 MHz, MeOD) δ 162.16, 160.55, 156.01, 136.81, 131.09, 128.19, 127.34, 125.40, 123.95, 122.31, 120.98, 118.27, 117.79, 114.84, 111.42, 110.93, 41.37, 40.63, 28.58, 24.91; UHPLC-MS analysis: t = 4.91 min

(95 % purity, method B), calc. for base $C_{21}H_{22}FN_7$ $m/z = 391.44$, found $m/z = 392.6$ $[M+1]^+$

N^2-(2-(1H-indol-3-yl)ethyl)-N^4-(3-fluorophenethyl)-1,3,5-triazine-2,4,6-triamine hydrochloride (24)

white solid, yield 80 %, mp: 196–199 °C; ^{1}H NMR (600 MHz, MeOD) δ 7.55 (d, $J = 7.9$ Hz, 1H), 7.35 (dd, $J = 7.9$, 4.4 Hz, 1H), 7.31–7.28 (m, 1H), 7.13–6.90 (m, 6H), 3.74 (t, $J = 7.0$ Hz, 1H), 3.70 (t, $J = 6.7$ Hz, 1H), 3.62 (brs, 1H), 3.53 (t, $J = 7.1$ Hz, 1H), 3.06 (t, $J = 6.9$ Hz, 2H), 2.91 (t, $J = 6.9$ Hz, 1H), 2.83 (t, $J = 7.1$ Hz, 1H); ^{13}C NMR (151 MHz, MeOD) δ 163.73, 162.15, 156.07, 141.61, 136.82, 129.82, 127.33, 124.43, 122.29, 121.00, 118.29, 117.77, 115.25, 112.80, 111.42, 110.96, 41.65, 41.41, 34.73, 24.96; UHPLC-MS analysis: t = 4.88 min (98 % purity, method B), calc. for base $C_{21}H_{22}FN_7$ $m/z = 391.44$, found $m/z = 392.3$ $[M+1]^+$

N^2-(2-(1H-indol-3-yl)ethyl)-N^4-(4-fluorophenethyl)-1,3,5-triazine-2,4,6-triamine hydrochloride (25)

white solid, yield 80 %, mp: 194–196 °C; ^{1}H NMR (400 MHz, MeOD) δ 7.56 (d, $J = 7.8$ Hz, 1H), 7.36 (d, $J = 8.1$ Hz, 1H), 7.29–7.23 (m, 1H), 7.16–7.06 (m, 3H), 7.05–6.88 (m, 3H), 3.78–3.67 (m, 2H), 3.60 (t, $J = 6.9$ Hz, 1H), 3.51 (t, $J = 7.3$ Hz, 1H), 3.06 (t, $J = 6.7$ Hz, 2H), 2.87 (t, $J = 7.0$ Hz, 1H), 2.80 (t, $J = 7.3$ Hz, 1H); ^{13}C NMR (101 MHz, MeOD) δ 162.82, 159.51, 155.88, 136.80, 134.55, 130.21, 127.30, 122.24, 121.00, 118.30, 117.78, 114.76, 114.55, 111.39, 110.96, 42.07, 41.44, 34.18, 24.93; UHPLC-MS analysis: t = 6.12 min (95 % purity, method B), calc. for base $C_{21}H_{22}FN_7$ $m/z = 391.44$, found $m/z = 392.29$ $[M+1]^+$

N^2-(2-(1H-indol-3-yl)ethyl)-N^4-(2-chlorophenethyl)-1,3,5-triazine-2,4,6-triamine hydrochloride (26)

white solid, yield 68 %, mp: 104–108 °C; ^{1}H NMR (600 MHz, MeOD) δ 7.54 (d, $J = 7.9$ Hz, 1H), 7.35 (td, $J = 15.3$, 7.6 Hz, 2H), 7.25–7.05 (m, 5H), 7.04–6.92 (m, 1H), 3.74–3.68 (m, 2H), 3.64 (d, $J = 6.8$ Hz, 1H), 3.58 (t, $J = 7.1$ Hz, 1H), 3.04 (t, $J = 6.9$ Hz, 3H), 2.98 (t, $J = 7.1$ Hz, 1H); ^{13}C NMR (151 MHz, MeOD) δ 159.82, 158.83, 155.95, 136.82, 136.28, 133.80, 131.05, 129.13, 127.89, 127.34, 126.76, 122.32, 121.00, 118.29, 117.82, 110.95, 41.40, 40.19, 32.94, 24.92; UHPLC-MS analysis: t = 6.35 min (95 % purity, method B), calc. for base $C_{21}H_{22}ClN_7$ $m/z = 407.90$, found $m/z = 408.25$ $[M+1]^+$

N^2-(2-(1H-indol-3-yl)ethyl)-N^4-(3-chlorophenethyl)-1,3,5-triazine-2,4,6-triamine hydrochloride (27)

white solid, yield 56 % mp: 185–188 °C; ^{1}H NMR (600 MHz, MeOD) δ 7.55 (d, $J = 7.9$ Hz, 1H), 7.35 (dd, $J = 7.9$, 4.4 Hz, 1H), 7.30–7.25 (m, 1H), 7.22–7.17 (m, 3H), 7.08 (dd, $J = 13.5$, 9.3 Hz, 2H), 7.04–6.90 (m, 1H), 3.72 (dt, $J = 18.5$, 6.9 Hz, 2H), 3.61 (d, $J = 6.5$ Hz, 1H), 3.51 (t, $J = 7.1$ Hz, 1H), 3.05 (t, $J = 7.1$ Hz, 2H), 2.88 (t, $J = 6.9$ Hz, 1H), 2.80 (t, $J = 7.1$ Hz, 1H); ^{13}C NMR (151 MHz, MeOD) δ 159.68, 158.72, 155.88, 141.12, 136.82, 133.83, 129.62, 128.57, 127.32, 127.04, 126.17, 122.34, 121.01, 118.31, 117.77, 110.98, 41.66, 41.46, 34.68, 24.95; UHPLC-MS analysis: t = 5.14 min (96 % purity, method A), calc. for base $C_{21}H_{22}ClN_7$ $m/z = 407.90$, found $m/z = 408.4$ $[M+1]^+$

N^2-(2-(1H-indol-3-yl)ethyl)-N^4-(4-chlorophenethyl)-1,3,5-triazine-2,4,6-triamine hydrochloride (28)

white solid, yield 62 %, mp: 140–144 °C; ^{1}H NMR (600 MHz, MeOD) δ 7.56 (d, $J = 7.8$ Hz, 1H), 7.35 (t, $J = 10.4$ Hz, 1H), 7.28 (brs, 1H), 7.23 (d, $J = 7.6$ Hz, 1H), 7.17 (d, $J = 7.7$ Hz, 1H), 7.09 (dd, $J = 14.3$, 7.1 Hz, 3H), 7.05–6.91 (m, 1H), 3.72 (dt, $J = 19.0$, 6.6 Hz, 2H), 3.60 (brs, 1H), 3.51 (t, $J = 7.0$ Hz, 1H), 3.06 (t, $J = 6.9$ Hz, 2H), 2.88 (brs, 1H), 2.80 (t, $J = 7.0$ Hz, 1H); ^{13}C NMR (151 MHz, MeOD) δ 159.80, 158.96, 156.03, 137.48, 136.82, 131.83, 130.13, 128.12, 127.32, 122.36, 122.24, 121.03, 118.33, 117.80, 110.98, 41.84, 41.43, 34.37, 24.96; UHPLC-MS analysis: t = 5.10 min (95 % purity, method A), calc. for base $C_{21}H_{22}ClN_7$ $m/z = 407.90$, found $m/z = 408.5$ $[M+1]^+$

N^2-(2-(1H-indol-3-yl)ethyl)-N^4-(4-methylphenethyl)-1,3,5-triazine-2,4,6-triamine hydrochloride (29)

white solid, yield 77 %, mp: 181–185 °C; ^{1}H NMR (600 MHz, MeOD) δ 7.55 (d, $J = 7.8$ Hz, 1H), 7.36 (d, $J = 8.1$ Hz, 1H), 7.17–7.00 (m, 7H), 3.73 (t, $J = 7.2$ Hz, 1H), 3.70 (t, $J = 6.3$ Hz, 1H), 3.59 (t, $J = 6.7$ Hz, 1H), 3.53 (t, $J = 7.3$ Hz, 1H), 3.05 (t, $J = 7.1$ Hz, 2H), 2.84 (t, $J = 6.6$ Hz, 1H), 2.79 (t, $J = 7.3$ Hz, 1H), 2.30 (d, $J = 17.0$ Hz, 3H); ^{13}C NMR (151 MHz, MeOD) δ 156.07, 136.83, 135.63, 135.53, 135.39, 128.74, 128.37, 127.34, 122.34, 122.26, 121.00, 118.32, 117.81, 111.46, 110.94, 42.17, 41.48, 34.68, 24.93, 19.67; UHPLC-MS analysis: t = 5.12 min (100 % purity, method A), calc. for base $C_{22}H_{25}N_7$ $m/z = 387.48$, found $m/z = 388.6$ $[M+1]^+$

N^2-(2-(1H-indol-3-yl)ethyl)-N^4-(4-(trifluoromethyl)phenethyl)-1,3,5-triazine-2,4,6-triamine hydrochloride (30)

white solid, yield 47 %, mp: 217–220 °C; ^{1}H NMR (600 MHz, MeOD) δ 7.58 (dd, $J = 26.7$, 7.3 Hz, 2H), 7.45 (t, $J = 8.2$ Hz, 2H), 7.36 (d, $J = 8.1$ Hz, 1H), 7.30 (d, $J = 7.8$ Hz, 1H), 7.14–7.05 (m, 2H), 7.04–6.89 (m, 1H), 3.77–3.63 (m, 3H), 3.54 (t, $J = 7.2$ Hz, 1H), 3.10–3.04 (m, 2H), 2.99 (s, 1H), 2.89 (t, $J = 7.2$ Hz, 1H); ^{13}C NMR (151 MHz, MeOD) δ 156.11, 143.37, 136.82, 129.23, 129.18, 127.31, 124.90, 124.88, 123.50, 122.34, 122.22, 121.01, 118.29, 117.77, 111.44, 110.97, 41.61, 41.42, 34.83, 24.96; UHPLC-MS analysis: t = 5. 20 min (97 % purity, method A), calc. for base $C_{22}H_{25}N_7$ $m/z = 441.45$, found $m/z = 442.5$ $[M+1]^+$

N^2-(2-(1H-indol-3-yl)ethyl)-N^4-(2-(thiophen-2-yl)ethyl)-1,3,5-triazine-2,4,6-triamine hydrochloride (31)

white solid, yield 56 %, mp: 150–154 °C; ^{1}H NMR (600 MHz, MeOD) δ 7.56 (d, $J = 7.9$ Hz, 1H), 7.35 (dd, $J = 8.0$, 4.3 Hz, 1H), 7.21 (dd, $J = 18.1$, 4.9 Hz, 1H), 7.09 (dd, $J = 19.2$, 8.9 Hz, 2H), 7.04–6.96 (m, 1H), 6.96–6.80 (m, 2H), 3.77–3.68 (m, 2H), 3.64 (t, $J = 6.7$ Hz, 1H), 3.56 (t, $J = 7.0$ Hz, 1H), 3.12 (t, $J = 6.4$ Hz, 1H), 3.06 (dd, $J = 11.5$, 6.7 Hz, 3H); ^{13}C NMR (151 MHz, MeOD) δ 156.08, 140.71, 140.56, 136.81, 127.33, 126.54, 125.18, 123.55, 123.47, 122.35, 120.99, 118.30, 117.82, 111.42, 110.94, 42.17, 41.46, 29.05, 24.95; UHPLC-MS analysis: t = 4. 86 min (97 % purity, method A), calc. for base $C_{19}H_{21}N_7S$ $m/z = 379.48$, found $m/z = 380.2$ $[M+1]^+$

N^2-(2-(1H-indol-3-yl)ethyl)-N^4-(2-(thiophen-3-yl)ethyl)-1,3,5-triazine-2,4,6-triamine hydrochloride (32)

white solid, yield 56 %, mp: 162–164 °C; ^{1}H NMR (600 MHz, MeOD) δ 7.56 (d, $J = 7.8$ Hz, 1H), 7.37–7.28 (m, 2H), 7.13–7.09 (m, 2H), 7.05 (m, 2H), 6.96 (dd, $J = 10.1$, 5.8 Hz, 1H), 3.72 (dt, $J = 20.0$, 6.9 Hz, 2H), 3.63 (t, $J = 6.7$ Hz, 1H), 3.56 (t, $J = 7.1$ Hz, 1H), 3.06 (t, $J = 7.0$ Hz, 2H), 2.93 (t, $J = 6.9$ Hz, 1H), 2.88 (t, $J = 7.1$ Hz, 1H); ^{13}C NMR (151 MHz, MeOD) δ 156.07, 138.89, 136.83, 127.83, 127.34, 125.30, 125.22, 122.29, 121.08, 121.02, 118.32, 117.79, 111.46, 111.21, 110.96, 41.46, 41.31, 29.40, 24.96; UHPLC-MS analysis: t = 4. 88 min (95 % purity, method A), calc. for base $C_{19}H_{21}N_7S$ $m/z = 379.48$, found $m/z = 380.5$ $[M+1]^+$

N^2-(2-(1H-indol-3-yl)ethyl)-N^4-(2-(furan-2-yl)ethyl)-1,3,5-triazine-2,4,6-triamine hydrochloride (33)

white solid, yield 78 %, mp: 138–140 °C; ^{1}H NMR (600 MHz, MeOD) δ 7.56 (t, $J = 7.4$ Hz, 1H), 7.36 (t, $J = 11.5$ Hz, 2H), 7.10 (dd, $J = 13.8$, 6.2 Hz, 2H), 7.00 (dt, $J = 26.4$, 7.4 Hz, 1H), 6.30 (d, $J = 10.4$ Hz, 1H), 6.14–6.07 (m, 1H), 3.72 (dt, $J = 18.5$, 6.7 Hz, 2H), 3.65 (t, $J = 6.7$ Hz, 1H), 3.58 (t, $J = 6.9$ Hz, 1H), 3.06 (t, $J = 7.0$ Hz, 2H), 2.93 (t, $J = 6.5$ Hz, 1H), 2.88 (t, $J = 6.9$ Hz, 1H); ^{13}C NMR (151 MHz, MeOD) δ 156.07, 152.67, 152.51, 141.35, 136.81, 127.33, 122.35, 120.99, 118.29,

117.80, 111.43, 111.18, 110.94, 109.89, 106.01, 41.45, 39.35, 27.40, 24.95; UHPLC-MS analysis: t = 4. 70 min (96 % purity, method A), calc. for base $C_{19}H_{21}N_7O$ *m/z* = 363.42, found *m/z* = 364.5 $[M+1]^+$

N^2-(2-(1H-indol-3-yl)ethyl)-N^4-(2-(1H-pyrrol-1-yl)ethyl)-1,3,5-triazine-2,4,6-triamine hydrochloride (34)

white solid, yield 78 %, mp: 143–147 °C; ^{1}H NMR (600 MHz, MeOD) δ 7.57 (t, *J* = 9.2 Hz, 1H), 7.35 (dd, *J* = 8.0, 2.0 Hz, 1H), 7.10 (dd, *J* = 8.9, 5.8 Hz, 2H), 7.02 (dd, *J* = 17.2, 7.6 Hz, 1H), 6.70 (s, 1H), 6.61 (s, 1H), 6.04 (d, *J* = 21.8 Hz, 2H), 4.09 (s, 1H), 3.97 (t, *J* = 6.0 Hz, 1H), 3.76–3.66 (m, 3H), 3.56 (t, *J* = 5.9 Hz, 1H), 3.05 (t, *J* = 7.0 Hz, 2H); ^{13}C NMR (151 MHz, MeOD) δ 156.10, 136.82, 127.34, 122.36, 121.03, 120.45, 120.39, 118.32, 117.79, 111.46, 111.00, 110.94, 107.87, 107.76, 107.57, 41.87, 41.41, 24.95, 24.44; UHPLC-MS analysis: t = 4. 70 min (96 % purity, method A), calc. for base $C_{19}H_{22}N_8$ *m/z* = 362.43, found *m/z* = 363.2 $[M+1]^+$

Synthesis of 4-((2-(1H-indol-3-yl)ethyl)amino)-6-(phenethylamino)-1,3,5-triazin-2-ol hydrochloride (35)

0.4 g (1.02 mmol) of intermediate **132** was dissolved in a mixture of dioxane (25 mL) and water (5 mL), and then 0.29 g (5.1 mmol) of KOH, ground in a mortar, was added. The resulting solution was refluxed for 3 days. When the reaction was completed, the mixture was cooled and 1 M HCl was added. Ethyl acetate was added to the partially precipitated solid to complete product precipitation. The precipitate was filtered, dissolved in hot acetone, and then filtered. The filtrate was cooled, and 4 M HCl in dioxane was added until the pH reached 2–3. Cold diethyl ether was added to the resulting solution to precipitate product **37** as a hydrochloride salt.

The synthesis of intermediate **132** is described in Supporting Information.

white solid, yield 79 %, mp: 105–109 °C; ^{1}H NMR (600 MHz, MeOD) δ 7.56 (d, *J* = 7.9 Hz, 1H), 7.36 (d, *J* = 8.1 Hz, 1H), 7.25 (t, *J* = 7.2 Hz, 2H), 7.22–7.17 (m, 3H), 7.12–7.07 (m, 2H), 6.95 (t, *J* = 7.4 Hz, 1H), 3.79 (t, *J* = 7.0 Hz, 2H), 3.54 (t, *J* = 7.3 Hz, 2H), 3.09 (t, *J* = 6.9 Hz, 2H), 2.85 (t, *J* = 7.3 Hz, 2H); ^{13}C NMR (151 MHz, MeOD) δ 156.45, 156.33, 147.73, 138.19, 136.85, 128.55, 128.25, 127.25, 126.26, 122.50, 121.11, 118.44, 117.72, 111.02, 110.98, 42.53, 42.09, 34.75, 24.75; UHPLC-MS analysis: t = 4. 40 min (97 % purity, method A), calc. for base $C_{21}H_{22}N_6O$ *m/z* = 374.44, found *m/z* = 375.3 $[M+1]^+$

Synthesis of 4-((2-(1H-indol-3-yl)ethyl)amino)-6-(phenethylamino)-1,3,5-triazine-2-thiol hydrochloride (36)

0.2 g (0.51 mmol) of intermediate **132** was dissolved in 8 mL of dioxane, and then 0.04 g (0.53 mmol) of thiourea was added. The resulting solution was heated at the boiling point of the solvent for 5 hours. When the reaction was completed, the mixture was cooled and 1 M HCl was added. Ethyl acetate was added to the partially precipitated solid to complete product precipitation. The precipitate was filtered, dissolved in hot acetone, and then filtered. The filtrate was cooled, and 4 M HCl in dioxane was added until the pH reached 2–3. Cold diethyl ether was added to the resulting solution to precipitate the white product as a hydrochloride salt.

white solid, yield 62 %, mp: 117–120 °C; ^{1}H NMR (600 MHz, MeOD) δ 7.57 (d, *J* = 7.9 Hz, 1H), 7.36 (d, *J* = 8.2 Hz, 1H), 7.28 (t, *J* = 7.3 Hz, 2H), 7.21 (dd, *J* = 17.0, 7.2 Hz, 3H), 7.13–7.09 (m, 2H), 6.98 (t, *J* = 7.5 Hz, 1H), 3.82 (t, *J* = 6.9 Hz, 2H), 3.55 (t, *J* = 7.2 Hz, 2H), 3.11 (t, *J* = 6.9 Hz, 2H), 2.86 (t, *J* = 7.2 Hz, 2H); ^{13}C NMR (151 MHz, MeOD) δ 174.28, 153.81, 138.04, 136.90, 128.54, 128.29, 127.21, 126.35, 122.54, 121.18, 118.48, 117.67, 113.63, 111.03, 110.86, 42.43, 42.05, 34.60, 24.66; UHPLC-MS analysis: t = 4. 91 min (95 % purity, method A), calc. for base $C_{21}H_{22}N_6S$ *m/z* = 390.50, found *m/z* = 391.3 $[M+1]$

Synthesis of N^2-(2-(1H-indol-3-yl)ethyl)-6-methyl-N^4-phenethyl-1,3,5-triazine-2,4-diamine hydrochloride (37)

0.2 g (0.70 mmol) of intermediate **141**, 0.21 g (1.75 mmol) of 2-phenylethylamine **129**, 0.29 g (2.1 mmol) of potassium carbonate (4.5 mmol) and 0.02 g (0.07 mmol) of TBAB was ground in a mortar and transferred to a sealed tube. Subsequently, 5 wt% DMF was added. The mixture was reacted in a microwave reactor at 50 W for 2.5 minutes. Reaction progress was monitored *via* TLC (chloroform: MeOH 90:10 v/v). The mixture was cooled down and extracted with chloroform (3 ×20 mL). Organic layers were combined, dried over $MgSO_4$ and concentrated. The crude product was purified via column chromatography with elution using chloroform 100 %, then chloroform: MeOH 97:3 v/v, then chloroform: MeOH 95:5 v/v, then chloroform: MeOH 93:7 v/v, then chloroform: MeOH 90:10 v/v. The colorless oil was then dissolved in acetone and pH was adjusted to 2–3 with 4 M HCl in 1,4-dioxane. The precipitating white solid was additionally crushed by the addition of cold diethyl ether. The white powder was filtered and rinsed with cold diethyl ether and then dried to yield the title compound.

The synthesis of intermediate **141** is described in Supporting Information.

white solid, yield 51 %, mp: 83–86 °C; ^{1}H NMR (600 MHz, MeOD) δ 7.56 (d, *J* = 7.9 Hz, 1H), 7.35 (d, *J* = 8.1 Hz, 1H), 7.24–7.20 (m, 2H), 7.17 (t, *J* = 8.5 Hz, 3H), 7.13–7.06 (m, 2H), 6.93 (t, *J* = 7.4 Hz, 1H), 3.76 (t, *J* = 7.1 Hz, 2H), 3.53 (t, *J* = 7.4 Hz, 2H), 3.07 (t, *J* = 7.1 Hz, 2H), 2.84 (t, *J* = 7.4 Hz, 2H), 2.28 (s, 3H); ^{13}C NMR (151 MHz, MeOD) δ 164.81, 158.68, 138.43, 136.80, 128.60, 128.51, 128.17, 127.27, 126.14, 122.41, 121.04, 118.36, 117.77, 111.22, 111.00, 42.16, 41.61, 34.61, 24.64, 19.78; UHPLC-MS analysis: t = 4. 60 min (98 % purity, method A), calc. for base $C_{22}H_{24}N_6$ *m/z* = 372.47, found *m/z* = 373.4 $[M+1]^+$

2.3. General procedure for the synthesis of final compounds 40–45

0.25 g (0.64 mmol) of intermediate **132**, 1.59 mmol of amines: **133**, **134**, **135**, **136**, **137** and **138**, 0.26 g (1.92 mmol) of potassium carbonate and 0.02 g (0.064 mmol) of TBAB (0.15 mmol) was ground in a mortar and transferred to a sealed tube. Subsequently, 5 wt% DMF was added. The mixture was reacted in a microwave reactor at 50 W for 2.5 minutes. Reaction progress was monitored via TLC (chloroform: MeOH 90:10 v/v). The mixture was cooled down and extracted with chloroform (3 ×20 mL). Organic layers were combined, dried over $MgSO_4$ and concentrated. The crude product was purified *via* column chromatography with elution using chloroform 100 %, then chloroform: MeOH 97:3 v/v, then chloroform: MeOH 95:5 v/v, then chloroform: MeOH 93:7 v/v, then chloroform: MeOH 90:10 v/v. The colorless oil was then dissolved in acetone and pH was adjusted to 2–3 with 4 M HCl in 1,4-dioxane. The precipitating white solid was additionally crushed by the addition of cold diethyl ether. The white powder was filtered and rinsed with cold diethyl ether and then dried to yield title compounds.

N^2-(2-(1H-indol-3-yl)ethyl)-N^4-phenethyl-1,3,5-triazine-2,4,6-triamine-d2 hydrochloride (38)

white solid, yield 93 %, mp: 193–198 °C; ^{1}H NMR (600 MHz, MeOD) δ 7.56 (d, *J* = 7.8 Hz, 1H), 7.36 (d, *J* = 8.1 Hz, 1H), 7.29 (d, *J* = 7.2 Hz, 1H), 7.26–7.15 (m, 4H), 7.10 (dd, *J* = 15.4, 8.7 Hz, 2H), 7.05–6.92 (m, 1H), 3.74 (t, *J* = 7.1 Hz, 1H), 3.70 (t, *J* = 6.5 Hz, 1H), 3.61 (t, *J* = 6.5 Hz, 1H), 3.55 (t, *J* = 7.2 Hz, 1H), 3.06 (brs, 2H), 2.89 (t, *J* = 6.7 Hz, 1H), 2.84 (t, *J* = 7.2 Hz, 1H); 13 C NMR (151 MHz, MeOD) δ 156.07, 138.69, 136.82, 128.50, 128.14, 127.33, 126.15, 126.05, 122.35, 122.26, 121.00, 118.32, 117.80, 111.44, 110.95, 42.07, 41.45, 35.10, 24.96; UHPLC-MS analysis: t = 6.24 min (100 % purity, method B), calc. for base $C_{21}H_{21}D_2N_7$ *m/z* = 375.47, found *m/z* = 375.25 $[M]^+$

N^2-(2-(1H-indol-3-yl)ethyl)-N^4-methyl-N^6-phenethyl-1,3,5-triazine-2,4,6-triamine hydrochloride (39)

white solid, yield 68 %, mp: 89–90 °C; ^{1}H NMR (600 MHz, MeOD) δ 7.55 (d, *J* = 7.5 Hz, 1H), 7.35 (d, *J* = 8.1 Hz, 1H), 7.32–7.16 (m, 5H),

7.10 (dd, $J = 12.8$, 7.6 Hz, 2H), 7.04–6.92 (m, 1H), 3.78–3.55 (m, 4H), 3.06 (d, $J = 7.0$ Hz, 2H), 2.97–2.83 (m, 5H); ^{13}C NMR (151 MHz, MeOD) δ 154.85, 154.09, 138.51, 136.82, 128.48, 128.17, 127.31, 126.15, 126.05, 122.37, 121.02, 118.32, 117.79, 111.15, 110.94, 41.61, 34.74, 26.20, 24.48, 19.51; UHPLC-MS analysis: t = 4.45 min (97 % purity, method A), calc. for base $C_{22}H_{25}N_7$ *m/z* = 387.48, found *m/z* = 388.4 $[M+1]^+$

N^2-(2-(1H-indol-3-yl)ethyl)-N^4,N^4-dimethyl-N^6-phenethyl-1,3,5-triazine-2,4,6-triamine hydrochloride (40)

white solid, yield 70 %, mp: 224–227 °C; ^{1}H NMR (600 MHz, MeOD) δ 7.56 (s, 1H), 7.39–6.90 (m, 9H), 3.74 (s, 2H), 3.64 (s, 2H), 3.23–3.00 (m, 8H), 2.91 (s, 2H); ^{13}C NMR (151 MHz, MeOD) δ 162.23, 154.20, 138.62, 136.85, 128.49, 128.22, 127.35, 126.17, 122.38, 121.01, 118.27, 117.80, 117.71, 111.28, 110.96, 41.82, 41.21, 35.70, 34.75, 24.60; UHPLC-MS analysis: t = 11.33 min (97 % purity, method A), calc. for base $C_{23}H_{27}N_7$ *m/z* = 401.51, found *m/z* = 402.6 $[M+1]^+$

N^2-(2-(1H-indol-3-yl)ethyl)-N^4-phenethyl-6-(pyrrolidin-1-yl)-1,3,5-triazine-2,4-diamine hydrochloride (41)

white solid, yield 77 %, mp: 199–204 °C;^{1}H NMR (600 MHz, MeOD) δ 7.57 (d, $J = 7.8$ Hz, 1H), 7.35 (dd, $J = 7.4$, 4.6 Hz, 1H), 7.29 (d, $J = 6.5$ Hz, 2H), 7.26–7.17 (m, 3H), 7.13–7.06 (m, 2H), 7.04–6.92 (m, 1H), 3.72 (brs, 2H), 3.64–3.54 (m, 3H), 3.47 (brs, 3H), 3.06 (brs, 2H), 2.88 (dt, $J = 14.6$, 7.1 Hz, 2H), 1.94 (brs, 4H); ^{13}C NMR (151 MHz, MeOD) δ 159.93, 154.16, 151.65, 138.68, 136.84, 128.48, 128.17, 127.29, 126.14, 122.40, 121.01, 118.31, 117.81, 111.35, 110.95, 46.59, 41.81, 41.12, 34.77, 24.75, 24.57; UHPLC-MS analysis: t = 12.67 min (99 % purity, method A), calc. for base $C_{25}H_{29}N_7$ *m/z* = 427.54, found *m/z* = 428.6 $[M+1]^+$

N^2-(2-(1H-indol-3-yl)ethyl)-N^4-phenethyl-6-(piperidin-1-yl)-1,3,5-triazine-2,4-diamine hydrochloride (42)

white solid, yield 59 %, mp: 173–179 °C; ^{1}H NMR (400 MHz, MeOD) δ 7.55 (d, $J = 7.8$ Hz, 1H), 7.35 (d, $J = 8.1$ Hz, 1H), 7.33–7.27 (m, 2H), 7.26–7.19 (m, 3H), 7.10 (t, $J = 7.2$ Hz, 2H), 7.01 (t, $J = 7.4$ Hz, 1H), 3.81 (d, $J = 15.6$ Hz, 3H), 3.72 (t, $J = 6.9$ Hz, 2H), 3.64 (t, $J = 6.8$ Hz, 3H), 3.06 (t, $J = 6.9$ Hz, 2H), 2.90 (t, $J = 7.1$ Hz, 2H), 1.72 (d, $J = 4.7$ Hz, 2H), 1.61 (brs, 4H); ^{13}C NMR (101 MHz, MeOD) δ 160.75, 154.57, 138.61, 136.82, 128.46, 128.21, 127.32, 126.17, 122.35, 121.01, 118.26, 117.80, 117.65, 111.24, 110.97, 44.91, 41.77, 41.22, 34.78, 25.54, 24.62, 24.01; UHPLC-MS analysis: t = 12.67 min (99 % purity, method A), calc. for base $C_{26}H_{31}N_7$ *m/z* = 441.57, found *m/z* = 428.6 $[M+1]^+$

N^2-(2-(1H-indol-3-yl)ethyl)-6-morpholino-N^4-phenethyl-1,3,5-triazine-2,4-diamine hydrochloride (43)

white solid, yield 86 %, mp: 213–216 °C; ^{1}H NMR (600 MHz, MeOD) δ 7.56 (brs, 1H), 7.4–7.2 (m, 6H), 7.11 (brs, 2H), 7.02 (s, 1H), 3.85–3.60 (m, 12H), 3.06 (brs, 2H), 2.90 (brs, 2H); ^{13}C NMR (151 MHz, MeOD) δ 161.49, 154.86, 154.76, 138.59, 136.86, 128.51, 128.24, 127.36, 126.22, 122.44, 121.07, 118.29, 117.68, 111.31, 111.01, 66.11, 44.14, 41.76, 41.21, 34.81, 24.74; UHPLC-MS analysis: t = 4.64 min (100 % purity, method A), calc. for base $C_{25}H_{29}N_7O$ *m/z* = 443.54, found *m/z* = 444.5 $[M+1]^+$

Synthesis of N^2-(2-(1H-indol-3-yl)ethyl)-6-(4-methylpiperazin-1-yl)-N^4-phenethyl-1,3,5-triazine-2,4-diamine hydrochloride (44)

0.25 g (0.81 mol) of intermediate **128** was dissolved in 15 mL of THF and the mixture was cooled to approximately 10–15°C. Subsequently, 0.21 mL (1.22 mmol) of DIPEA was added, followed by 0.22 mL (2.02 mmol) of *N*-methylpiperazine **130**. The resulting mixture was stirred at room temperature for 12 hours. When the reaction was completed, the DIPEA hydrochloride precipitate was filtered off, and 0.35 mL (2.02 mmol) of fresh DIPEA and 0.25 g (2.02 mmol) of 2-phenylethylamine **129** was added to the filtrate containing intermediate **131**. The mixture was then heated under reflux for further 60 hours. Reaction progress was monitored *via* TLC (chloroform: MeOH 90:10 v/v). The mixture was cooled down and extracted with chloroform (3 ×20 mL). Organic layers were combined, dried over $MgSO_4$ and concentrated. The crude product was purified via column chromatography with elution using chloroform 100 %, then chloroform: MeOH 97:3 v/v, then chloroform: MeOH 95:5 v/v, then chloroform: MeOH 93:7 v/v, then chloroform: MeOH 90:10 v/v. The colorless oil was then dissolved in acetone and pH was adjusted to 2–3 with 4 M HCl in 1,4-dioxane. The precipitating white solid was additionally crushed by the addition of cold diethyl ether. The white powder was filtered and rinsed with cold diethyl ether and then dried to yield title compounds.

The synthesis of intermediate **128** is described in the patent application [38].

white solid, yield 52 %, mp: 184–187 °C; ^{1}H NMR (600 MHz, MeOD) δ 7.56 (d, $J = 7.8$ Hz, 1H), 7.38 (d, $J = 8.1$ Hz, 1H), 7.32–7.29 (m, 2H), 7.23 (dd, $J = 15.1$, 7.4 Hz, 3H), 7.12 (t, $J = 7.4$ Hz, 2H), 7.03 (t, $J = 7.4$ Hz, 1H), 3.77 (t, $J = 6.5$ Hz, 2H), 3.66 (s, 2H), 3.60–3.12 (m, 8H), 3.06 (t, $J = 6.5$ Hz, 2H), 2.94 (s, 3H), 2.90 (t, $J = 7.0$ Hz, 2H); ^{13}C NMR (151 MHz, MeOD) δ 161.85, 155.10, 154.98, 138.53, 136.83, 128.55, 128.25, 127.36, 126.25, 122.65, 121.10, 118.35, 117.72, 111.25, 111.09, 52.52, 42.26, 41.92, 41.26, 40.48, 34.76, 24.79; UHPLC-MS analysis: t = 4.64 min (98 % purity, method A), calc. for base $C_{26}H_{32}N_8$ *m/z* = 456.59, found *m/z* = 457.5 $[M+1]^+$

Synthesis of N^2-(2-(1H-indol-3-yl)ethyl)-N^4-phenethyl-N^6-phenyl-1,3,5-triazine-2,4,6-triamine hydrochloride (45)

0.25 g (0.64 mmol) of intermediate **132**, 0.15 mL (1.59 mmol) of aniline **139**, 0.26 g (1.92 mmol) of potassium carbonate and 0.02 g (0.064 mmol) of TBAB (0.15 mmol) was ground in a mortar and transferred to a sealed tube. Subsequently, 5 wt% DMF was added. The mixture was reacted in a microwave reactor at 50 W for 2.5 minutes. Reaction progress was monitored *via* TLC (chloroform: MeOH 90:10 v/v). The mixture was cooled down and extracted with chloroform (3 ×20 mL). Organic layers were combined, dried over $MgSO_4$ and concentrated. The crude product was purified *via* column chromatography with elution using chloroform 100 %, then chloroform: MeOH 97:3 v/v, then chloroform: MeOH 95:5 v/v, then chloroform: MeOH 93:7 v/v, then chloroform: MeOH 90:10 v/v. The colorless oil was then dissolved in acetone and pH was adjusted to 2–3 with 4 M HCl in 1,4-dioxane. The precipitating white solid was additionally crushed by the addition of cold diethyl ether. The white powder was filtered and rinsed with cold diethyl ether and then dried to yield the title compound.

beige solid, yield 58 %, mp: 64–66 °C; ^{1}H NMR (600 MHz, MeOD) δ 7.68 (brs, 2H), 7.59 (d, $J = 7.7$ Hz, 1H), 7.34 (d, $J = 8.1$ Hz, 1H), 7.32–7.14 (m, 8H), 7.12–7.05 (m, 2H), 7.03–6.96 (m, 2H), 3.70 (brs, 2H), 3.59 (brs, 2H), 3.04 (brs, 2H), 2.87 (t, $J = 7.0$ Hz, 2H); ^{13}C NMR (151 MHz, MeOD) δ 165.48, 162.36, 139.86, 139.48, 136.80, 128.49, 128.37, 128.16, 128.04, 127.47, 125.80, 122.06, 121.94, 120.89, 119.95, 118.20, 118.06, 112.15, 110.80, 41.98, 41.12, 35.74, 25.38; UHPLC-MS analysis: t = 4.64 min (98 % purity, method A), calc. for base $C_{27}H_{27}N_7$ *m/z* = 449.55, found *m/z* = 450.5 $[M+1]^+$

Synthesis of N^2-(2-(1H-indol-3-yl)ethyl)-N^4-phenethyl-1,3,5-triazine-2,4-diamine hydrochloride (46)

0.4 g (1.01 mmol) of intermediate **132** was dissolved in a mixture of THF (8 mL) and methanol (8 mL), and 0.35 mL (2.02 mmol) of DIPEA and 0.11 g (1.01 mmol) of Pd/C was added. The mixture was stirred at room temperature under hydrogen atmosphere (balloon) for 24 hours. When the reaction was completed, the palladium was filtered off, and the filtrate was concentrated. The crude product was purified via column chromatography with elution using chloroform 100 %, then chloroform: MeOH 97:3 v/v, then chloroform: MeOH 95:5 v/v, then

chloroform: MeOH 93:7 v/v, then chloroform: MeOH 90:10 v/v. The colorless oil was then dissolved in acetone and pH was adjusted to 2–3 with 4 M HCl in 1,4-dioxane. The precipitating white solid was additionally crushed by the addition of cold diethyl ether. The white powder was filtered and rinsed with cold diethyl ether and then dried to yield the title compound.

beige solid, yield 60 %, mp: 110–112 °C; ^{1}H NMR (600 MHz, MeOD) δ 7.56 (d, J = 7.9 Hz, 1H), 7.35 (d, J = 8.1 Hz, 1H), 7.25–7.21 (m, 2H), 7.18 (t, J = 8.9 Hz, 3H), 7.11–7.06 (m, 2H), 6.94 (t, J = 7.4 Hz, 1H), 3.78 (t, J = 7.1 Hz, 2H), 3.54 (t, J = 7.3 Hz, 2H), 3.09 (t, J = 7.1 Hz, 2H), 2.85 (t, J = 7.3 Hz, 2H); ^{13}C NMR (151 MHz, MeOD) δ 154.35, 138.39, 136.82, 128.57, 128.53, 128.19, 127.28, 126.18, 122.40, 121.06, 118.40, 117.74, 111.19, 111.00, 110.96, 42.11, 41.60, 34.49, 24.54; UHPLC-MS analysis: t = 4.88 min (99 % purity, method A), calc. for base $C_{21}H_{22}N_6$ m/z = 358.44, found m/z = 359.3 $[M+1]^+$

2.4. General procedure for the synthesis of final compounds 49, 50

0.25 g (0.87 mmol) of intermediate **143**, 2.18 mmol of amines: **129** or **116**, 0.36 g (2.61 mmol) of potassium carbonate and 0.03 g (0.087 mmol) of TBAB (0.15 mmol) was ground in a mortar and transferred to a sealed tube. Subsequently, 5 wt% DMF was added. The mixture was reacted in a microwave reactor at 50 W for 40 minutes. Subsequently, another portion of amines (2.18 mmol) was added and the mixture was reacted in a microwave reactor at 50 W for 40 minutes again. Reaction progress was monitored *via* TLC (chloroform: MeOH 90:10 v/v). The mixture was cooled down and extracted with chloroform (3 ×20 mL). Organic layers were combined, dried over $MgSO_4$ and concentrated. The crude product was purified *via* column chromatography with elution using chloroform 100 %, then chloroform: MeOH 97:3 v/v, then chloroform: MeOH 95:5 v/v, then chloroform: MeOH 93:7 v/v, then chloroform: MeOH 90:10 v/v. The colorless oil was then dissolved in acetone and pH was adjusted to 2–3 with 4 M HCl in 1,4-dioxane. The precipitating white solid was additionally crushed by the addition of cold diethyl ether. The white powder was filtered and rinsed with cold diethyl ether and then dried to yield title compounds.

The synthesis of intermediate **143** is described in Supporting Information.

N^4-(2-(1H-indol-3-yl)ethyl)-N^6-phenethylpyrimidine-2,4,6-triamine hydrochloride (47)

white solid, yield 57 %, mp: 104–109 °C, ^{1}H NMR (600 MHz, MeOD) δ 7.57 (d, J = 7.9 Hz, 1H), 7.36 (d, J = 8.1 Hz, 1H), 7.30 (t, J = 7.5 Hz, 2H), 7.25–7.19 (m, 3H), 7.12 (s, 1H), 7.09 (t, J = 7.3 Hz, 2H), 3.56 (t, J = 6.6 Hz, 2H), 3.38 (brs, 2H), 3.06 (t, J = 6.9 Hz, 2H), 2.85 (t, J = 7.0 Hz, 2H); ^{13}C NMR (151 MHz, MeOD) δ 157.94, 153.57, 138.51, 136.84, 128.52, 128.40, 128.21, 127.26, 126.20, 122.61, 121.10, 118.43, 117.73, 111.13, 111.01, 70.43, 42.66, 42.20, 34.70, 24.63; UHPLC-MS analysis: t = 4.58 min (100 % purity, method A), calc. for base $C_{22}H_{24}N_6$ m/z = 372.47, found m/z = 373.2 $[M+1]^+$

N^4-(2-(1H-indol-3-yl)ethyl)-N^6-(4-fluorophenethyl)pyrimidine-2,4,6-triamine (48)

white solid, yield 65 %, mp: 112–114 °C; ^{1}H NMR (600 MHz, MeOD) δ 7.57 (d, J = 7.8 Hz, 1H), 7.36 (d, J = 8.1 Hz, 1H), 7.27–7.22 (m, 2H), 7.13 (s, 1H), 7.09 (t, J = 7.5 Hz, 1H), 7.04–7.00 (m, 3H), 3.57 (t, J = 6.0 Hz, 2H), 3.33 (s, 2H), 3.06 (t, J = 6.7 Hz, 2H), 2.83 (d, J = 5.9 Hz, 2H); ^{13}C NMR (151 MHz, MeOD) δ 162.55, 160.94, 153.21, 136.82, 134.44, 130.29, 130.24, 127.24, 122.67, 121.10, 118.44, 117.73, 114.84, 114.70, 111.03, 70.33, 42.66, 42.27, 33.80, 24.61; UHPLC-MS analysis: t = 6.10 min (97 % purity, method B), calc. for base $C_{22}H_{23}FN_6$ m/z = 390.46, found m/z = 391.33 $[M+1]^+$

2.5. Receptor binding

Cell cultures (HEK293 for 5-HT_7 and 5-HT_{1A} receptors) and cell membranes were prepared, and radioligand binding assays ([^{3}H]-8-OH-DPAT for 5-HT_{1A}R and [^{3}H]-5-CT for 5-HT_7R) were performed in accordance with standard protocols [41].

2.6. Functional assay

Functional assays were performed according to our previous paper [31].

2.7. Cholinesterase activity

The target compounds were tested for their inhibitory potency against cholinesterases using Ellman's protocol [60], modified for 96-well microplates. All the reagents were purchased from Sigma–Aldrich (Steinheim, Germany). The stock solutions of the target compounds were prepared in DMSO and diluted with water to yield the desired final concentrations.

The enzymes (AChE from Electrophorus electricus and BuChE from horse serum) were prepared as 5 U/mL aqueous stock solutions and diluted before use to a final concentration of 0.384 U/mL. Then 20 μL of prepared enzyme solutions (AChE or BuChE) each was added to the reaction mixture in the wells, containing 25 μL of the target compound (in case of blank samples, water or water/DMSO mixture), 200 μL of 0.1 M phosphate buffer (pH = 8.0) and 20 μL of 5,5′ -dithiobis-(2-nitrobenzoic acid) DTNB (0.0025 M). All those reagents were pre-incubated for 5 min at 25°C for the reactions with the animal enzymes (eeAChE or eqBuChe). The enzymatic reaction was initiated by the addition of 20 μL of acetylthiocholine iodide ATC substrate (0.00375 M) or butyrylthiocholine iodide BTC (0.00375 M) solutions (depending on the enzyme used). After 5 min of incubation, changes in absorbance were measured at 412 nm, using the EnSpire multimode microplate reader (PerkinElmer, Waltham, MA, USA). Target compounds were tested at the screening concentrations of 10 μM for inhibitory potencies toward animal cholinesterases. Percentage enzyme inhibition was calculated based on the formula 100-(S/B)x100, where S and B were the respective enzyme activities with and without the test compound, respectively. For compounds showing > 50 % inhibition of enzyme (eeAChE or eqBuChE) activity at 10 μM, IC_{50} values were determined measuring absorbance at seven different inhibitor concentrations. The obtained percentages of enzyme inhibition were plotted against the applied inhibitor concentrations, using nonlinear regression (GraphPad Prism 9; GraphPad Software, San Diego, CA, USA). Tacrine and donepezil were tested as the references. All the experiments were performed in triplicate.

2.8. Kinetic study

The kinetic studies were performed with compounds **18** and **50** based on Ellman's method [60]. The aqueous BuChE stock solution (5 U/mL) was diluted before use to a concentration of 0.384 U/mL. Stock solutions of **18** and **50** were prepared in DMSO and diluted in demineralized water to six different contestations giving enzyme activities between 30 % and 80 %. For each concentration of the compound, the aqueous BTC substrate was added to the wells at concentrations of 0.3, 0.24, 0.18, 0.12, 0.06, and 0.04 mM. Experimental data are based on n = 1 independent measurement per condition. For the control (water), four replicates were measured per BTC substrate concentration, while for the inhibitor conditions, two replicates were performed per BTC concentration. Consequently, statistical significance was not assessed. V_{max} and K_m values of Michaelis–Menten kinetics were calculated by nonlinear regression from substrate–velocity curves. Lineweaver-Burk and Cornish-Bowden plots were calculated using linear regression in GraphPad Prism 5 (GraphPad Software, San Diego,

CA, USA).

2.9. Molecular modeling

The general docking protocol was performed according to our previous publication [31] using the crystal structure of the 5-HT_7 receptor with the parent ligand of 5-CT (PDB: 7XCT). In terms of docking to BuChE PDB: 7AWH was used. Automated Protein Preparation Wizard (Schrodinger, Maestro v13.4) was used to evaluate appropriate amino acid ionization states, to check for steric clashes and to assign bond ordering. Optimized three-dimensional structures for the ligands were determined by LigPrep (OPLS4) and the protonation state at pH 7.4 ± 2.0 using Epik. The ligands were docked by Induced Fit Docking (IFD) using extended sampling protocols. A grid box size of 15 Å was centered on the rest of E7.34 and D3.32 (for 5-HT7R) or Asp70 (for BuChE). Refined residues were set up to 5 Å of ligand poses. Selected ligand poses were prepared and generated using Maestro v13.4.

2.10. Molecular dynamics

The long-time-scale molecular dynamics were performed in all-atom approach using NAMD 2.13, with standard all-atom forcefield CHARMM [61] which is available in all of the above. The membrane and simulation system were built in QwikMD beta tool in VMD 1.9.3 [62], using POPC (1-palmitoyl-2-oleoylphosphatidylcholine), solvent explicit, buffer 15 A salt cons 0.15 mol/L NaCl.

2.10.1. β-amyloid inhibition

Spectrofluorimetric assays, measuring ThT fluorescence in the presence of amyloid, were performed according to our previous paper [50,51,63]. The *in vitro* inhibition of β-amyloid aggregation was assessed through a ThT fluorescence-based method, using 2 % 1,1,1,3,3,3-hexafluoroisopropanol (HFIP) as an aggregation enhancer. Fluorimetric reads were performed in an Infinite M1000 Pro multiplate reader (Tecan, Cernusco sul Naviglio, Italy). Each concentration point was run in triplicate. In this medium-throughput assay, Aβ40 peptide was used as more manageable than Aβ42 and less prone to the formation of pre-aggregates. Aβ samples were co-incubated with test molecules in PBS at 100 μM final concentration and antiaggregating activities were measured after 2 h of incubation at 25°C. Coincubation samples were prepared as described above in 96-well black, non-binding microplates (Greiner Bio-One GmbH, Frickenhausen, Germany).

2.11. Danio rerio toxicity model

The toxicity *in vivo* model with *Danio rerio* was applied according to our previous paper [32].

2.12. Hepatotoxicity and neurotoxicity

Hepatotoxicity was estimated using the hepatoma HepG2 cell line purchased from the American Type Culture Collection (ATCC® HB-8065™). The CellTiter 96® AQueous Non-Radioactive Cell Proliferation Assay (MTS) used for the estimation of cell viability was purchased from Promega (Madison, WI, USA). Compound **50** was tested in quadruplicate in two independent experiments at six concentrations (0.1, 1, 10, 25, 50 and 100 μM). The results of the MTS assay conducted after the incubation of **50** with cells for 72 h provided data for the calculation of IC_{50} values using GraphPad Prism 8.0.1 software. Serial dilutions of the antiproliferative medication doxorubicin (Sigma-Aldrich, St. Louis, MO, USA) were used as a reference. Absorbance in the MTS assay was measured at 490 nm using a Tecan Spark multimode plate reader (Tecan, Männedorf, Switzerland).

Neurotoxicity was tested using the neuroblastoma SH-SY5Y cell line, purchased from ATCC® (CRL-2266™, Manassas, VA, USA). The general procedure was similar to the hepatotoxicity assay described above. The only difference was that compound **50** was incubated for 48 h.

2.13. CYP activity

The possibility of drug-drug interactions was estimated using luminescent CYP3A4 and CYP2D6 assays purchased from Promega (Madison, WI, USA). The compounds were tested in triplicate in five concentrations (0.01, 0.1, 1, 10 and 25 μM). Serial dilutions of the respective reference CYP inhibitors (ketoconazole for CYP3A4 and quinidine QD for CYP2D6) were used as the reference. Both inhibitors were purchased from Sigma-Aldrich (St. Louis, MO, USA). IC50 values were calculated using GraphPad Prism 8.0.1 software. Luminescence signals were measured using a Tecan Spark multimode plate reader (Tecan, Männedorf, Switzerland).

2.14. Metabolic stability

Mouse liver microsomes (MLMs), obtained from Sigma-Aldrich (St. Louis USA), were used for the metabolic stability assay. Compounds **40** and **50** were incubated with MLMs for 120 min in the Tris-HCl buffer in the presence of the NADPH Regeneration System (Promega, Madison, WI, USA). The reactions were stopped by the addition of cold methanol. After centrifugation the supernatants were subsequently analyzed using the UPLC-MS ACQUITY™ TQD system (Waters, Milford, CT, USA). UPLC and MS data interpretation was supported by the MetaSite 6.0.1 program from Molecular Discovery Ltd. (Hertfordshire, UK), which enables the determination of the most probable sites of metabolism as well as metabolic pathways. The unstable drug verapamil (Sigma-Aldrich, St. Louis, MO, USA) was used as a reference.

2.15. Animals

Swiss albino mice were housed 4 per cage group in 12 h light/dark cycles with free access to food and water (room temperature 21 ± 1°C). Each experimental group consisted of 6–10 animals randomly allocated to prevent bias. 6-week-old male Swiss albino mice (25–30 g) were used for the experiments. All experiments were performed as approved by the Local Ethics Committee. The experiment was in accordance with the National Institute of Health Guidelines for the Care and Use of Laboratory Animals and approved by the European Community Council Directive for the Care and Use of Laboratory Animals of September 22, 2010 (2010/63/EU).

2.16. Maximum tolerated dose (MTD) assessment

The Maximum Tolerated Dose (MTD) was determined using a modified OECD 425 “Up-and-Down Procedure” [58]. This approach involves sequential administration of the test compound to individual animals at escalating doses, with a 48-hour interval between each dose, to observe for signs of toxicity or adverse effects. The study commenced with a dose of 1 × the MTD, as established from prior zebrafish model studies and literature data on the toxicity of structurally similar compounds. The MTD assessment started with Dose 1, given to a single mouse. If this dose induced toxic effects, the next mouse would receive a dose that was a half of Dose 1. This reduced dose would then be considered the MTD. If toxic effects persisted even at a half of Dose 1, the dose would be further reduced to a quarter of Dose 1. The protocol allows dose adjustments up to four times lower or higher, depending on observed toxicity. If toxic effects were observed at a quarter of Dose 1, the experiment would be terminated, and further pharmacokinetic and therapeutic experiments would not proceed. However, if no toxic effects were noted, two additional mice would be administered this dose to confirm its safety. If the initial dose proved non-toxic, the next mouse would receive a dose twice as high. If this higher dose resulted in toxic effects, two additional mice would be administered Dose 1 to validate its safety as the MTD. If no toxic effects were observed, the next mouse

would receive a dose four times higher than Dose 1. In the absence of toxic effects at this level, this dose would be given to two more mice to determine the upper limit of the MTD.

2.17. Spontaneous Locomotor Activity

The locomotor activity of the mice was measured using Opto-Varimex-4 Auto-Track (Columbus Instruments, United States). After injections of saline or substances (5, 10 mg/kg), the animals were placed individually in an actimeter for 60 min. A grid of infrared photocells were used to track the movement of animals within a defined area of the cage, providing detailed data on their locomotor activity.

2.18. Passive avoidance (PA) Test

Memory-related responses were evaluated using the passive avoidance (PA) test [64]. The apparatus for the PA task consisted of an acrylic box divided into two compartments: a light compartment (10 × 13 × 15 cm) and a dark compartment (25 × 20 × 15 cm) equipped with an electric floor.

The experiment involved two stages: the pre-test and the test. In the pre-test, the mice were first allowed to habituate in the light compartment for 30 seconds. After this habituation period, the door separating the two compartments was opened, allowing the mice to enter the dark compartment. Once inside, the door was closed, and the mice received a mild foot shock (0.15 mA for 2 seconds). On the following day, the test was conducted using the same procedure, but without administering the shock. The time taken by the mice to move from the light compartment to the dark one was recorded as latency time: TL1 for the pre-test and TL2 for the test.

$$IL = (TL2 - TL1)/TL1$$

This methodology allows the examination of different stages of memory depending on the timing of drug administration and the interval between training and testing. Administering the drug before the first trial (pre-test) is used to assess its impact on the acquisition of new information. In contrast, administering the drug immediately after the pre-test evaluates its effect on the consolidation of the acquired information.

3. Results and discussion

3.1. Chemistry

The general synthesis of all the tested compounds **1–50** involved a three-step *N*-alkylation reaction according to the protocol described in our previous papers under microwave irradiation [32,37]. Substrate **51** for the synthesis of set I compounds was prepared according to the previously published paper [37]. Subsequently, compound **51** was reacted with commercially available piperazines **52–54** under microwave irradiation in the presence of catalytical amount of TBAB (tetrabutylammonium bromide) over 2.5 min to yield title compounds **1–3** (Scheme 1) in 68–81 % of yields. Compounds of set II were obtained similarly using intermediate **55** [34,38] and commercially available amines **53**, **54**, **56** and **57** (Scheme 2) in 53–78 % of yields.

The synthesis of set III (Scheme 3) was started with preparing intermediates **88–103** according to a described procedure [31]. The first step of this synthesis was a reaction between **58** and commercially available arylpiperazine **59–69** or freshly prepared **70–73** in the presence of potassium carbonate in boiling acetonitrile (ACN). Subsequently, the isolated products were transformed into primary amines *via* a reaction with 40 % methylamine solution in water. The yields were in the range of 15–89 %.

Arylpiperazines **70–73** were prepared as shown in Scheme 4. In the first stage, Suzuki coupling was initiated between 2-iodoaniline **104** and appropriate boronic acids **105–108** in the presence of $Pd(dppf)Cl_2$ catalyst and 5 M NaOH solution. After 4 hours of refluxing in THF (tetrahydrofuran) the reaction was completed. The crude product was extracted with DCM (dichloromethane) and purified *via* column chromatography to prepare final compounds with yields ranging from 50–80 %. Biphenyl anilines **109–112** were subsequently cyclized with bis(2-chloroethyl)amine hydrochloride (**113**) to yield title arylpiperazines **70–73** [39].

The synthesis of set IV compounds shown in Scheme 5 was conducted similarly to our previously reported papers [31,34]. Intermediate **55** was reacted with commercially available phenylethylamines **114–121** and their heterocyclic analogs **122–125** under microwave conditions in 47–88 % of yields.

The synthesis of set V compounds was slightly different than the previous ones (Scheme 6). In the first stage intermediate **128** was prepared *via* alkylation of tryptamine (**126**) with cyanuric chloride (**127**). The reaction was carried out at 0 °C in THF in the presence of DIPEA (*N*,*N*-diisopropylethylamine). Subsequently, isolated product **128** was reacted with phenylethylamine **129** in THF for 15 h at RT. Crude product **132** was used in the next step without any further purification. Final compounds **40–45** were obtained *via* a microwave-assisted *N*-alkylation reaction between intermediate **132** and commercial amines **133–139**.

Because of extremely low yield (a few %) for compound **46** obtained *via* the same route as for **40–45** and **47**, this compound was synthetized through a different pathway. Intermediate **128** was reacted with *N*-methylpiperazine **130** at room temperature in the presence of DIPEA. After 15 hours of stirring, solid DIPEA-HCl was filtered off, and another portion of DIPEA was added to the filtrate followed by the addition of 2-

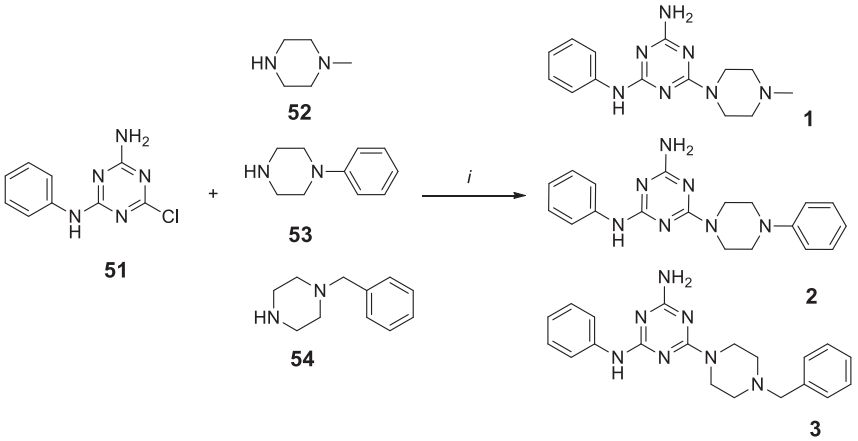

Scheme 1. Synthesis pathway of set I compounds. *i* – K_2CO_3, TBAB, DMF (*N*,*N*-dimethylformamide), MW P = 50 W, 2.5 min.

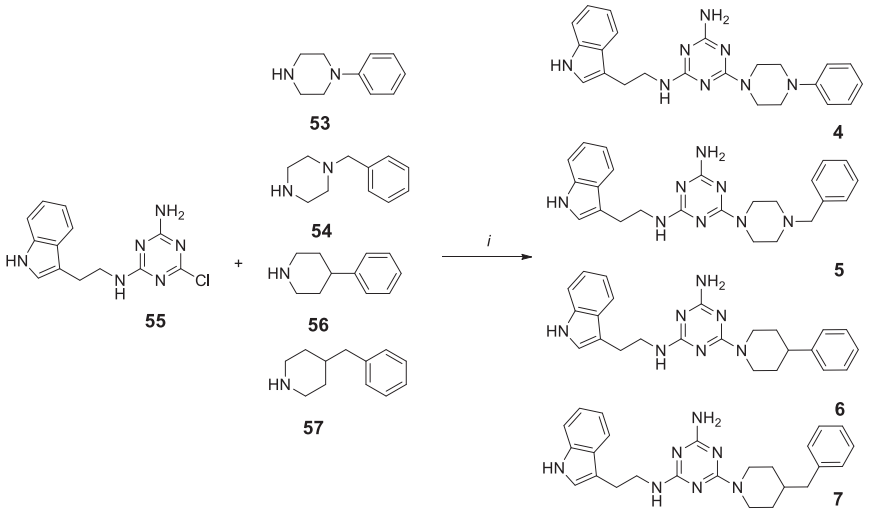

Scheme 2. Synthesis pathway of set II compounds. *i* – K_2CO_3, TBAB, DMF, MW P = 50 W, 2.5 min.

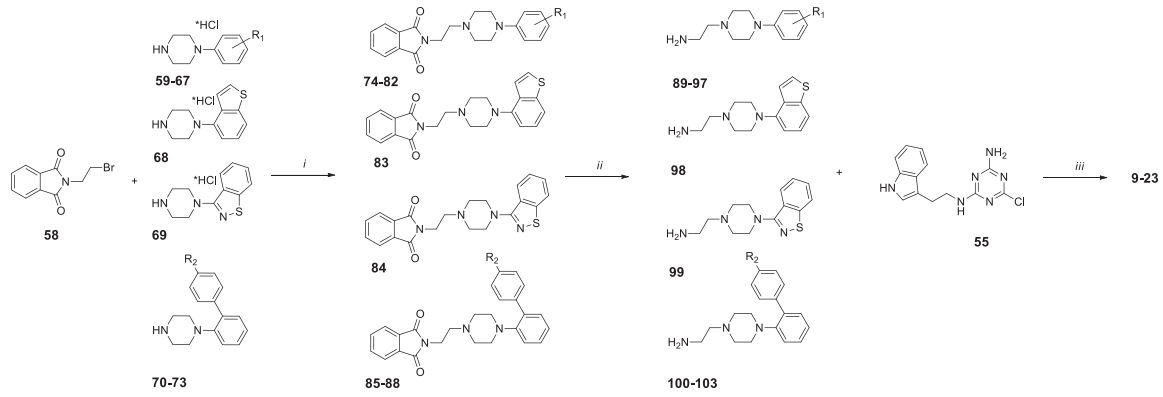

Scheme 3. Synthesis pathway of set III compounds. *i* – K_2CO_3, ACN, 90 °C, 15 h; *ii* – 40 % $MeNH_2$ 15 h r.t. then 2 M NaOH, 1 h, r.t.; *iii* – K_2CO_3, TBAB, DMF, MW P = 50 W, 2.5 min. R_1 substituent order: *o*-F, *m*-F, *p*-F, *o*-Cl, *m*-Cl, *p*-Cl, *o*-OMe, *m*-OMe, *p*-OMe; R_2 substituent order: H, F, Cl, OMe.

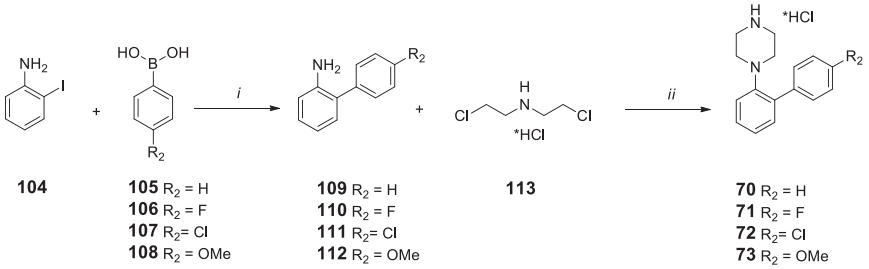

Scheme 4. Synthesis pathway of arylpiperazines 70–73. *i* – $Pd(dppf)Cl_2$, 5 M NaOH, toluene, reflux, 4 h; *ii* – K_2CO_3, pTSA, xylene, reflux, 72 h.

phenylethylamine (**129**). The reaction was refluxed over 24 hours followed by water work-up and purification to obtain **46** with 52 % yield. Direct isolation of **131** resulted in product decomposition during work-up. Compound **39** was obtained in an *N*-alkylation reaction supported with microwave irradiation between intermediate **141** and 2-phenylethylamine (**129**) over 2.5 min. Intermediate **141** was obtained *via* freshly prepared 2,4-dichloro-6-methyl-1,3,5-triazine (**140**) and tryptamine (**126**) according to the protocol described above. The incorporation of non-amine nucleophiles (-OH and -SH) was presented in Scheme 6. The reaction was carried out in a boiling solvent over a few days (compound **37**) or a few hours (compound **38**) according to the data reported by Lebel O [40]. The chlorine atom (compound **48**) was removed in hydrogen atmosphere (balloon) *via* a heterogeneous reaction on Pd/C with 2 eq. of DIPEA with quantitative yield. The synthesis of set VI compounds (Scheme 7) required much longer microwave irradiation, but other reaction parameters were the same as for the synthesis of set IV. Intermediate **143** was obtained in a reaction between tryptamine (**126**) and commercially available 4,6-dichloropyrimidin-2-amine (**142**) in the presence of triethylamine. After 24 hours of reaction in boiling methanol, the mixture was cooled and the TEA-HCl salt was filtered off. Unreacted tryptamine **126** was removed *via* the addition of chloroform during the work-up stage. The crude product was purified *via* column chromatography to obtain amber-like viscous oil which turned to a creamy sponge after longer drying *in vacuo*. Final products **49** and **50**

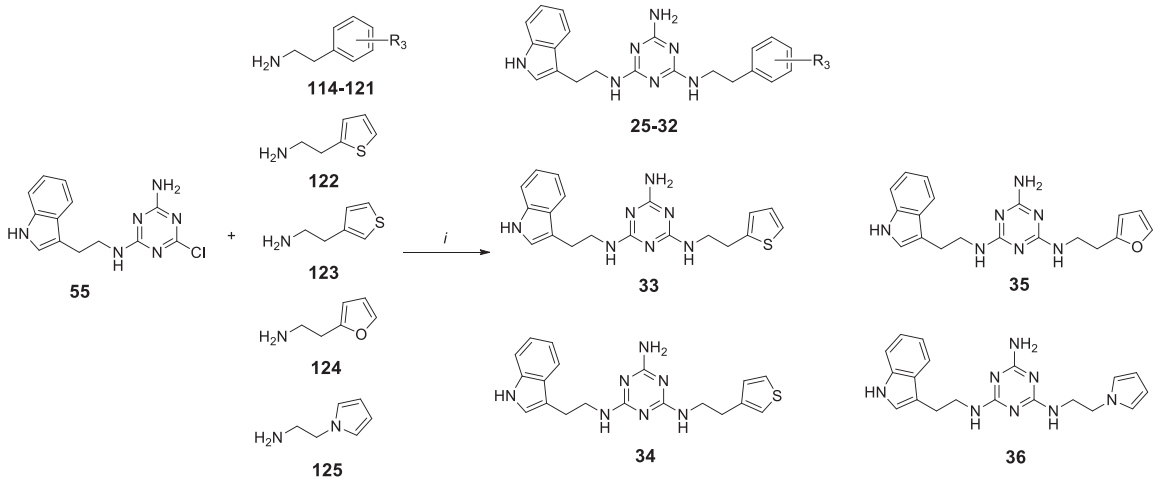

Scheme 5. Synthesis pathway of set IV compounds. *i* – K_2CO_3, TBAB, DMF, MW P = 50 W, 2.5 min. R_3 substituent order: *o*-F, *m*-F, *p*-F, *o*-Cl, *m*-Cl, *p*-Cl, *p*-Me, *p*-CF_3.

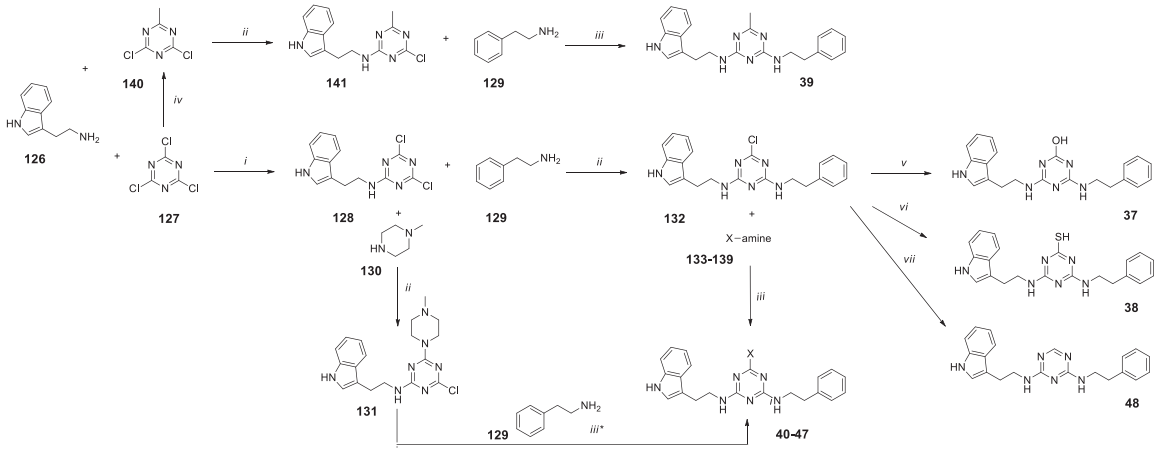

Scheme 6. Synthesis pathway of set V compounds. *i* – DIPEA, THF, 0 °C, 20 min; *ii* – DIPEA, THF, room temp., 15 h; *iii* – K_2CO_3, TBAB, DMF, MW P = 50 W, 2.5 min or (iii*) reflux for 72 h; *iv* – CH_3MgBr, DCM, 0 °C, 3 h; *v* – KOH, H_2O/1,4-dioxane (1:5 vol.), reflux, 3 days; *vi* – thiourea, 1,4-dioxane, reflux, 5 h; *vii* – hydrogen balloon, Pd/C, DIPEA, THF/MeOH (1:1 vol.), 24 h. **40**–**47** X substituent order: deuterated amine, *N*-methylamine, *N,N*-dimethylamine, pyrrolidine, piperidine, morpholine, *N*-methylpiperazine (derived from **131**), aniline. X-amine: **133** deuterated ammonia (ammonia-d_3), **134** *N*-methylamine, **135** *N,N*-dimethylamine, **136** pyrrolidine, **137** piperidine, **138** morpholine, **139** aniline.

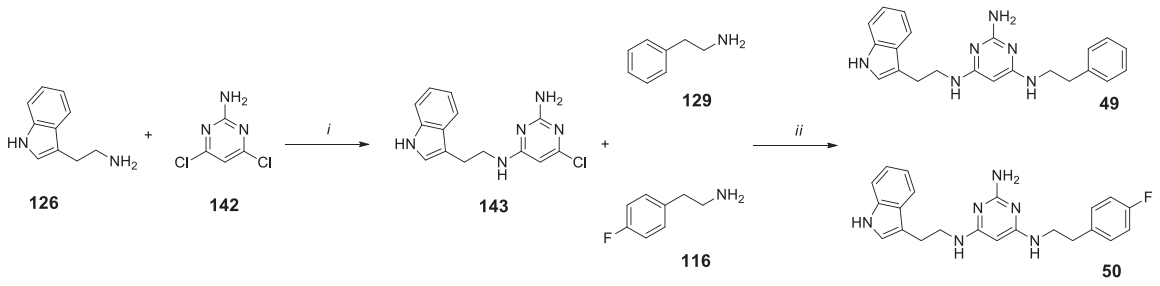

Scheme 7. Synthesis pathway of set VI compounds. *i* – TEA, MeOH, 70 °C, 24 h; *ii* – K_2CO_3, TBAB, DMF, MW P = 50 W, 40 min.

were obtained in the reaction between intermediate **143** and amines **129** or **116** under microwave conditions with yield of 57 % and 65 % respectively.

***In vitro* pharmacology:** *5-HT$_7$ receptor binding, functional assay for 5-HT$_7$R, cholinesterase activity and kinetic study for BuChE*

To evaluate the activity of the compounds, 5-HT$_7$R radioligand binding was evaluated for all the obtained molecules. Because the long-chain arylpiperazine motif is characteristic for activity toward aminergic GPCR receptors, including serotonin receptors, and due to the fact that the binding pocket of the 5-HT$_7$ receptor is similar to that of the 5-HT$_{1A}$ receptor, selected ligands from set III, with affinity for the 5-HT$_7$ receptor with a K_i value below 100 nM, were tested for their affinity to the 5-HT$_{1A}$ receptor as off-target. In general each compound was tested in triplicate at seven concentrations. Only for molecules exhibiting 5-HT$_7$R activity were functional assays using the cAMP measurement assay and cholinesterase activity, including kinetic studies, performed

according to previously published papers [41,42].

According to Table 1, set I compounds turned out to be inactive. The exchange of the aniline aryl ring and its replacement with the tryptamine motif, which was verified in previous studies, resulted in a slight increase in 5-HT$_7$R binding; however activities were still poor with K_i of more than 100 nM. The most active compound in this group was **7** with $K_i = 430$ nM. The poor results from sets I and II prompted us to replace the aniline-triazine core with a the tryptamine-triazine core functionalized with ethyl arylpiperazines, and the pharmacological profile is shown in Table 2.

All set III compounds exhibited good or average activities with submicromolar affinities in most cases with K_i below 200 nM. As we expected, all the tested compounds (apart from **18** $K_i = 144$ nM) did not show significant activity toward 5-HT$_{1A}$R. Comparing the influence of the presence of substituents on the aryl ring (compounds **9–17**) or when the aryl was replaced with a heterocyclic system (**18**, **19**) to compound **8**, it can be observed that the affinity for the 5-HT$_7$ receptor was comparable or slightly decreased. The fluorine atom (**9**, **10**, **11**) was found to be the most preferable compared to the chlorine and methoxy group which was the most unpreferable. In terms of the position, *para* substitution (**11**, 5-HT$_7$R $K_i = 12$ nM) was the most preferable. For the chlorine substituent, as well as the methoxy group, the *meta* position generated the highest binding values. In fluorinated and chlorinated compounds, the *ortho* position tended to be unpreferable while for the methoxy substituent, the *para* position abolished activity toward 5-HT$_7$R. The replacement of a substituted aryl onto heterocycles in **18** ($K_i = 7$ nM) and **19** ($K_i = 19$ nM) did not appreciably improve the affinity of the compounds, but the compounds still had very good affinity to 5-HT$_7$R. In terms of compound **18**, we noticed additional average binding to 5-HT$_{1A}$R which may result from the presence of an additional hydrogen bond acceptor in the benzisothiazole moiety. Although the 2-biphenylpiperazine scaffold has been reported as highly potent in terms of 5-HT$_7$R binding, we did not confirm its utility in our studies. Compounds **20–22** were more than 10-fold weaker in comparison to unsubstituted ligand **8** or **11** or **14** substituted in the *para* position. Interesting phenomena were noted when comparing ligand **23** ($K_i = 98$ nM) and **17** ($K_i = 1760$ nM). In this case, significant (18-fold) improvement of activity was found. For all compounds with 5-HT$_7$R $K_i < 100$ nM (**10**, **11**, **13**, **14**, **18**, **19**) cAMP production was measured to evaluate antagonist function. It turned out that the selected compounds were highly potent (apart from **20** and **23**) antagonists of the 5-HT$_7$ receptor with K_b ranging from 1–6 nM. Ligands with K_i below 100 nM were subjected to cholinesterase activity screening. The analysis of results toward AChE showed that all tested compounds in this set were not able to inhibit enzyme activity within 50% at the highest tested dose of 10 μM (Table 2). Better results were achieved for BuChE. The compounds exhibited nearly three times higher activity compared to AChE. Ligands **10**, **18** and **19** were characterized by IC$_{50}$ equal to 5.73 μM, 4.75 μM and 6.22 μM, respectively. Surprisingly, it turned out that the 2-biphenyl-piperazines **20** and **23**, despite their relatively weak activity toward the 5-HT$_7$ receptor, they were one of the most active compounds among the set III. Both compounds exhibited comparable IC$_{50}$ values of 3.13 μM and 3.75 μM respectively.

Table 1
In vitro activity for set I and II compounds. Human receptors stably expressed in HEK293 cells.

Set No.	Cmpd. No.	5-HT$_7$R	5-HT$_{1A}$R
		K_i [nM]	K_i [nM]
I	1	17650 ± 2648	n.d.
	2	46360 ± 9272	n.d.
	3	51180 ± 8701	n.d.
II	4 *	798 ± 96	12960 ± 2722
	5	2019 ± 303	n.d.
	6	3801 ± 228	n.d.
	7	430 ± 39	12960 ± 1299

n.d. – not determined; * – data taken from ref31. Each compound was tested in triplicate at 7 concentrations (0.1 nM to 100 μM). Inhibition constants (K_i) were calculated from the Cheng-Prusoff equation [43]. Results are expressed as means of at least two separate experiments ± standard deviation (SD).

As shown in Table 3, all compounds also had submicromolar affinities to K_i below 500 nM except for two compounds **36** and **38** whereby K_i toward the 5-HT$_7$ receptor was more than 1 mM. Overall, optimizing the phenylethyl region (set IV) proved to be much more beneficial than substituting different nucleophiles for the NH$_2$ group (set V). According to our previous research, only small substituents, such as fluorine (**25–27**) or chlorine (**28–30**), were tolerated well. Upon deeper analysis of the influence of fluorine and chlorine atoms and their attachment to the aryl ring, the following conclusions can be drawn: a) fluorine induces the highest activity among the studied group of compounds; b) there is an observed increase in affinity for the 5-HT$_7$ receptor when the heteroatom (F or Cl) is positioned in the following order: *ortho* > *meta* > *para*. Replacement of *para*-F (**27**) or *para*-Cl (**30**) onto *para*-methyl (**31**) caused a 16-fold and a 10-fold decrease of 5-HT$_7$R affinity, respectively. Although fluorine is considered an important bioisostere of hydrogen [44,45] often enhancing the potential of a molecule by improving pharmacology or pharmacokinetic properties or reducing toxicity, in the case of compound **32** (5-HT$_7$R $K_i = 340$ nM), its application unfortunately significantly reduced affinity for the 5-HT$_7$ receptor. In terms of compounds being heterocyclic analogs of phenylethylamine, compound **34** (5-HT$_7$R $K_i = 6$ nM) exhibited the highest activity in the considered group. As noted before, the modification of the amine group in set V did not provide improvement of activity toward the 5-HT$_7$ receptor. The NH$_2$ group is crucial for the high activity of compound **24** toward the 5-HT$_7$ receptor. Its absence significantly reduces activity (**42**, $K_i = 486$ nM). The deuterated NH$_2$ group also maintains high affinity (**40**, $K_i = 19$ nM), although slightly lower than the unmodified NH$_2$ group. Substituting the NH$_2$ group with various EDG substituents (OH, SH) and acyclic and cyclic amines generally leads to reduced activity. The most favorable results were obtained for methylamine (**41**, $K_i = 41$ nM) and the methyl group (**39**, $K_i = 44$ nM). The most significant reduction in activity was observed with SH group substitution (**38**, $K_i = 1619$ nM). The last compound set contained only two ligands being pyrimidine. Both compounds exhibited the highest activity toward 5-HT$_7$R with $K_i = 1$ nM over all synthetized molecules. Analog compounds containing the triazine core (**25** and **27**) showed slightly lower activity; however, more in-depth medicinal chemistry studies are ongoing in terms of pyrimidines. For set IV, V and VI ligands with K_i lower than 200 nM, functional assays with cAMP measurement were performed. It turned out that all the compounds showed an antagonistic mode with K_b ranging from 1 −74 nM. Similarly to set III, the tested compounds were not active toward AChE inhibition, while their activity against BuChE was more than four times higher than for AChE. The activity against BuChE of all tested compounds from series IV and V ranged from 5.78 μM to 8.53 μM. Evaluating the impact of the fluorine atom's position for compounds **25–27**, we did not observe significant differences in activity. Similar conclusions can be drawn for compounds containing chlorine in the aromatic ring **29–31**, with the exception that in the case of the *ortho* position, the molecule lost enzymatic activity. Analyzing the chemical structure of compound **40**, it can be inferred that halogens increase the activity of molecules in terms of affinity to BuChE. The most potent compound was **50** with IC$_{50}$ equal to 2.53 μM. The activity of **50** was similar as for donepezil, a known BuChE inhibitor [46].

To determine the mechanism of eqBuChE inhibition, we carried out kinetic studies with two the most potent BuChE compounds **18** and **50**. Lineweaver–Burk plots (1/V vs. I/S, Fig. 4) for **18** and **50** showed a series of converging lines above the x-axis, while Cornish−Bowden plots (S/V vs. I, Fig. 5) showed converging lines below the x-axis, profiling a mixed-type mechanism of eqBuChE inhibition. For both compounds the plots revealed increased slopes (decreased V_{max}) at increasing inhibitor concentrations, and different intercepts at the x-axis (increased K_m).

Table 2
In vitro activity for set III compounds. Human receptors stably expressed in HEK293 cells.

Set No.	Cmpd. No.	5-HT$_7$R	5-HT$_{1A}$R	5-HT$_7$R	AChE	BuChE	
		K_i [nM]	K_i [nM]	K_b [nM]	% inh.[a]/IC_{50}	% inh.[b]	IC_{50} [μM]
	8 *	7 ± 2	2836 ± 425	34 ± 3	n.d.	n.d.	n.d.
III	9	132 ± 17	n.d.	n.d.	n.d.	n.d.	n.d.
	10	44 ± 4	936 ± 75	1 ± 0.1	15.5 ± 0.2 %	73.7 ± 1.7 %	5.73 ± 0.16
	11	12 ± 1	1678 ± 402	1 ± 0.03	< 10 %	31 ± 1	n.d.
	12	795 ± 181	n.d.	n.d.	n.d.	n.d.	n.d.
	13	13 ± 2	908 ± 190	1 ± 0.2	10 ± 1 %	38 ± 2 %	n.d.
	14	36 ± 8	4467 ± 224	6 ± 0.6	10.3 ± 1.7 %	35 ± 2 %	n.d.
	15	726 ± 99	n.d.	n.d.	n.d.	n.d.	n.d.
	16	118 ± 21	n.d.	n.d.	n.d.	n.d.	n.d.
	17	1760 ± 376	n.d.	n.d.	n.d.	n.d.	n.d.
	18	7 ± 0.5	144 ± 6	2 ± 0.2	21 ± 4 %	62 ± 2 %	4.75 ± 0.1
	19	19 ± 0.8	396 ± 67	3 ± 0.1	35 ± 4 %	54 ± 3 %	6.22 ± 0.07
	20	99 ± 10	391 ± 35	108 ± 21	24.6 ± 1.5 %	79.5 ± 1.2 %	3.13 ± 0.08
	21	247 ± 40	n.d.	n.d.	n.d.	n.d.	n.d.
	22	371 ± 26	n.d.	n.d.	n.d.	n.d.	n.d.
	23	98 ± 13	1660 ± 232	111 ± 24	25.3 ± 2.9 %	76.3 ± 0.6 %	3.75 ± 0.1
	donepezil	n.d.	n.d.	n.d.	0.011 μM	-	1.83

n.d. – not determined; * - data taken from ref31. **Radioligand binding:** each compound was tested in triplicate at 7 concentrations (0.1 nM to 100 μM). Inhibition constants (K_i and K_b) were calculated from the Cheng-Prusoff equation [43]. Results are expressed as means of at least two separate experiments ± standard deviation (SD); **Cholinesterase activity:** [a] – percent inhibition of AChE from electric eel with tested cmpd. at 10 μM; [b] – percent inhibition of BuChE from horse serum with tested cmpd. at 10 μM. Values are expressed as the means ± the standard error of the mean (SEM) of at least three experiments (n = 3), each performed in triplicate.

Mixed types of eqBuChE inhibition with increasing K_m at increasing concentrations of **18** or **50** indicate higher affinity of the inhibitor to the free enzyme than to the enzyme−substrate complex.

3.2. Molecular modeling

Lead compounds from set III (**18**, K_i = 7 nM) and set VI (**50**, K_i = 1 nM) were chosen for molecular modeling studies in terms of 5-HT$_7$ binding and human BuChE activity (Figs. 6, 7 and Supporting Information). The interesting SAR results for the entire set V in the context of 5-HT$_7$ receptor binding prompted us to explain the lack of activity for most compounds, despite minor structural changes, and why the CH_3 substituent (compound **39**) was tolerated but did not form a conserved hydrogen bond with E7.36. Since the crystallized 5-HT$_7$_5-CT complex [47] had recently become available, compound **24** (Fig. 6A) was re-docked to examine whether the binding mode we described in our previous publication was consistent with the new one derived from the crystal structure. It turned out that bio-conformation was the same, and compound **24** formed identical types of bonds as previously described. Docking revealed that ligand **18** (Fig. 6C) was anchored between TMh3 and TMh6-TMh7 of 5-HT$_7$R with more linear bioconformation. The 1-(benzo[*b*]thiophen-4-yl)piperazine moiety occupies a hydrophobic binding pocket located deeply in the receptor where the benzotiophene ring forms F6.51 and F6.52 T-type hydrophobic π-π stacking. The protonated piperazine nitrogen atom forms a conserve salt bridge with D3.32 while nitrogen atoms of the triazine ring form three hydrogen bonds with R7.35, L232 and I233. The amine substituent attached to the triazine ring is involved in hydrogen interaction with E7.34 and another one with L7.31. In the case of compound **50** (Fig. 6D) lacking the long-chain arylpiperazine motif, tryptamine is oriented toward the internal binding pocket of the receptor. The indole ring is involved in hydrophobic π-π interaction with F6.52 (T-shape), while the NH group forms a hydrogen bond with Ser5.43. The central part of the structure, the pyrimidine ring, interacts with Ser6.55, also forming a hydrogen bond. An additional hydrogen bond is observed between the secondary amine group of tryptamine and D3.32. Moreover, as with the entire group of compounds, a typical hydrogen bond is observed between the amino substituent and E7.34. 4-fluorophenylethylamine is oriented toward the external side of the receptor and points toward the cavity between TMh2 and TMh3, with the potential to form an additional cation-π bond between the aryl ring and R7.35.

Two lead compounds were subjected to molecular docking to determine the binding mode (Fig. 7A and Fig. 7B). The crystal structure chosen was PDB: 7AWH. Both compounds exhibit a binding arrangement in the enzyme similar to the crystallized parent ligand (S8K609), adopting a bent shape. For compound **18** (BuChE, IC_{50} = 4.75 μM), the arylpiperazine is located in a hydrophobic binding pocket facing the interior of the enzyme, where the benzothiophene interacts with Trp82 and Phe329 *via* hydrophobic π-π interactions. The protonated nitrogen atom of the piperazine forms a salt bridge with Asp70, while the amine group forms hydrogen bonds with Ser287 and Thr284. The indole forms an additional hydrophobic interaction with Phe329. In the case of compound **50** (BuChE, IC_{50} = 2.53 μM), an opposite orientation is observed in the binding pocket. The aromatic ring of the indole faces the inner side of the receptor, interacting *via* a π-π bond with Trp82, while the indole nitrogen forms a hydrogen bond with His483. Similarly to compound **18**, the NH_2 group attached to triazine forms a hydrogen bond with Leu287, and the NH group of the 4-fluorophenylethylamine forms a hydrogen bond with Leu286. The benzene ring of the 4-fluorophenylethylamine also forms a hydrophobic π-π interaction with Phe329. The described binding mode is consistent with results of other research groups [28,48,49].

Using docking studies, we also proposed a potential explanation why the amine (cmpd. **24**), methyl (cmpd. **39**), deuterated amine (cmpd. **40**) or methylamine (cmpd. **41**) substituents were preferred for maintaining affinity for the 5-HT$_7$ receptor (Fig. 9). For small nucleophiles, such as OH (**37**) or SH (**38**) groups (Fig. 8), it appears that under docking conditions (pH = 7.4, similar to physiological conditions), the compound exists in tautomeric form B rather than A. In such conditions, no hydrogen bond formation with E7.34 is observed. Cyclic aliphatic amines and *N*,*N*-dimethylamine **42** exhibit weak affinity because they are too bulky, preventing them from fitting into the binding pocket and thus blocking potential hydrogen bond formation between nitrogen and E7.34. Surprisingly, however, compound **39** (Fig. 6B), which is unable to form a hydrogen bond with E7.34, still shows affinity for the 5-HT$_7$ receptor. According to molecular dynamics results, it turns out that the methyl group electrostatically repels the carboxyl group of E7.34, while the adjacent R6.58 is drawn closer to the triazine ring, forming a stable cation-π bond at a distance ranging from 3–4 Å (Supporting Information).(Fig. 9)

3.2.1. *β-amyloid inhibition*

As mentioned in the introduction, the formation of β-amyloid plaques may be one possible explanation for the mechanism of Alzheimer's

Table 3
In vitro activity for set IV, V and VI compounds. 5-HT_7R stably expressed in HEK293 cells.

Set No.	Cmpd. No.	5-HT_7R	5-HT_7R	AChE	BuChE	
		K_i [nM]	K_b [nM]	% inh.[a]/IC	50 % inh.[b]	IC_{50} [μM]
IV	25	33 ± 4	26 ± 3	< 10 %	59.1 ± 1.6 %	8.11 ± 0.22
	26	7 ± 0.5	18 ± 3	< 10 %	61.9 ± 0.6 %	7.46 ± 0.19
	27	3 ± 0.2	4 ± 0.6	< 10 %	56.8 ± 1.2 %	8.53 ± 0.18
	28	214 ± 35	n.d.	n.d.	n.d.	n.d.
	29	12 ± 1	1 ± 2	< 10 %	38.9 ± 1.2 %	n.d.
	30	5 ± 0.15	7 ± 2	17.6 ± 0.4 %	70.1 ± 1 %	5.78 ± 0.16
	31	49 ± 9	40 ± 18	< 10 %	71.5 ± 1 %	5.88 ± 0.18
	32	340 ± 75	n.d.	n.d.	n.d.	n.d.
	33	119 ± 13	n.d.	n.d.	n.d.	n.d.
	34	6 ± 0.35	6 ± 0.6	< 10 %	65 ± 2 %	6.06 ± 0.1
	35	191 ± 14	n.d.	n.d.	n.d.	n.d.
	36	1254 ± 242	n.d.	n.d.	n.d.	n.d.
V	37	233 ± 17	n.d.	n.d.	n.d.	n.d.
	38	1619 ± 372	n.d.	n.d.	n.d.	n.d.
	39	44 ± 2	14 ± 1	< 10 %	42 ± 2 %	n.d.
	40	19 ± 1	11 ± 2	< 10 %	43 ± 1 %	n.d.
	41	41 ± 4	10 ± 1.5	< 10 %	53 ± 1 %	8.15 ± 0.13
	42	486 ± 100	n.d.	n.d.	n.d.	n.d.
	43	157 ± 11	n.d.	n.d.	n.d.	n.d.
	44	433 ± 39	n.d.	n.d.	n.d.	n.d.
	45	371 ± 30	n.d.	n.d.	n.d.	n.d.
	46	351 ± 80	n.d.	n.d.	n.d.	n.d.
	47	157 ± 43	n.d.	n.d.	n.d.	n.d.
	48	462 ± 33	n.d.	n.d.	n.d.	n.d.
VI	49	1 ± 0.05	1 ± 0.17	n.d.	n.d.	n.d.
	50	1 ± 0.1	2 ± 0.3	10 ± 1 %	79 ± 1 %	2.53 ± 0.28
	donepezil	n.d.	n.d.	0.011 μM	-	1.83 μM

n.d. – not determined; **Radioligand binding:** each compound was tested in triplicate at 7 concentrations (0.1 nM to 100 μM). Inhibition constants (K_i and K_b) were calculated from the Cheng-Prusoff equation [43]. Results are expressed as means of at least two separate experiments ± standard deviation (SD); **Cholinesterase activity:**

[a] – percent inhibition of AChE from electric eel with tested cmpd. at 10 μM;

[b] – percent inhibition of BuChE from horse serum with tested cmpd. at 10 μM. Values are expressed as the means ± the standard error of the mean (SEM) of at least three experiments (n = 3), each performed in triplicate.

Disease. Despite some doubts regarding targeting the Aβ protein, it remains an interesting molecular target, and many research groups are focusing on it. Since the compounds under consideration have never been studied for their inhibition of β-amyloid plaque formation, we decided to investigate for the first time those compounds which exhibited the best pharmacological properties. Compounds **18**, **19**, **41**, and **50** were assayed for their properties to affect and inhibit the $Aβ_{1–40}$ self-induced aggregation, through the test measuring the thioflavin T (ThT) fluorescence (Table 4) [50,51]. Quercetin, known as a strong *in vitro* inhibitor of Aβ aggregation, was also tested as positive control. The selected compounds were tested at one point concentration 100 μM, thus showing a inhibition percentage ranging between 30 % and 55 %, without any apparent dependence upon the structure. Derivative **19**, **41**, and **50** appeared as weak inhibitors of amyloid self-induced aggregation (30–40 % inhibition). In contrast, compound **50** showed the highest observed activity with an inhibition percentage of 53 % at 100 μM concentration. The pharmacophore to achieve anti-Aβ activity has been established by a planar heterocyclic scaffold, acting as an intercalating moiety for disruption of amyloid aggregate β-sheet secondary structure, decorated with suitably small polar and H-bonding groups. The weak observed activity of tested compounds may be mainly determined by the lack of these groups in suitable positions [52–54].

3.3. ADME and toxicology

Taking into account the fact that a large portion of chemical compounds are disqualified from progressing to clinical trials because of significant toxicity [55], we decided to estimate preliminary ADME parameters along with toxicology at the early stages of research. First, we assessed compounds **18**, **19**, **34** and **50** for general toxicity, including cardiotoxicity, using a larval *Danio rerio* model [56]. Subsequently, the selected compounds were subjected to MTD (maximum tolerated dosage) evaluation in an animal model or forwarded to more detailed *in vitro* ADME-T studies: metabolic stability, potential drug-drug interaction (CYP activity), hepatotoxicity and neurotoxicity.

3.3.1. Danio rerio toxicity model

All four compounds were tested for general toxicity on *Danio rerio* in the larval form (Fig. 10). The test was conducted according to the OECD protocol [57], with the compounds incubated for 96 hours. The dose at which 50 % of the larvae were observed to die was evaluated, and the concentration at which a statistically significant decrease in the heart rate was observed was monitored. The studies showed that two compounds containing a heterocyclic motif (**34**, LD_{50} = 6.347 μg/mL) or a 4-fluorphenethyl analog (**50**, LD_{50} = 9.791 μg/mL) exhibited higher toxicity compared to the compounds containing long-chain arylpiperazine motifs (**18**, LD_{50} = 205.1 μg/mL and **19**, LD_{50} = 202.5 μg/mL). The results obtained in the assessment of the heart rate (Supporting Information) showed that for compounds **34** and **50** cardiotoxicity was observed at concentrations of 7 μg/mL and 8 μg/mL, respectively. For long-chain arylpiperazine derivatives, no cardiotoxicity was observed at concentrations up to 200 μg/mL. Based on the studies, compound **18**, which demonstrated a high safety profile and good pharmacological properties, was selected for further *in vivo* studies.

3.3.2. Hepatotoxicity and neurotoxicity

Due to the higher toxicity of compounds **34** and **50** in the *Danio rerio* model compared to compounds **18** and **19**, these compounds were subjected to extended *in vitro* ADME-T studies. Based on the best results for 5-HT_7 receptor affinity and BuChE inhibition, as well as slightly lower toxicity of compound **50** compared to **34**, compound **50** was selected for these studies. The studies were conducted using two cell lines, HepG2 (to assess hepatotoxicity) and SH-SY5Y (to assess neurotoxicity), using the MTS assay (Fig. 11; cell morphology changes in Supporting Information). It was found that compound **50** exhibited moderate hepatotoxicity (IC_{50} = 20.28 μM). Doxorubicin (Dox), the reference hepatotoxic compound, was over 10 times more toxic (IC_{50} = 1.91 μM) than compound **50**. The tested molecule showed lower neurotoxicity compared to hepatotoxicity. Calculated IC_{50} = 31 μM against the SH-SY5Y cell line was approx. 75 times higher than for Dox, the reference compound with significant neurotoxicity (IC_{50} = 0.41 μM). The IC_{50} values for compound **50**, determined in both HepG2 and SH-SY5Y cell lines, were significantly higher than the values for 5-

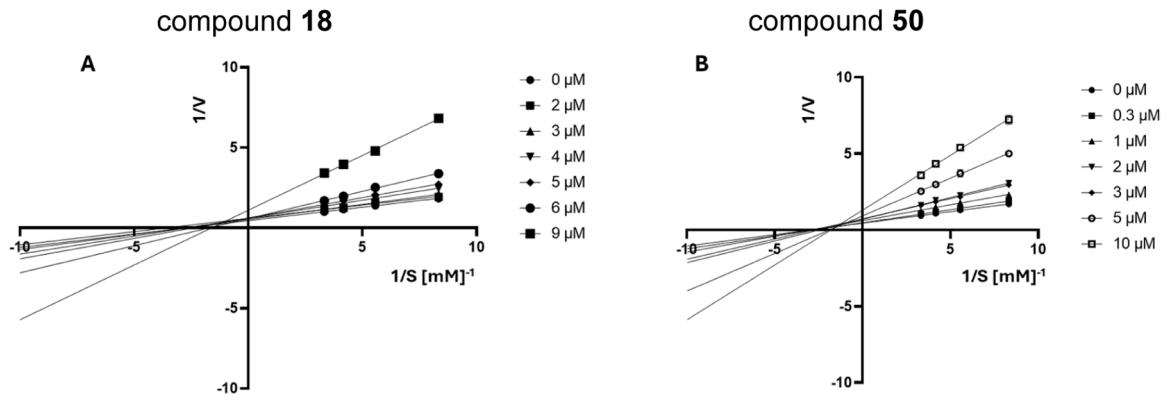

Fig. 4. Lineweaver–Burk plots of mixed-type eqBuChE inhibition by compound **18** (A) and compound **50** (B). S = butyrylthiocholine (BTC) concentration; V = initial velocity rate. The R-squared values for the linear regression range from 0.9741 to 0.9959 for compound **18** and from 0.9535 to 0.9909 for compound **50** at all tested concentrations (see supplementary material, Table S3, for further details). Experimental data are based on a single (n = 1) independent measurement per condition.

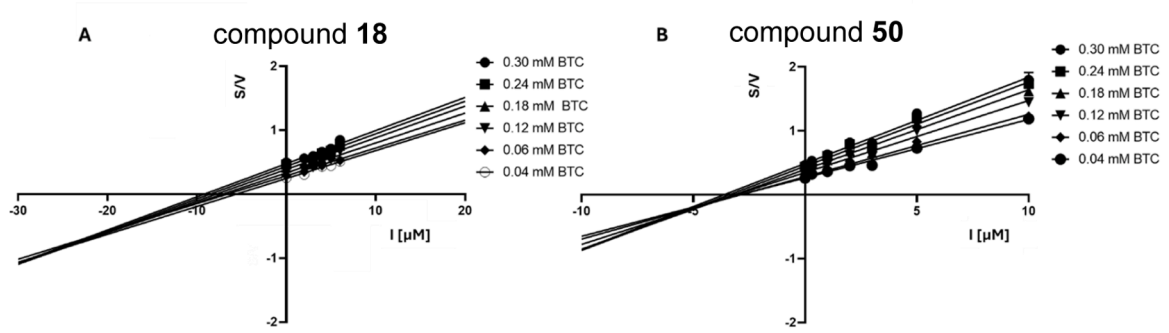

Fig. 5. Cornish−Bowden plots of mixed-type eqBuChE inhibition by compound **18** (A) and compound **50** (B). S = butyrylthiocholine (BTC) concentration; V = initial velocity rate; I = inhibitor concentration. The R-squared values for the linear regression range from 0.9073 to 0.9605 for compound **18** and from 0.9717 to 0.9900 for compound **50** at all tested concentrations (see supplementary material, Table S4, for further details). Experimental data are based on a single ($n = 1$) independent measurement per condition.

HT_7 receptor affinity or BuChE activity, which may indicate the relative safety of the molecule.

3.3.3. *CYP activity*

Compound **50** was also tested for potential drug-drug interactions, specifically by measuring its activity toward the CYP3A4 and CYP2D6 isoenzymes (Fig. 12). Both of these cytochrome P450 isoforms are among those most important for the metabolism of drugs, toxins, and other xenobiotics. Potential drugs that show high activity toward these enzymes may interact with other medications and cause various side effects. As shown in Fig. 12, the activity toward the CYP3A4 and CYP2D6 isoenzymes was at the IC_{50} level of 13.95 μM and 0.95 μM, respectively. Ketoconazole (for CYP3A4) and quinidine (for CYP2D6), as strong inhibitors, were used as reference compounds. They were found to be 126-fold stronger for CYP3A4 and 52-fold stronger for CYP2D6.

3.3.4. *Metabolic stability*

Preliminary metabolic stability was determined based on the percentage of the remaining compound after incubation with mouse liver microsomes (MLM) for 2 hours. Compound **50** and compound **40** were tested (Table 5). As mentioned in the introduction, there are several drugs in which the deuterium atom was introduced instead of the proton [36]. This modification improved the PK parameters, making this strategy potentially promising for enhancing the bioavailability of molecules. Therefore, we decided to synthesize them and test whether there would be a change in the metabolic stability of compound **24** compared to compound **40**. In terms of 5-HT_7 receptor affinity, no significant changes were observed. To our surprise, the introduction of a deuterated amine did not improve metabolic stability, and the compound still exhibited poor stability. Moreover, compound **40** showed a greater number of metabolites than compound **24**. Compound **50**, with a pyrimidine core, exhibited moderately good stability. After 2 hours of incubation with MLM, nearly 50 % of the compound remained in the tested sample. Additionally Table 5 presents the potential metabolites and identifies the sites in the molecule that are susceptible to liver enzyme activity, as illustrated by the MetaSite program (Supplement data).

3.4. *In vivo study: maximum tolerated dose and procognitive properties*

To initiate the study, a safe and effective dose for both substances for use in subsequent behavioral studies was determined. This involved conducting a Maximum Tolerated Dose (MTD) study following a modified OECD 425 guideline [58]. The purpose of this MTD study was to establish the maximum dose that can be tolerated without causing significant toxic effects for each of the new substances. This dose-finding step is crucial as it ensures animal safety during behavioral testing and provides a baseline for comparing the efficacy of the substances in cognitive enhancement and other behavioral outcomes.

Both compounds **18** and **50** demonstrated high acute toxicity at doses of 100 mg/kg, indicating that this dose far exceeded the maximum tolerated level. For both compounds, doses of 50 mg/kg and 25 mg/kg resulted in severe lethargy and mortality, suggesting that these doses were also above the tolerated threshold. However, doses of 10 mg/kg and 5 mg/kg were found to be safe for both **18** and **50**. Mice at these dose levels showed minimal or no adverse effects, which implies that these doses were within the maximum tolerated dose range. The initial mild lethargy observed at 10 mg/kg indicated that the dose was

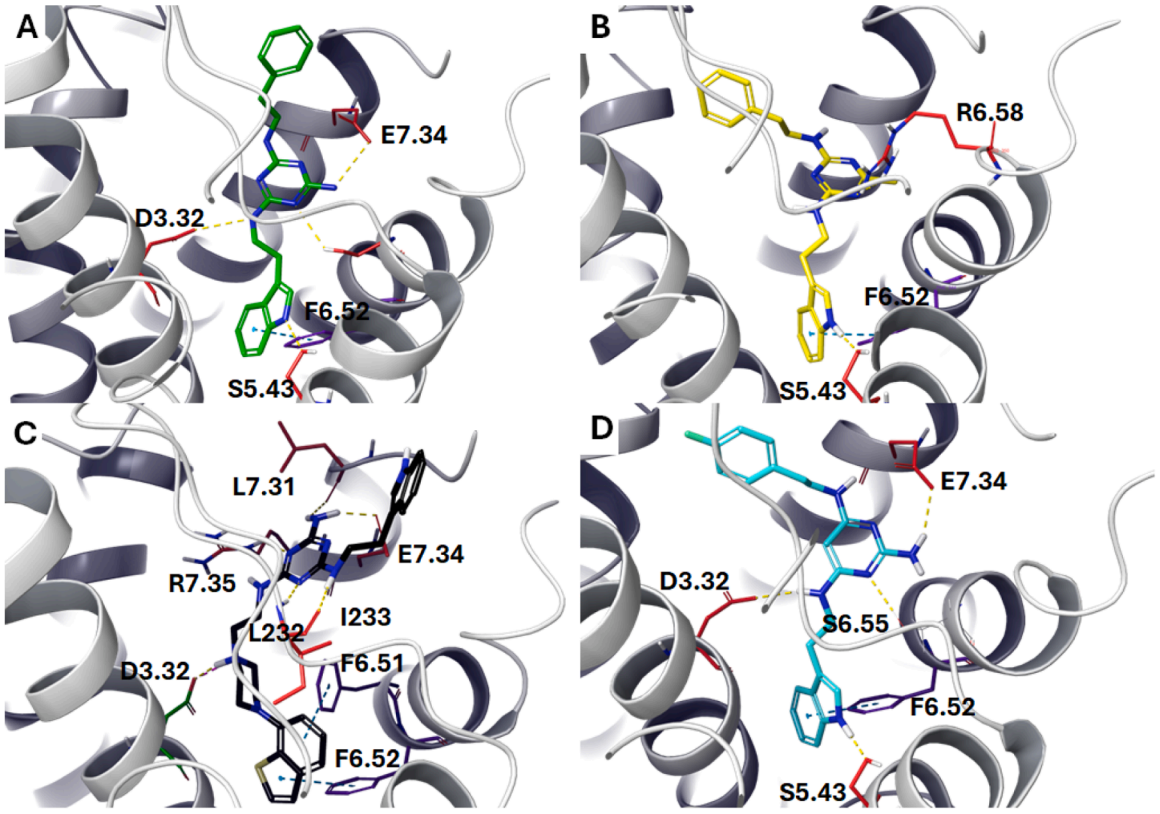

Fig. 6. Binding mode of compounds: **24** (A, green), **39** (B, yellow) **18** (C, black) and **50** (D, cyan) obtained in a docking study to the 5-HT$_7$ receptor (PDB: 7XTC). Red: amino acids responsible for the formation of hydrogen bonds. Magenta: amino acids responsible for the formation of hydrogen bons. Green: amino acid responsible for the formation of salt bridges (only in cmpd. **18**). Dotted yellow lines represent hydrogen bonds.

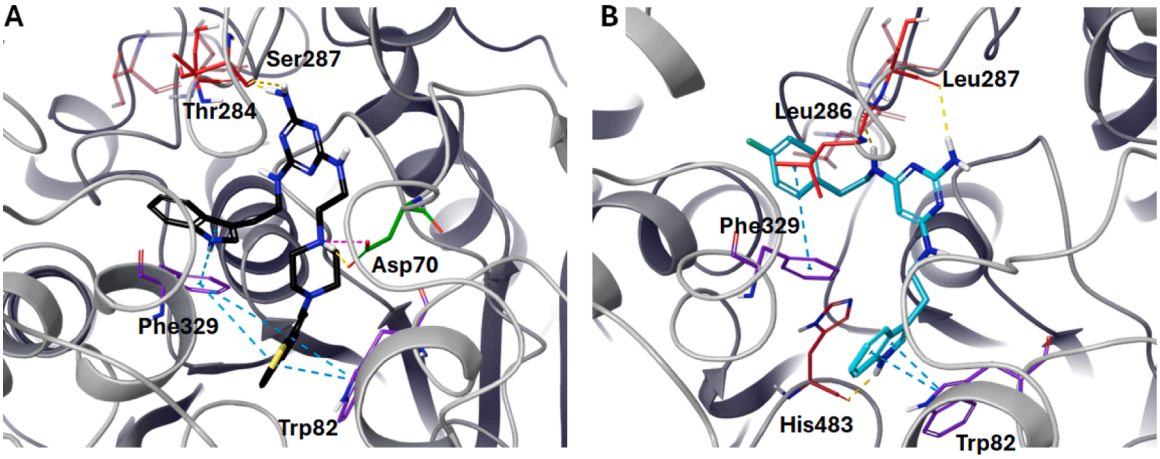

Fig. 7. Binding mode of compounds **18** (A, black) and **50** (B, cyan) obtained in a docking study to BuChE (PDB: 7AWH). Red: amino acids responsible for the formation of hydrogen bonds. Magenta: amino acids responsible for the formation of hydrogen bons. Green: amino acid responsible for the formation of salt bridges (only in cmpd. **18**). Dotted yellow lines represent hydrogen bonds. Dotted magenta lines represent salt bridges.

approaching the upper limit of safety, and 5 mg/kg appeared to be the safest dose for further studies. More details in Supplement data.

Using the safe doses of 5 mg/kg and 10 mg/kg, a locomotor activity test was conducted to ensure that the drug's effects would not significantly influence the results of subsequent behavioral testing. In these behavioral tests, such as the Passive Avoidance (PA) test, the time taken for an animal to move from one compartment of the apparatus to another is measured. If a drug were to impair the locomotor activity of the subjects, it would render the results of the PA test unreliable, as the observed effects might be due to altered movement capabilities rather than the intended cognitive function changes. Therefore, confirming that these doses do not affect basic locomotor activity is crucial for validating the efficacy and accuracy of the behavioral assays, such as those assessing memory acquisition and consolidation, which rely on the animal's ability to move freely and without impairment.

The locomotor activity tests revealed that both compounds significantly reduced movement at a dose of 10 mg/kg body weight (Fig. 13). Due to this observed impairment in locomotor function, it was determined that such doses could potentially confound the results of memory and cognitive function tests, such as those used in Passive Avoidance

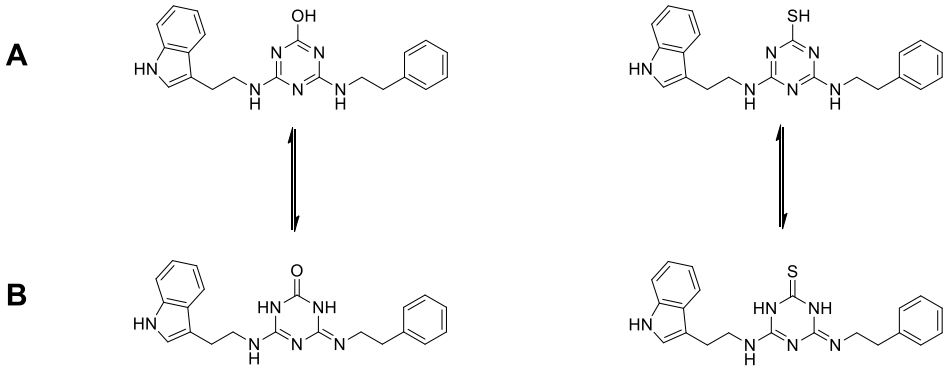

Fig. 8. Possible tautomeric state structures of the hydroxyl derivative (**37**) and the tiol derivative (**38**).

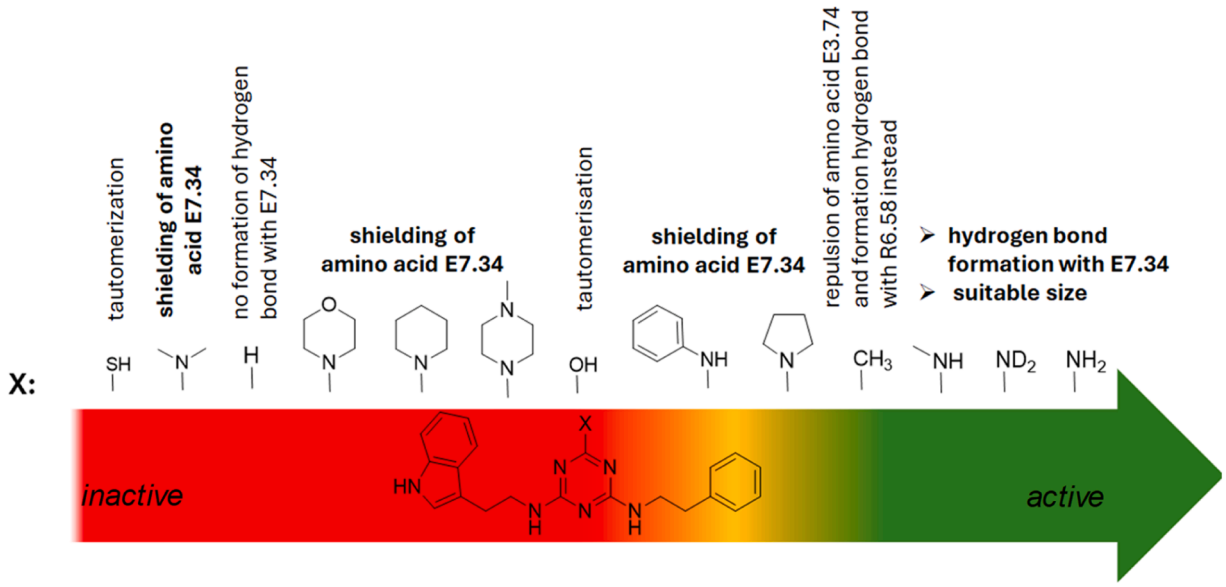

Fig. 9. Potential impact of different substituents (**X**) on binding to the 5-HT$_7$ receptor.

Table 4
18, 19, 34 and 50 screening against β-amyloid plaque formation.

Cmpd. No.	% inhibition at 100 μM
18	53 ± 3 %
19	37 ± 6 %
34	37 ± 6 %
50	31 ± 3 %
quercetin	95 ± 1 %

Each value represents the mean + /- SD of n = 4 different determination. From the statistical analysis obtained by applying the One-way ANOVA with a Bonferroni post-test, compairing alla pairs of values, all tested compounds resulted significantly different from reference compound Quercetin ($p < 0.001$ ***)

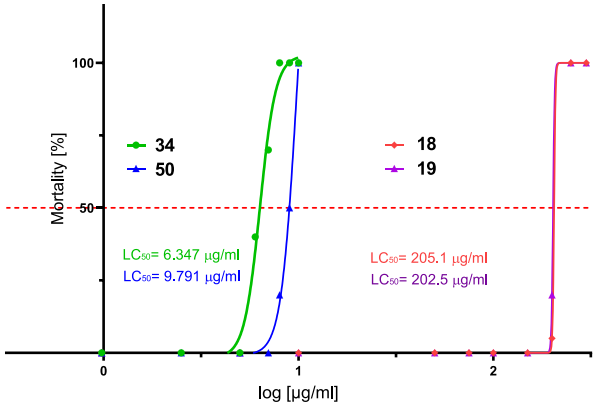

Fig. 10. Effect of compounds **18**, **19**, **34**, and **50** on *Danio rerio* mortality ($n = 10$). Experiments were performed in triplicate.

(PA) experiments, where unrestricted movement is essential for reliable results. Consequently, to minimize the risk of locomotor interference, lower doses of 2.5 mg/kg and 5 mg/kg body weight were selected for further memory testing. These adjusted doses aimed to assess the compounds' effects on memory acquisition and consolidation without the confounding factor of reduced locomotor activity.

The passive avoidance (PA) test was used to analyze cognitive enhancement. This behavioral test evaluates both the acquisition (learning) and consolidation (memory retention) phases. The test assesses the rodent's ability to learn and remember an aversive stimulus, a crucial measure of cognitive enhancement properties. Mice are placed in the light compartment of PA and then, guided by instinct, they go to the dark compartment, where they receive a mild foot shock upon entering. The time taken to enter the dark compartment (latency time) is measured both during training (acquisition phase) and on subsequent

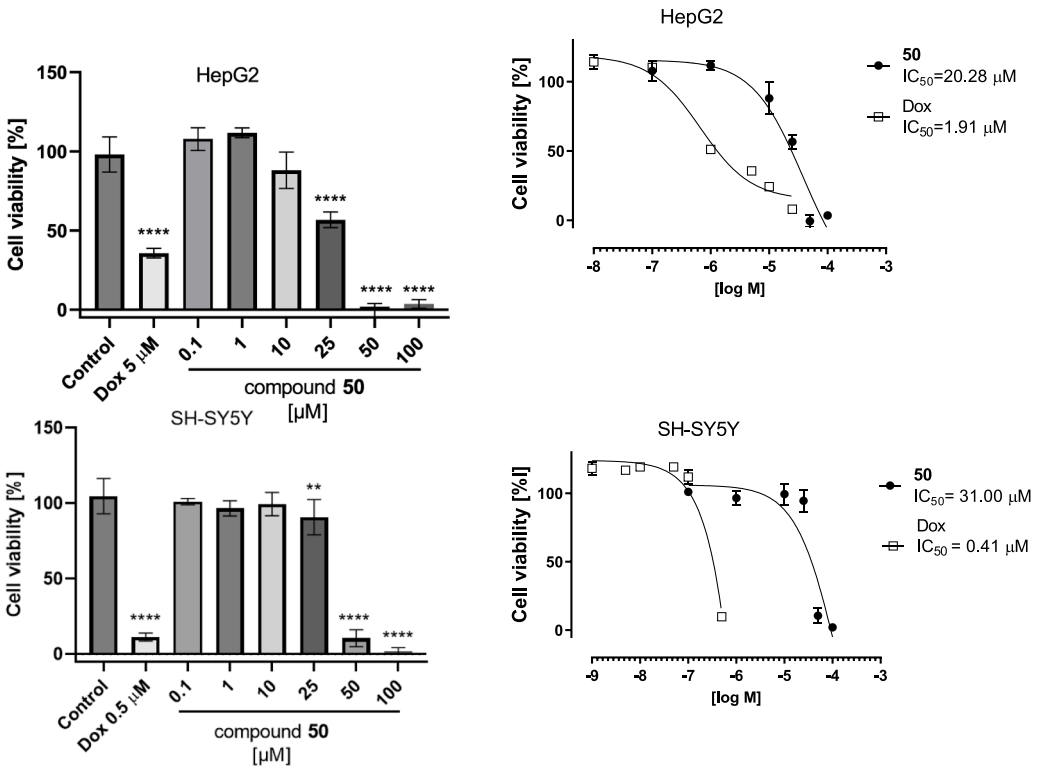

Fig. 11. Calculated IC_{50} value of **50** in hepatoma HepG2 cells and neuroblastoma SH-SY5Y cells. The statistical significance (GraphPad Prism 8.0.1) was evaluated by a one-way ANOVA, followed by Dunnett's Comparison Test. n = 8 (two independent experiments, each in quadriplicate), (**p < 0.01, ****p < 0.0001 compared with control).

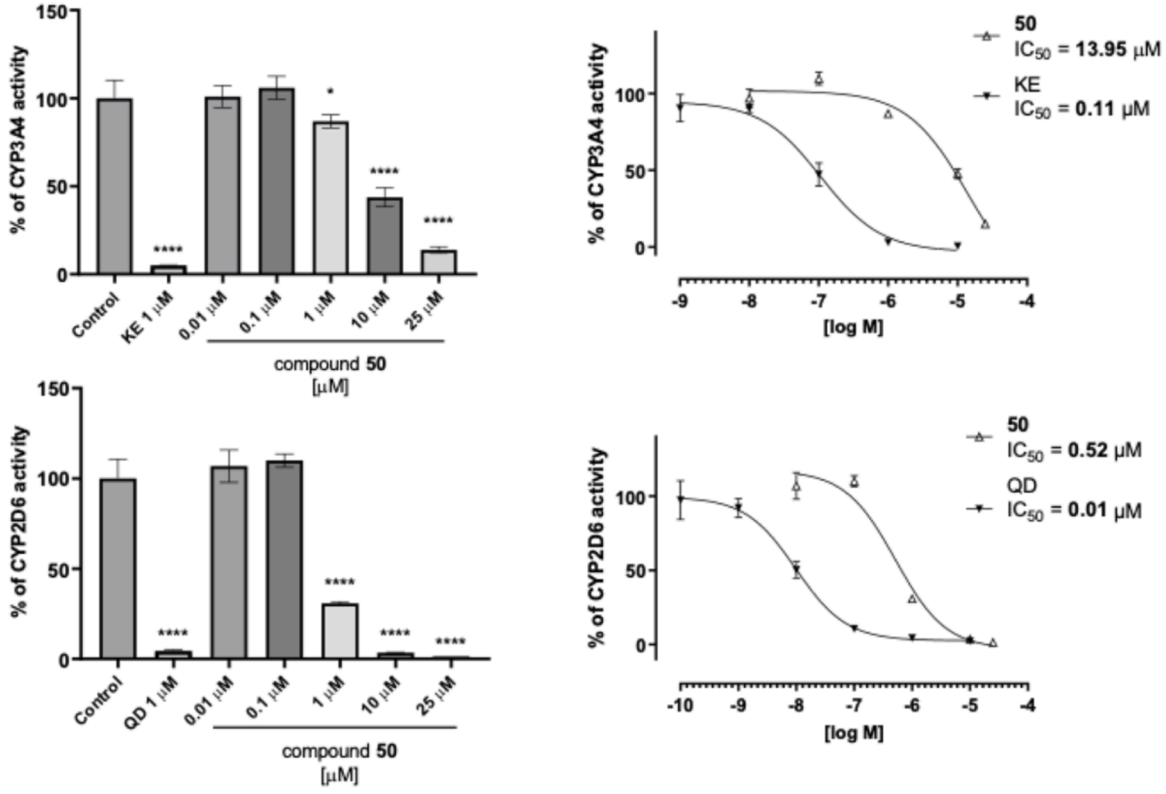

Fig. 12. Effect on CYP3A4 and CYP2D6 activity of the tested compounds and the reference inhibitors: ketoconazole (KE) and quinidine (QD). The statistical significance (GraphPad Prism 8.0.1) was evaluated by a one-way ANOVA, followed by Dunnett's Comparison Test. n = 8 (two independent experiments, each in triplicate), (*p < 0.05, ****p < 0.0001 compared with control). Incubation time 25 min for both CYP's.

Table 5
Metabolic stability summary: % remaining, molecular masses, and metabolic pathways of compounds **40** and **50** and Verapamil (reference unstable drug) after incubation with mouse liver microsomes (MLMs). Main metabolic pathways are marked in red.

Substrate	Molecular mass (*m/z*)	% remaining compound	Molecular mass of the metabolite (*m/z*)	Metabolic pathway
40	374.26	**17.84**	390.21 (**M1**)	***hydroxylation***
			406.26 (**M2**)	*double hydroxylation*
			372.27(**M3**)	*dehydrogenation*
			388.23 (**M4**)	*oxidation*
			390.29 (**M5**)	*hydroxylation*
			406.19 (**M6**)	*double hydroxylation*
			406.32 (**M7**)	*oxidation*
			388.30 (**M8**)	
50	391.29	**45.81**	407.25 (**M1**)	***hydroxylation***
			421.22 (**M2**)	*hydroxylation and oxidation*
			389.29 (**M3**)	*dehydrogenation*
			407.32 (**M4**)	*hydroxylation*
			423.35 (**M5**)	*double hydroxylation*
			407.25 (**M6**)	*hydroxylation*
			- (**M7**)	*not determined*
Verapamil	455.54	**23.93**	441.42 (**M1**)	***demethylation***
			441.42 (**M2**)	*demethylation*
			291.35 (**M3**)	*defragmentation*
			293.34 (**M4**)	*decomposition/ hydroxylation*
			277.33 (**M5**)	*defragmentation*

days (consolidation phase). By comparing the results of new substances with those from mice administered with known cognitive enhancers, such as rivastigmine, the potential of enhancing memory and learning can be determined. Rivastigmine, a well-known inhibitor of both acetylcholinesterase (AChE) and butyrylcholinesterase (BuChE), enhances cognitive function by preventing the breakdown of acetylcholine, thereby increasing its availability in the brain. The action of rivastigmine against both AChE and BuChE contributes to its effectiveness in treating cognitive symptoms in diseases such as Alzheimer's.

Our results show that there is a slight trend suggesting that compound **50** might have some memory-enhancing effects when compared to rivastigmine, particularly in the acquisition phase. However, the findings did not reach statistical significance (Fig. 14).

To further evaluate the procognitive potential of the tested substances, we sought to determine their effectiveness in reversing scopolamine-induced memory impairments (1 mg/kg body weight), focusing on both memory consolidation and acquisition. Scopolamine is a potent antagonist with high affinity for cholinergic muscarinic receptors capable of crossing the blood-brain barrier. By blocking these muscarinic receptors, scopolamine induces cognitive impairment in humans, rodents, and non-human primates. This blockade mimics the age-related degeneration of cholinergic neurons in the basal forebrain, making scopolamine a commonly used model for studying cognitive impairment *in vivo*. The induced memory deficits are particularly valuable for researching potential cognitive enhancers and understanding the mechanisms underlying memory loss associated with neurodegenerative conditions [59].

Our results indicate that compound **50** shows a significant promise in counteracting memory deficits, demonstrating efficacy in both the consolidation and acquisition phases of memory (Fig. 15). This suggests that **50** may have robust procognitive properties, making it a potential candidate for further development as a cognitive enhancer. On the other hand, compound **18** exhibited a positive effect on memory consolidation at higher doses, suggesting some procognitive capabilities in this domain. However, it failed to show significant activity in enhancing memory acquisition, indicating that its procognitive effects might be more limited or dose-dependent.

4. Conclusion

The aim of this study was to synthesize the *first-in-class* dual 5-HT$_7$ receptor antagonists with additional activity toward butyrylcholinesterase (BuChE). All compounds were obtained via quick and efficient reactions under microwave irradiation. The first set of compounds, inspired by the work of Tiwari and Hoda [33], turned out to be inactive against the 5-HT$_7$ receptor. Replacing the aniline group with tryptamine (set II) did not yield significant results, but it was demonstrated that a piperazine ring (compound **7**) directly attached to triazine could be a potentially useful motif. With a slightly modified structure, enriched with a long-chain arylpiperazine motif, it was possible to obtain compounds exhibiting activity against the 5-HT$_7$ receptor, with K_i values below 200 nM in most cases. Due to the presence of the long-chain arylpiperazine system, it was crucial that the compounds did not show significant affinity for the 5-HT$_{1A}$ receptor as an off-target. For small substituents (F, Cl), it was observed that the *para* position (for compound **11**) or the *meta* position (for compound **13**) was preferred, and the best results were obtained in the presence of a chlorine atom. The presence of heterocyclic substituents was also well tolerated. Unfortunately, in the case of 2-biphenylpiperazines (compounds **20–23**), satisfactory results were not achieved. Compounds with high affinity for the 5-HT$_7$ receptor in functional tests proved to be antagonists of this receptor. Selected active compounds were evaluated for cholinergic

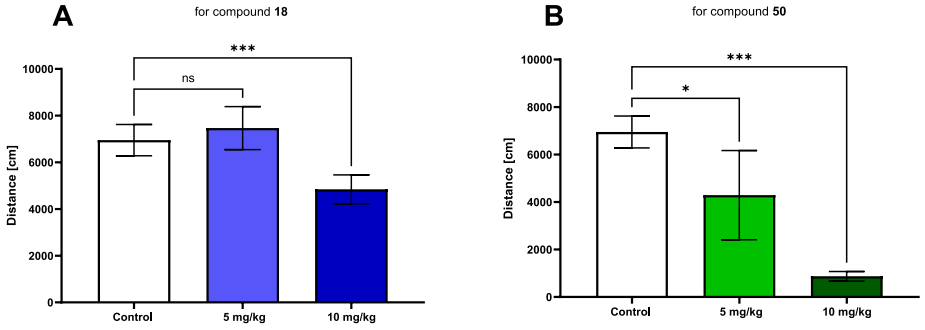

Fig. 13. Effect of tested compounds on locomotor activity. (A) Compound **18** at doses of 5 and 10 mg/kg; (B) Compound **50** at doses of 5 and 10 mg/kg; $n = 8$; One-way ANOVA followed by Tukey's post-hoc test: *$p < 0,05$, * **$p < 0.00$. ns – not statistically significant.

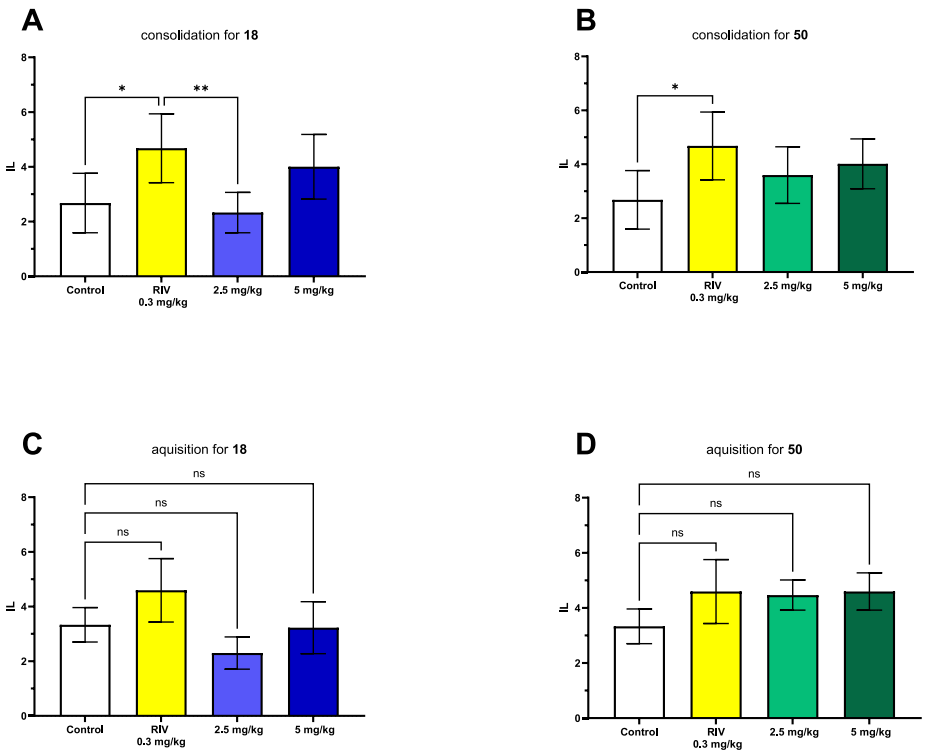

Fig. 14. Passive avoidance results for tested compounds. (A) Compound **18** at doses of 2.5 and 5 mg/kg for memory consolidation; (B) Compound **50** at doses of 2.5 and 5 mg/kg for memory consolidation; (C) Compound **18** at doses of 2.5 and 5 mg/kg for memory acquisition; (D) Compound **50** at doses of 2.5 and 5 mg/kg for memory acquisition, compared to rivastigmine (0.3 mg/kg); $n = 8$. One-way ANOVA followed by Tukey's post-hoc test: *$p < 0{,}05$, * *$p < 0.01$. RIV – rivastigmine. ns – not statistically significant.

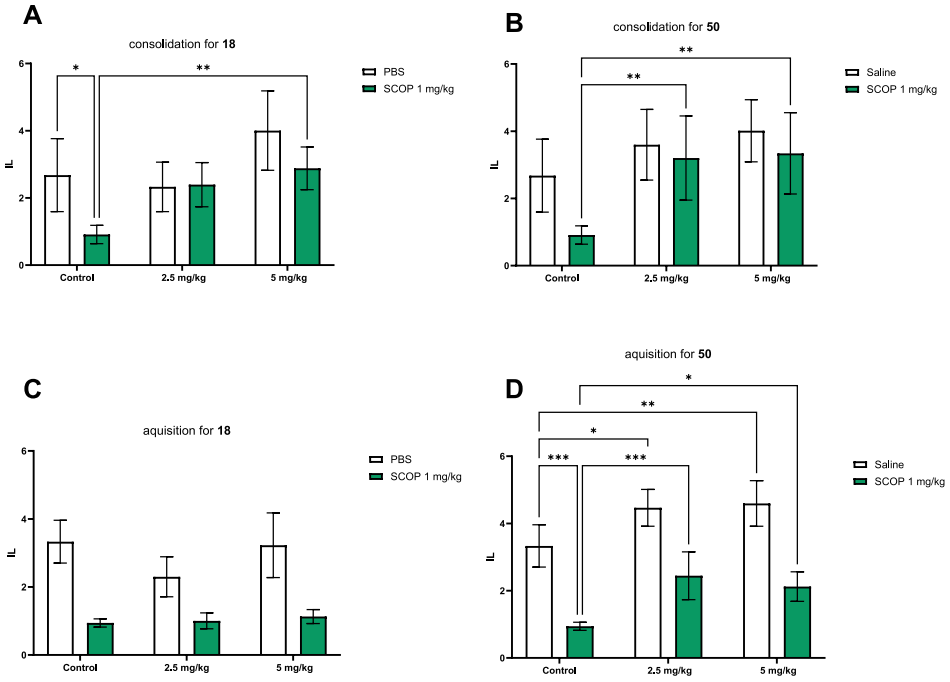

Fig. 15. Passive Avoidance results for tested compounds. (A) Compound **18** at doses of 2.5 and 5 mg/kg for memory consolidation; (B) Compound **50** at doses of 2.5 and 5 mg/kg for memory consolidation; (C) Compound **18** at doses of 2.5 and 5 mg/kg for memory acquisition; (D) Compound **50** at doses of 2.5 and 5 mg/kg for memory acquisition, following cognitive impairment induced by a single administration of scopolamine (1 mg/kg); $n = 8$. Two-way ANOVA followed by Šídák's post-hoc test: *$p < 0{,}05$, * *$p < 0.01$, * ** $p < 0.001$. SCOP – scopolamine.

activity, showing a greater tendency for BuChE activity than for AChE. Two compounds from series III, **18** and **19**, were characterized by IC_{50} values of 4.75 μM and 6.22 μM, respectively. The next two sets, IV and V, involved the modification of the aromatic system (compounds **25–32**) and the heterocyclic system (compound **33–36**) of phenylethylamine and the amino group attached to triazine, respectively. Similarly to set III, in set IV, chlorine, and especially fluorine, provided the highest affinity for the 5-HT_7 receptor. Ligands with a heterocyclic system, on the other hand, decreased receptor affinity, except for compound **34**. Replacing the amino group with another nucleophile or completely removing the substituent negatively impacted 5-HT_7 receptor affinity. Surprisingly, compound **39** with a methyl substituent turned out to be similarly active as the parent ligand **8**. Set VI appears to be very promising. The two obtained compounds with a pyrimidine core proved to be the most active among all the studied compounds, with K_i values of 1 nM. All the active compounds of set IV-VI, similarly to set III, turned out to be antagonists. The compounds also showed a preference for BuChE, with compound **50** being the most active, with an IC_{50} value of 2.53 μM. The two lead compounds, **18** and **50**, exhibit a binding mode consistent with the literature. Molecular docking suggests that the high activity of compound **39** is due to the methyl group electrostatically pushing away amino acid E7.34, while the attraction of R6.58 is observed, leading to the formation of a hydrogen bond with a length of 2.51 Å. Representative compounds **18**, **19**, **34** and **50** did not exhibit a significant potential for β-amyloid inhibition.

The above compounds were tested for general toxicity and cardiotoxicity using the *Danio rerio in vivo* model. It was found that compounds **18** and **19** with a long-chain arylpiperazine motif had low toxicity ($LD_{50} = 205.1$ μg/mL and $LD_{50} = 202.5$ μg/mL, respectively). In contrast, compounds **34** and **50** exhibited slightly higher toxicity and cardiotoxicity ($LD_{50} < 10$ μg/mL). Therefore, these compounds were subjected to more detailed ADME-Tox studies. Compound **50** demonstrated moderate hepatotoxicity and neurotoxicity, but the IC_{50} values were still 10 times higher than those for reference compounds. Studies of CYP3A4 and CYP2D6 isoenzyme activity indicated that the compounds should potentially not show drug-drug interactions. Molecule **50** also exhibited moderate metabolic stability, significantly higher than those described by us so far [31,32]. Additionally, we demonstrated that the introduction of deuterium instead of hydrogen did not improve metabolic stability. The studies performed on a mouse *in vivo* model enabled determination of the Maximum Tolerated Dose (MTD) for compounds **18** and **50** and successfully identified safe and effective dose levels for subsequent behavioral and cognitive testing. MTD studies revealed that while higher doses (25–100 mg/kg) of both compounds resulted in severe lethargy and mortality, lower doses of 10 mg/kg and 5 mg/kg were within the tolerated range, with minimal or no adverse effects observed. However, due to a significant reduction in locomotor activity at 10 mg/kg, further investigations were carried out using lower doses of 2.5 mg/kg and 5 mg/kg to minimize interference in cognitive tests.

In behavioral studies on cognitive functions, a slight trend indicated that compound **50** might enhance memory acquisition compared to the known cognitive enhancer rivastigmine, although this trend was not statistically significant. More compellingly, both **18** and **50** were evaluated for their ability to reverse scopolamine-induced memory impairments which mimic cognitive deficits through the blockade of acetylcholine receptors. Compound **18**, while showing some efficacy in improving memory consolidation at higher doses, did not demonstrate significant benefits in memory acquisition. Compound **50** demonstrated considerable potential in reversing these impairments, effectively enhancing both memory consolidation and acquisition. This points to a more limited or dose-dependent procognitive effect of **18**, potentially restricting its application compared to **50**. Overall, these findings highlight the potential of compound **50**, particularly in reversing cognitive impairments caused by scopolamine, and support its further exploration as a candidate for cognitive enhancement therapies. The conducted pilot studies indicate a promising potential of a dual molecule exhibiting 5-HT_7 receptor antagonism with simultaneous BuChE inhibition, which could have potential applications in CNS disorders, particularly in Alzheimer's disease. Nevertheless, ongoing chemical and pharmacological studies will provide more data on the use of the 5-HT_7R/BuChE strategy in the disease.

Author contributions

These authors contributed equally.

CRediT authorship contribution statement

Jaśkowska Jolanta: Writing – review & editing. **Zaręba Przemysław:** Visualization, Methodology, Investigation. **Plażuk Damian:** Writing – review & editing, Investigation. **Sudoł-Tałaj Sylwia:** Methodology, Investigation. **Boguszewska-Czubara Anna:** Methodology, Investigation. **Purgatorio Rosa:** Methodology, Investigation. **de Candia Modesto:** Writing – review & editing, Methodology, Investigation. **Więckowska Anna:** Writing – review & editing. **Zaręba Paula:** Visualization, Software, Methodology, Investigation. **Drabczyk Anna:** Software, Methodology, Investigation. **Latacz Gniewomir:** Writing – review & editing, Methodology, Investigation. **Kułaga Damian:** Writing – review & editing, Writing – original draft, Visualization, Validation, Supervision, Software, Resources, Project administration, Methodology, Investigation, Funding acquisition, Formal analysis, Data curation, Conceptualization. **Satała Grzegorz:** Methodology, Investigation.

Declaration of Competing Interest

The authors declare the following financial interests/personal relationships which may be considered as potential competing interests: Damian Kulaga reports financial support was provided by Cracow University of Technology. If there are other authors, they declare that they have no known competing financial interests or personal relationships that could have appeared to influence the work reported in this paper.

Acknowledgements

The entire research study (organic synthesis, *in vitro* screening, *in vivo* screening and molecular modelling) was funded by the National Center for Research and Development (Project No. LIDER/41/0206/L-12/20/NCBR/2021). The hepatotoxicity and neurotoxicity studies were carried out with the use of research infrastructure co-financed by the Smart Growth Operational Programme POIR 4.2 project no. POIR.04.02.00–00-D023/20.

Supporting information

The document contains: all spectra, physiochemical properties of intermediates, synthesis protocols, cardiotoxicity in the *Danio rerio in vivo* model for **34**, **50**, **18** and **19**, cell morphology changes under compound **50** treatment, toxicity in the mouse model and the R-squared values for the linear regression.

Appendix A. Supporting information

Supplementary data associated with this article can be found in the online version at doi:10.1016/j.biopha.2025.117995.

Data availability

Data will be made available on request.

References

[1] X.X. Zhang, Y. Tian, Z.T. Wang, Y.H. Ma, L. Tan, J.T. Yu, The Epidemiology of Alzheimer's disease: modifiable risk factors and prevention, J. Prev. Alzheimers Dis. 8 (3) (2021) 313–321, https://doi.org/10.14283/jpad.2021.15.

[2] 2024 Alzheimer's Disease Facts and Figures. *Alzheimers Dement.* 2024, *20* (5), 3708–3821,doi: 10.1002/alz.13809.

[3] S.H. Barage, K.D. Sonawane, Amyloid cascade hypothesis: pathogenesis and therapeutic strategies in Alzheimer's disease, Neuropeptides 52 (2015) 1–18, https://doi.org/10.1016/j.npep.2015.06.008.

[4] Y. Zhang, H. Chen, R. Li, K. Sterling, W. Song, Amyloid β-based therapy for Alzheimer's disease: challenges, successes, and future, Sig. Transduct. Target. Ther. 8 (2023) 248, https://doi.org/10.1038/s41392–023–01484–7.

[5] F. Panza, M. Lozupone, The challenges of anti-tau therapeutics in Alzheimer disease, Nat. Rev. Neurol. 18 (9) (2022) 577–578, https://doi.org/10.1038/s41582–022–00702–0.

[6] G. Marucci, M. Buccioni, D.D. Ben, C. Lambertucci, R. Volpini, F. Amenta, Neuropharmacology 190 (2021) 108352,, https://doi.org/10.1016/j.neuropharm.2020.108352.

[7] T.H. Ferreira-Vieira, I.M. Guimaraes, F.R. Silva, F.M. Ribeiro, Alzheimer's disease: targeting the cholinergic system, Curr. Neuropharmacol. 14 (1) (2016) 101–115, https://doi.org/10.2174/1570159x13666150716165726.

[8] F. Amenta, L. Parnetti, V. Gallai, A. Wallin, Treatment of cognitive dysfunction associated with Alzheimer's disease with cholinergic precursors: ineffective treatments or inappropriate approaches? Mech. Ageing Dev. 122 (16) (2001) 2025–2040, https://doi.org/10.1016/S0047–6374(01)00310–4.

[9] E. Perry, I. McKeith, C. Ballard, Butyrylcholinesterase and progression of cognitive deficits in dementia with lewy bodies, Neurology 60 (11) (2003) 1852–1853, https://doi.org/10.1212/01.wnl.0000068336.84399.9e.

[10] G. Marucci, M. Buccioni, D. Dal Ben, C. Lambertucci, R. Volpini, F. Amenta, Efficacy of acetylcholinesterase inhibitors in Alzheimer's disease, Neuropharmacology 190 (2021) 108352, https://doi.org/10.1016/j.neuropharm.2020.108352.

[11] R.A. Hansen, G. Gartlehner, A.P. Webb, L.C. Morgan, C.G. Moore, D.E. Jonas, Efficacy and safety of donepezil, galantamine, and rivastigmine for the treatment of Alzheimer's disease: a systematic review and meta-analysis, Clin. Interv. Aging 3 (2) (2008) 211–225, https://doi.org/10.2147/cia.S12159936.

[12] K.Z. Peters, J.F. Cheer, R. Tonini, Modulating the neuromodulators: dopamine, serotonin, and the endocannabinoid system, Trends Neurosci. 44 (6) (2021) 464–477, https://doi.org/10.1016/j.tins.2021.02.001.

[13] M. Butzlaff, E. Ponimaskin, The role of serotonin receptors in Alzheimer's disease, Opera Med. Physiol. 2 (1) (2016) 77–86, https://doi.org/10.20388/OMP2016.001.0018.

[14] J.A. González-Vera, R.A. Medina, M. Martín-Fontecha, A. Gonzalez, T. de la Fuente, H. Vázquez-Villa, J. García-Cárceles, J. Botta, P.J. McCormick, B. Benhamú, L. Pardo, M.L. López-Rodríguez, A new serotonin 5-HT$_6$ receptor antagonist with procognitive activity – importance of a halogen bond interaction to stabilize the binding, Sci. Rep. 7 (2017) 41293, https://doi.org/10.1038/srep41293.

[15] P. Pyka, W. Haberek, M. Więcek, E. Szymańska, W. Ali, A. Cios, M. Jastrzębska-Więsek, G. Satała, S. Podlewska, S. Di Giacomo, A. Di Sotto, S. Garbo, T. Karcz, C. Lambona, F. Marocco, G. Latacz, S. Sudoł-Tałaj, B. Mordyl, M. Głuch-Lutwin, A. Siwek, K. Czarnota-Łydka, D. Gogola, A. Olejarz-Maciej, N. Wilczyńska-Zawal, E. Honkisz-Orzechowska, M. Starek, M. Dąbrowska, K. Kucwaj-Brysz, R. Fioravanti, M.J. Nasim, M. Hittinger, A. Partyka, A. Wesołowska, C. Battistelli, C. Zwergel, J. Handzlik, First-in-class selenium-containing potent serotonin receptor 5-HT$_6$ agents with a beneficial neuroprotective profile against Alzheimer's disease, J. Med. Chem. 67 (2) (2024) 1580–1610, https://doi.org/10.1021/acs.jmedchem.3c02148.

[16] D.V. Eremin, E.M. Kondaurova, A.Y. Rodnyy, C.A. Molobekova, D.A. Kudlay, V. S. Naumenko, Serotonin receptors as a potential target in the treatment of Alzheimer's disease, *Biochem.* Mosc. 88 (2023) 2023–2042, https://doi.org/10.1134/S0006297923120064.

[17] I.X. Lou, J. Chen, K. Ali, A.L. Shaikh, Q. Chen, Mapping new pharmacological interventions for cognitive function in Alzheimer's disease: a systematic review of randomized clinical trials, Front. Pharmacol. 14 (2023), https://doi.org/10.3389/fphar.2023.1190604.

[18] M. Solas, D. Van Dam, J. Janssens, U. Ocariz, Y. Vermeiren, P.P. De Deyn, M. J. Ramirez, 5-HT$_7$ receptors in Alzheimer's disease, Neurochem. Int. 150 (2021) 105185, https://doi.org/10.1016/j.neuint.2021.105185.

[19] A. Quintero-Villegas, S.I. Valdés-Ferrer, Central nervous system effects of 5-HT$_7$ receptors: a potential target for neurodegenerative Diseases, Mol. Med. 28 (1) (2022) 70, https://doi.org/10.1186/s10020–022–00497–2.

[20] K. Jahreis, A. Brüge, S. Borsdorf, F.E. Müller, W. Sun, S. Jia, D.M. Kang, N. Boesen, S. Shin, S. Lim, A. Koroleva, G. Satała, A.J. Bojarski, E. Rakuša, A. Fink, G. Doblhammer-Reiter, Y.K. Kim, A. Dityatev, E. Ponimaskin, J. Labus, Amisulpride as a potential disease-modifying drug in the treatment of tauopathies, Alzheimers Dement 19 (12) (2023) 5482–5497, https://doi.org/10.1002/alz.13090.

[21] K. Kucwaj-Brysz, H. Baltrukevich, K. Czarnota, J. Handzlik, Chemical Update on the potential for serotonin 5-HT$_6$ and 5-HT$_7$ receptor agents in the treatment of Alzheimer's disease, Bioorg. Med. Chem. Lett. 49 (2021) 128275, https://doi.org/10.1016/j.bmcl.2021.128275.

[22] J. Labus, K.F. Röhrs, J. Ackmann, H. Varbanov, F.E. Müller, S. Jia, K. Jahreis, A. L. Vollbrecht, M. Butzlaff, Y. Schill, D. Guseva, K. Böhm, R. Kaushik, M. Bijata, P. Marin, S. Chaumont-Dubel, A. Zeug, A. Dityatev, E. Ponimaskin, Amelioration of tau pathology and memory deficits by targeting 5-HT$_7$ receptor, Prog. Neurobiol. 197 (2021) 101900, https://doi.org/10.1016/j.pneurobio.2020.101900.

[23] M.T. Gabr, S. Brogi, MicroRNA-based multitarget approach for Alzheimer's disease: discovery of the first-in-class dual inhibitor of acetylcholinesterase and MicroRNA-15b biogenesis, J. Med. Chem. 63 (17) (2020) 9695–9704, https://doi.org/10.1021/acs.jmedchem.0c00756.

[24] Ch Pathak, U.D. Kabra, A comprehensive review of multi-target directed ligands in the treatment of Alzheimer's disease, Bioorg. Chem. 144 (2024) 107152, https://doi.org/10.1016/j.bioorg.2024.107152.

[25] I. Góral, T. Wichur, E. Sługocka, J. Godyń, N. Szałaj, P. Zaręba, M. Głuch-Lutwin, B. Mordyl, D. Panek, A. Więckowska, Connecting GSK-3β inhibitory activity with IKK-β or ROCK-1 inhibition to target tau aggregation and neuroinflammation in Alzheimer's disease—discovery, *In Vitro* and *In Cellulo* activity of thiazole-based inhibitors, Molecules 29 (11) (2024) 2616, https://doi.org/10.3390/molecules29112616.

[26] K. Czarnota-Łydka, S. Sudoł-Tałaj, K. Kucwaj-Brysz, R. Kurczab, G. Satała, M. de Candia, F. Samarelli, C.D. Altomare, A. Carocci, A. Barbarossa, E. Żesławska, M. Głuch-Lutwin, B. Mordyl, M. Kubacka, N. Wilczyńska-Zawal, M. Jastrzębska-Więsek, A. Partyka, N. Khan, M. Więcek, W. Nitek, E. Honkisz-Orzechowska, G. Latacz, A. Wesołowska, A. Carrieri, J. Handzlik, Synthesis, Computational and experimental pharmacological studies for (Thio)Ether-Triazine 5-HT$_6$R ligands with noticeable action on AChE/BChE and chalcogen-dependent intrinsic activity in search for new class of drugs against Alzheimer's disease, Eur. J. Med. Chem. 259 (2023) 115695, https://doi.org/10.1016/j.ejmech.2023.115695.

[27] K. Kucwaj-Brysz, W. Ali, R. Kurczab, S. Sudoł-Tałaj, N. Wilczyńska-Zawal, M. Jastrzębska-Więsek, G. Satała, B. Mordyl, E. Żesławska, A. Olejarz-Maciej, K. Czarnota, G. Latacz, A. Partyka, A. Wesołowska, W. Nitek, J. Handzlik, An exit beyond the pharmacophore model for 5-HT$_6$R agents—a new strategy to gain dual 5-HT$_6$/5-HT$_{2A}$ action for triazine derivatives with procognitive potential, Bioorg. Chem. 121 (2022) 105695, https://doi.org/10.1016/j.bioorg.2022.105695.

[28] A. Pasieka, D. Panek, P. Zaręba, E. Sługocka, N. Gucwa, A. Espargaró, G. Latacz, N. Khan, A. Bucki, R. Sabaté, A. Więckowska, B. Malawska, Novel drug-like fluorenyl derivatives as selective butyrylcholinesterase and β-amyloid inhibitors for the treatment of Alzheimer's disease, 117333, Bioorg. Med. Chem. (2023) *88–89*, https://doi.org/10.1016/j.bmc.2023.117333.

[29] R.J. Mattson, D.J. Denhart, J.D. Catt, M.F. Dee, J.A. Deskus, J.L. Ditta, J. Epperson, H.D. King, A. Gao, M.A. Poss, A. Purandare, D. Tortolani, Y. Zhao, H. Yang, S. Yeola, J. Palmer, J. Torrente, A. Stark, G. Johnson, Aminotriazine 5-HT$_7$ antagonists, Bioorg. Med. Chem. Lett. 14 (16) (2004) 4245–4248, https://doi.org/10.1016/j.bmcl.2004.06.008.

[30] J.-b Su, W.-l Wu, C.-E. Dong, S. Yang, Y.-y Feng, T. Qin, K.-q Chen, J.-j Qian, J.-p Zou, Y.-H. Liu, S.-m Liu, W.-W. Liu, D.-H. Shi, Synthesis, Characterization, crystal structure, and biological evaluation of 1,3,5-triazine-quinoline derivatives as butyrylcholinesterase inhibitors, J. Mol. Struct. 1274 (Part 2) (2023) 134391, https://doi.org/10.1016/j.molstruc.2022.134391.

[31] D. Kułaga, A.K. Drabczyk, G. Satała, G. Latacz, K. Rózga, D. Plażuk, J. Jaśkowska, Design and synthesis of new potent 5-HT$_7$ receptor ligands as a candidate for the treatment of central nervous system diseases, Eur. J. Med. Chem. 227 (2022) 113931, https://doi.org/10.1016/j.ejmech.2021.113931.

[32] D. Kułaga, A.K. Drabczyk, G. Satała, G. Latacz, A. Boguszewska-Czubara, D. Plażuk, J. Jaśkowska, Design, synthesis, and biological evaluation of novel 1,3,5-triazines: effect of aromatic ring decoration on affinity to 5-HT$_7$ receptor, Int. J. Mol. Sci. 23 (21) (2022) 13308, https://doi.org/10.3390/ijms232113308.

[33] E. Jameel, P. Meena, M. Maqbool, J. Kumar, W. Ahmed, S. Mumtazuddin, M. Tiwari, N. Hoda, B. Jayaram, Rational Design, Synthesis, and biological screening of triazine-triazolopyrimidine hybrids as multitarget anti-alzheimer agents, Eur. J. Med. Chem. 136 (2017) 36–51, https://doi.org/10.1016/j.ejmech.2017.04.064.

[34] D. Kułaga, J. Jaśkowska, G. Satała, G. Latacz, P. Śliwa, Aminotriazines with indole motif as novel 5-HT$_7$ receptor ligands with atypical binding mode, Bioorg. Chem. 104 (2020) 104254, https://doi.org/10.1016/j.bioorg.2020.104254.

[35] E. Lacivita, D. Patarnello, N. Stroth, A. Caroli, M. Niso, M. Contino, P. De Giorgio, P. Di Pilato, N.A. Colabufo, F. Berardi, R. Perrone, P. Svenningsson, P.B. Hedlund, M. Leopoldo, Investigations on the 1-(2-Biphenyl)piperazine motif: identification of new potent and selective ligands for the serotonin7 (5-HT$_7$) receptor with agonist or antagonist action in vitro or ex vivo, J. Med. Chem. 55 (14) (2012) 6375–6380, https://doi.org/10.1021/jm3003679.

[36] R.M.C. Di Martino, B.D. Maxwell, T. Pirali, Deuterium in drug discovery: progress, opportunities, and challenges, Nat. Rev. Drug Discov. 22 (8) (2023) 562–584, https://doi.org/10.1038/s41573–023–00703–8.

[37] D. Kułaga, A.K. Drabczyk, P. Zaręba, J. Jaśkowska, J. Chrzan, K.E. Greber, K. Ciura, D. Plażuk, E. Wielgus, Green synthesis of 1,3,5-triazine derivatives using a sonochemical protocol, Ultrason. Sonochem. 108 (2024) 106951, https://doi.org/10.1016/j.ultsonch.2024.106951.

[38] D. Kułaga, J. Jaśkowska, G. Satała, New derivatives of indoleaminotriazines and method of their production, PL433527A1 (Oct 11, 2021).

[39] N.R. Pai, D.S. Dubhashi, S. Vishwasrao, D. Pusalkar, An efficient synthesis of neuroleptic drugs under microwave irradiation, J. Chem. Pharm. Res. 2 (5) (2010) 506–517.

[40] J.D. Wuest, O. Lebel, Anarchy in the solid state: structural dependence on glass-forming ability in triazine-based molecular glasses, Tetrahedron 65 (36) (2009) 7393–7402, https://doi.org/10.1016/j.tet.2009.07.026.

[41] A.S. Hogendorf, A. Hogendorf, R. Kurczab, G. Satała, T. Lenda, M. Walczak, G. Latacz, J. Handzlik, K. Kieć-Kononowicz, J.M. Wierońska, M. Woźniak, P. Cieślik, R. Bugno, J. Staroń, A.J. Bojarski, Low-basicity 5-HT$_7$ receptor agonists

synthesized using the van leusen multicomponent protocol, Sci. Rep. 7 (1) (2017) 1444, https://doi.org/10.1038/s41598–017–00822–4.
[42] D. Łażewska, P. Zaręba, J. Godyń, A. Doroz-Płonka, A. Frank, D. Reiner-Link, M. Bajda, D. Stary, S. Mogilski, A. Olejarz-Maciej, et al., Biphenylalkoxyamine derivatives–histamine H_3 receptor ligands with butyrylcholinesterase inhibitory activity, Molecules 26 (2021) 3580, https://doi.org/10.3390/molecules26123580.
[43] Y. Cheng, W.H. Prusoff, Relationship between the inhibition constant (K_i) and the concentration of inhibitor which causes 50 percent inhibition (IC_{50}) of an enzymatic reaction, Biochem. Pharmacol. 22 (23) (1973) 3099–3108, https://doi.org/10.1016/0006–2952(73)90196–2.
[44] N.A. Meanwell, The influence of bioisosteres in drug design: tactical applications to address developability problems, Tactics Contemp. Drug Des. 9 (2014) 283–381, https://doi.org/10.1007/7355_2013_29. Erratum in: https://doi.org/10.1007/7355_2014_74.
[45] N.A. Meanwell, Fluorine and fluorinated motifs in the design and application of bioisosteres for drug design, J. Med. Chem. 61 (14) (2018) 5822–5880, https://doi.org/10.1021/acs.jmedchem.7b01788.
[46] H. Ogura, T. Kosasa, Y. Kuriya, Y. Yamanishi, Comparison of inhibitory activities of donepezil and other cholinesterase inhibitors on acetylcholinesterase and butyrylcholinesterase in vitro, Methods Find. Exp. Clin. Pharmacol. 22 (8) (2000) 609–613, https://doi.org/10.1358/mf.2000.22.8.701373.
[47] S. Huang, P. Xu, D.D. Shen, I.A. Simon, C. Mao, Y. Tan, H. Zhang, K. Harpsoe, H. Li, Y. Zhang, C. You, X. Yu, Y. Jiang, Y. Zhang, D.E. Gloriam, H.E. Xu, Serotonin 7 (5-HT_7) receptor-Gs-Nb35 complex. PDB ID: 7XTC, Mol. Cell 82 (14) (2022) 2681–2695, https://doi.org/10.2210/pdb7xtc/pdb, https://doi.org/10.1016/j.molcel.2022.05.031.
[48] P. Zaręba, K. Łątka, G. Mazur, B. Gryzło, A. Pasieka, J. Godyń, D. Panek, A. Skrzypczak-Wiercioch, G.C. Höfner, G. Latacz, M. Maj, A. Espargaró, R. Sabaté, K. Jóźwiak, K.T. Wanner, K. Sałat, B. Malawska, K. Kulig, M. Bajda, Discovery of novel multifunctional ligands targeting GABA transporters, butyrylcholinesterase, β-secretase, and amyloid β aggregation as potential treatment of Alzheimer's disease, Eur. J. Med. Chem. 261 (2023) 115832, https://doi.org/10.1016/j.ejmech.2023.115832.
[49] D. Panek, A. Pasieka, G. Latacz, P. Zaręba, M. Szczęch, J. Godyń, F. Chantegreil, F. Nachon, X. Brazzolotto, A. Skrzypczak-Wiercioch, M. Walczak, M. Smolik, K. Sałat, G. Höfner, K. Wanner, A. Więckowska, B. Malawska, Discovery of new, highly potent and selective inhibitors of BuChE: design, synthesis, in vitro and in vivo evaluation, and crystallography studies, Eur. J. Med. Chem. 249 (2023) 115135, https://doi.org/10.1016/j.ejmech.2023.115135.
[50] F. Samarelli, R. Purgatorio, G. Lopopolo, C. Deruvo, M. Catto, M. Andresini, A. Carrieri, O. Nicolotti, A. De Palma, D.V. Miniero, M. de Candia, C.D. Altomare, Novel 6-Alkyl-Bridged 4-Arylalkylpiperazin-1-yl derivatives of azepino[4,3-b]indol-1(2H)-one as potent BChE-selective inhibitors showing protective effects against neurodegenerative insults, Eur. J. Med. Chem. 270 (2024) 116353, https://doi.org/10.1016/j.ejmech.2024.116353.
[51] R. Purgatorio, L.N. Kulikova, L. Pisani, M. Catto, M. de Candia, A. Carrieri, S. Cellamare, A. De Palma, A.A. Beloglazkin, G.R. Raesi, L.G. Voskressensky, C. D. Altomare, Scouting around 1,2,3,4-tetrahydrochromeno[3,2-c]pyridin-10-ones for single- and multitarget ligands directed towards relevant alzheimer's targets, ChemMedChem 15 (20) (2020) 1947–1955, https://doi.org/10.1002/cmdc.202000468.
[52] R. Purgatorio, M. de Candia, M. Catto, A. Carrieri, L. Pisani, A. De Palma, M. Toma, O.A. Ivanova, L.G. Voskressensky, C.D. Altomare, Investigating 1,2,3,4,5,6-Hexahydroazepino[4,3-b]indole as a scaffold of butyrylcholinesterase-selective inhibitors with additional neuroprotective activities for Alzheimer's disease, Eur. J. Med. Chem. 177 (2019) 414–424, https://doi.org/10.1016/j.ejmech.2019.05.062.
[53] R. Purgatorio, M. de Candia, A. De Palma, F. De Santis, L. Pisani, F. Campagna, S. Cellamare, C.D. Altomare, M. Catto, Insights into structure-activity relationships of 3-arylhydrazonoindolin-2-one derivatives for their multitarget activity on β-amyloid aggregation and neurotoxicity, Molecules 23 (7) (2018) 1544, https://doi.org/10.3390/molecules23071544.
[54] R. Purgatorio, N. Gambacorta, M. Catto, M. de Candia, L. Pisani, A. Espargaró, R. Sabaté, S. Cellamare, O. Nicolotti, C.D. Altomare, Pharmacophore modeling and 3D-QSAR study of indole and isatin derivatives as antiamyloidogenic agents targeting Alzheimer's disease, Molecules 25 (23) (2020) 5773, https://doi.org/10.3390/molecules25235773.
[55] D. Sun, W. Gao, H. Hu, S. Zhou, Why 90% of clinical drug development fails and how to improve it? Acta Pharm. Sin. B 12 (7) (2022) 3049–3062, https://doi.org/10.1016/j.apsb.2022.02.002.
[56] M.V. Caballero, M. Candiracci, Zebrafish as screening model for detecting toxicity and drug efficacy, J. Unexplored Med. Data 3 (4) (2018), https://doi.org/10.20517/2572–8180.2017.15.
[57] Busquet, F.; Halder, B.T.; Braunbeck, T.; Gourmelon, L.A.; Kleensang, A.; Belanger, S.; Carr, G.; Walter-rohde, S. *OECD Guidlines forthe Testing of Chemicals 236—Fish Embryo Acute Toxicity (FET) Test*; The OECD Observer; Organisation for Economic Co-operationand Development: Paris, France, 2013.
[58] OECD. *Test No. 425: Acute Oral Toxicity: Up-and-Down Procedure*, OECD Guidelines for the Testing of Chemicals, Section 4, OECD Publishing, Paris, 2022, https://doi.org/10.1787/9789264071049-en.
[59] J. Kowalczyk, Ł. Kurach, A. Boguszewska-Czubara, K. Skalicka-Woźniak, M. Kruk-Słomka, J. Kurzepa, M. Wydrzynska-Kuźma, G. Biała, A. Skiba, B. Budzyńska, Bergapten improves scopolamine-induced memory impairment in mice via cholinergic and antioxidative mechanisms, Front. Neurosci. 14 (2020) 730, https://doi.org/10.3389/fnins.2020.00730.
[60] G.L. Ellman, K.D. Courtney, V. Andres, R.M. Featherstone, A new and rapid colorimetric determination of acetylcholinesterase activity, Biochem. Pharmacol. 7 (1961) 88–95, https://doi.org/10.1016/0006–2952(61)90145–9.
[61] B.R. Brooks, C.L. Brooks, I.I.I. Mackerell, A.D. Nilsson Jr., L. Petrella, R.J. Roux, B. Won, Y. Archontis, G. Bartels, C. Boresch, S. Caflisch, A. Caves, L. Cui, Q. Dinner, A.R. Feig, M. Fischer, S. Gao, J. Hodoscek, M. Im, W. Kuczera, K. Lazaridis, T. Ma, J. Ovchinnikov, V. Paci, E. Pastor, R.W. Post, C.B. Pu, J.Z. Schaefer, M. Tidor, B. Venable, R.M. Woodcock, H.L. Wu, X. Yang, W. York, D.M. Karplus, M. CHARMM: the biomolecular simulation program, J. Comput. Chem. 30 (10) (2009) 1545–1614, https://doi.org/10.1002/jcc.21287.
[62] K. Vanommeslaeghe, E. Hatcher, C. Acharya, S. Kundu, S. Zhong, J. Shim, E. Darian, O. Guvench, P. Lopes, I. Vorobyov, A.D. Mackerell Jr, CHARMM general force field: a force field for drug-like molecules compatible with the CHARMM all-atom additive biological force fields, J. Comput. Chem. 31 (4) (2010) 671–690, https://doi.org/10.1002/jcc.21367.
[63] R. Purgatorio, M. De Candia, A. De Palma, F. De Santis, L. Pisani, F. Campagna, S. Cellamare, C.D. Altomare, M. Catto, Insights into structure-activity relationships of 3-arylhydrazonoindolin-2-one derivatives for their multitarget activity on β-amyloid aggregation and neurotoxicity, Molecules 23 (2018) 1544, https://doi.org/10.3390/molecules23071544.
[64] K. Stępnik, W. Kukula-Koch, A. Boguszewska-Czubara, K. Gawel, Astragaloside IV as a memory-enhancing agent: in silico studies with in vivo analysis and post mortem ADME-tox profiling in mice, Int. J. Mol. Sci. 25 (7) (2024) 4021, https://doi.org/10.3390/ijms25074021.
[65] S. Singh, M.K. Mandal, A. Masih, S.K. Ghosh, H.R. Bhat, U.P. Singh, 1,3,5-Triazine: a versatile pharmacophore with diverse biological activities, Arch. Pharm. 354 (6) (2021) 2000363, https://doi.org/10.1002/ardp.202000363.
[66] J. Labus, K.F. Röhrs, J. Ackmann, H. Varbanov, F. Müller, S. Jia, K. Jahreis, A. Vollbrecht, M. Butzlaff, Y. Schill, D. Guseva, K. Böhm, R. Kaushik, M. Bijata, P. Marin, S. Chaumont-Dubel, A. Zeug, A. Dityatev, E. Ponimaskin, Amelioration of Tau pathology and memory deficits by targeting 5-HT_7 receptor, Prog. Neurobiol. 197 (2021) 101900, https://doi.org/10.1016/j.pneurobio.2020.101900.